공학박사 학위논문

Development and investigation of ion selective materials for high performance capacitive deionization

고성능 축전식 담수화 공정을 위한 이온 선택성 물질 개발과 역할 규명

2018년 2월

서울대학교 대학원

화학생물공학부

윤 홍 식

Development and investigation of ion selective materials for high performance capacitive deionization

By

Hongsik Yoon

under the supervision of

Professor Jeyong Yoon, Ph. D.

A dissertation submitted in partial fulfillment of the requirements for the Degree of Doctor of Philosophy

February 2018

SCHOOL OF CHEMICAL AND BIOLOGICAL ENGINEERING

SEOUL NATIONAL UNIVERSITY

Development and investigation of ion selective materials for highly performed capacitive deionization

고성능 축전식 담수화 공정을 위한 이온 선택성 물질 개발과 역할 규명

지도교수 윤 제 용

이 논문을 공학박사 학위논문으로 제출함.

2018년 2월

서울대학교 대학원

화학생물공학부

윤 홍 식

윤홍식의 공학박사 학위논문을 인준함.

위 원 장 이 규 태 (인)

부위원장 윤 제 용 (인)

위 원 최 장 욱 (인)

위 원 강 경 석 (인)

위 원 김 광 제 (인)

Abstracts

Development and investigation of ion selective materials for highly performed capacitive deionization

Hongsik Yoon

School of Chemical and Biological Engineering

The Graduates School

Seoul National University

Capacitive deionization (CDI) is an emerging desalination process that produces fresh water from saline. CDI has been getting attentions due to its energy efficiency compared to the traditional desalination processes such as thermal distillation and reverse osmosis (RO). However, there is an intrinsic limitation in traditional CDI system. It is ‘co-ion expulsion’ issue. When the electrical double layer formed on the electrode, some of charges are wasted, leading to the deionization performance reduction. To overcome these disadvantages, ion selective materials such as ion exchange membrane and battery materials have been introduced in CDI system. Recently, various

materials have been vigorously developed for CDI system. However, the suitable ion selective material has been still required which would be expected to be highly performed, cost effective, and easily processible. Therefore, this study develops new ion selective materials to enhanced CDI performance. In addition, the effect of the ion selective materials on the CDI performances was also investigated.

First, Ca-alginate was proposed as an alternative to cation exchange membrane (CEM) in CDI system for hardness control. Ca-alginate, a cost effective and eco-friendly polymer gel, is widely used in pharmaceutical, water treatment, and food-industries. Ca-alginate was successfully coated on the negative electrode using phase separation via sodium-calcium exchange. As a major result, the CDI with Ca-alginate coated electrode (CA-CDI) showed superior deionization performance (approximately 44%) than conventional CDI system. Moreover, MCDI system with Ca-alginate coated electrode had comparable deionization capacity and charge efficiency to conventional MCDI system with commercial cation and anion exchange membranes.

Secondly, Ag coating on to the carbon electrode was proposed to enhance the deionization performances. The Ag coated carbon composite electrode was made by coating a small amount of Ag onto a carbon capacitive

electrode, exhibiting the characteristics of a battery and a capacitor together. As major results, the CDI deionization capacity (88% more), rate (39% more), and charge efficiency (76% → 92%) were dramatically enhanced due to the Ag coating. The significant improvements in deionization performances are explained by the enhanced specific capacity combining the capacitance in the carbon electrode with the Ag mediated charge transfer reaction. In addition, the hybrid CDI with Ag coated carbon composite electrode (73.3 kJ $mole^{-1}$) is superior to membrane assisted CDI (136.7 kJ $mole^{-1}$) in terms of energy consumption for deionization due to its low voltage feasible operation.

Lastly, it was investigated how the characteristics of ion exchange membrane (IEM) affect the membrane CDI (MCDI) performance. As MCDI performances, deionization capacity, maximum average deionization rate (MADR), and charge efficiency were analyzed. As major results, only MADR was significantly affected by change of IEM characteristics. In addition, MADR showed good positive relationship with transport number divided by total electrical resistance.

In conclusion, the research works of this dissertation indicate that the fascinated ion selective materials such as Ca-alginate and Ag coating significantly developed a superior deionization performance and showed great potential for further development in the CDI (MCDI) systems. In

addition, the study revealing the relationship between t_+/R_{CEM} and MADR would be expected to provide a good insight to develop of highly fast rate-capable MCDI.

Keywords: Water treatment, Desalination, Capacitive deionization, Silver, Ca-alginate

Student number: 2013-30283

Contents

List of figures

List of tables

1. Introduction

1.1. Backgrounds

Water scarcity is one of the most serious challenges faced by the global society (Shannon et al. 2008). Desalination systems such as distillation and reverse osmosis (RO) process have been receiving attention as a potential solution, despite the burden of its high-energy requirements. However, since the energy efficiency of current desalination technologies has approached the theoretical limit, the development of alternative desalination techniques has been intensively pursued to reduce energy consumption (Elimelech and Phillip 2011).

Capacitive deionization (CDI) technology has recently been introduced as an alternative desalination (Farmer et al. 1996, Welgemoed and Schutte 2005). CDI technology operates in a low voltage range where no electron transfer reaction occurs. However, the CDI process inevitably wastes some of the charge required for ion adsorption (Avraham et al. 2009, Biesheuvel and Van der Wal 2010). This is because, when the electric double layer is formed, it consumes charges to expel the co-ions (i.e. ions having the same potential as the potential of the electrode) existing on the electrode surface. To overcome this limitation, ion selective materials such as ion exchange membrane have been introduced. One of them is well known as membrane assisted capacitive deionization (MCDI) systems. MCDI system has been firstly developed by Lee et al. (Lee et al. 2006). MCDI is

assembled with the ion selective membranes and electrodes. The ion selective membranes located in front of the electrodes has dramatically improved desalination performance and charge efficiency by alleviating the 'co-ion expulsion' or ‘co-ion repulsion’(Biesheuvel and Van der Wal 2010). Due to the ion selective membrane (i.e. exchange membrane (IEM)), MCDI has three major advantages over conventional CDI systems. First, MCDI showed much better deionization performance than CDI. This is because the IEM of MCDI mitigates the above-mentioned co-ion repulsion. Second, MCDI showed better stability in the deionization performance over conventional CDI (Omosebi et al. 2014). This seems to be due to the fact that IEM protects CDI electrodes from oxidation-induced aging. Third, MCDI can enhance the water recovery by reducing the amount of stream concentrated by stop-flow operation (Biesheuvel and Van der Wal 2010). Despite its many advantages, MCDI was limited due to the expensive price of commercial IEM. Accordingly, various attempts have been made to develop ion selective materials that are expected to be competitive with commercial IEMs.

Various membrane materials have been introduced for MCDI. For example, Vinylbenzyl chloride-styrene-ethyl methacrylate copolymer (Koo et al. 2012), 4-styrenesulfonic acid sodium salt hydrate methacrylic acid methyl methacrylate copolymer (Kwak et al. 2012), Na Vinylbenzene Sulfonate-Grafted

Polyvinylidene fluoride (PVDF) have been developed from Hwang's group (Kang et al. 2015). In addition, Liu group developed Cross-linked quaternised Polyvinyl alcohol (PVA) (Tian et al. 2014), and Zou group developed RGO/Polyaniline/PVDF for anion exchange membrane (Zhang et al. 2015), respectively. On the other hand, various coating materials have been also studied. For example, PVA/ Sulfosuccinic acid, Sulfonated poly(arylene ether sulfone) random copolymer, Polyvinyl alcohol/Sulfosuccinic acid and Sulfonated poly(phenylene oxide) were proposed as a cation selective coating materials (Asquith et al. 2014, Gu et al. 2016, Kim et al. 2016a, Kim et al. 2015a). An aminated polysulfone was proposed as anion exchanging coating materials.

However, the suitable ion selective material has been still required which would be expected to be highly performed, cost effective, and easily processible. In addition, until now, a systematic research has been limitedly conducted on how the overall characteristics of IEM, including electrical resistance, affect the performance of MCDI.

1.2. Objectives

This study develops new and fascinated ion selective materials to enhanced CDI performance. In addition, it is investigated the influence of the ion selective materials on the CDI performances.

First, we propose Ca-alginate as a cation selective coating material and used it in asymmetric CDI and MCDI systems to control the hardness in water. Second, Ag coating on to the carbon composite electrode is proposed where this composite electrode has the characteristics of a battery and a capacitor together. Ag has been known as a representative ion selective materials through Ag/AgCl reaction as well as traditional battery material. Since Ag is an expensive rare metal, small amount of Ag was deposited onto the capacitive carbon electrode with a photo induced reduction. Third, it was investigated how the characteristics of cation exchange membrane (CEM) affects the MCDI performance which is evaluated by deionization capacity, maximum average deionization rate (MADR), and charge efficiency. As characteristics of IEM, electrical resistance, ion exchange capacity, water content, and transport number was examined.

2. Literature review

2.1. Capacitive deionization

The capacitive deionization is an electrochemical based desalination technology (Welgemoed and Schutte 2005). This system is operated by the electrochemical adsorption/desorption process. When the electrical voltage is applied between the electrodes, the electrical double layer is formed on the electrode. Then, the ions have different charge with the electrode move to the electrodes, resulting in the desalination of the feed solution. Since CDI is based on the capacitor system, this system has 2 advantages in aspect of energy consumption. Firstly, CDI is available for the energy saving operation due to its operation voltage range. CDI proceeds under non-faradaic reaction and operates at a low potential range (about 1.2 V). Assuming that they operate at the same current and efficiency conditions, the CDI can save the energy consumption due to the low potential operation. Secondly, CDI can recover the energy consumed at the charging step. Because, during the deionization step, the energy levels of both electrodes are increased. In the discharge step, ions adsorbed on the electrode are released and energy is produced. Indeed, it was reported that 83% of energy used for deionization step was recovered (Anderson et al. 2010). Accordingly, CDI has been expected to be energy-efficient for treating the low-grade saline water in

comparison with the conventional desalination technology (Zhao et al. 2013). Additionally, CDI showed its great potential to be applied for the hardness control, wastewater treatment, producing distilled water (Lee et al. 2006, Lee and Choi 2012, Seo et al. 2010, Yoon et al. 2016).

However, CDI has an intrinsic limitation which is 'co-ion expulsion'. When an electric double layer is formed on the surface of the electrode, the ions having same charge with the electrode (co-ion) are pushed toward the bulk solution from the electrode surface (Avraham et al. 2009, Biesheuvel and Van der Wal 2010). Due to the migration of the co-ions, some charges are inevitably consumed, resulting in the reduction of the charge efficiency (i.e. the amount of charge used for desalting through ion adsorption versus the amount of charge consumed). In order to overcome the limitation of CDI, various attempts have been made though controlling the operation condition. For example, Kim et al. reported that they alleviate the co-ion expulsion with discharge voltage control (Kim et al. 2015c). However, such a method would require sacrifice in performance such as desalting capacity. Recently, the introduction of ion selective materials such as ion exchange membranes (IEM) has successfully solved co-ion expulsion issue without loss of the deionization performances.

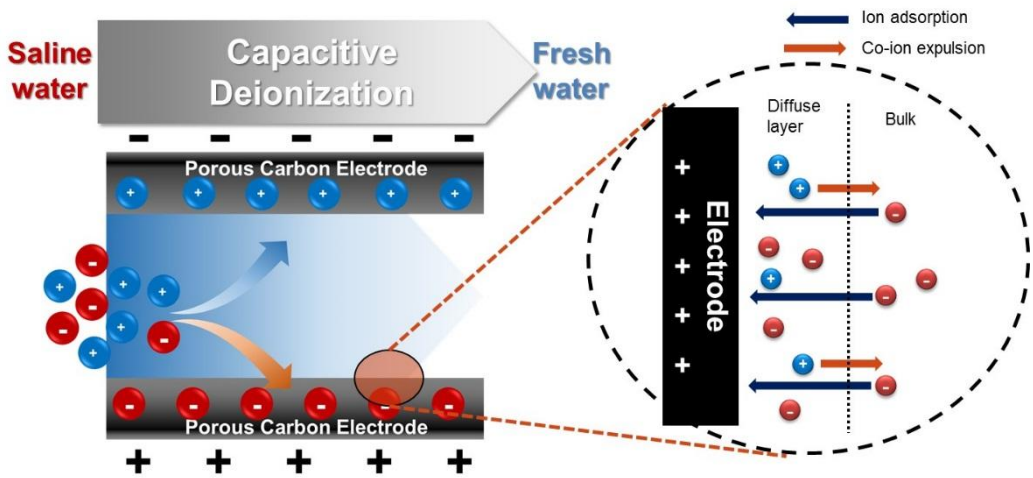

Figure II. 1 Schematic of capacitive deionization and co-ion expulsion

2.2. Membrane capacitive deionization (MCDI)

2.2.1. Ion exchange membrane (IEM)

Ion exchange membrane (IEM) is one of the most representative ion selective materials (Sata 2007). The ion exchange membrane is a membrane that allows selective permeation of positive / negative ions. The ion exchange membrane is divided into two part. One is a substrate part and the other is a functional group part which enables selective permeation characteristics. Usually, the type of ion exchange membrane is determined depending on the functional group. The ion exchange membrane types and the functional groups are summarized in Table 1. As the cation exchange membrane, a polymer containing sulfone group ($-SO_3^-$) is widely used. And a polymer having a carboxyl group and a phosphoric acid group is also utilized for cation exchange membrane materials although it is weakly acidic. As the anion exchange membrane, a polymer containing a trivalent amine group ($-N(CH_3)_3OH$ / $-N(CH_3OH)(CH_3)_2OH$) is mainly used. It is known that the membranes used as commercial cation exchange membranes are mainly composed of sulfone groups and trivalent amine groups.

Table II. 1 Cation/anion exchange groups and their apparent pKa (Sata 2007).

Cation exchange groups	Apparent pKa	Anion exchange groups	Apparent pKa
$-CF_2SO_3H$	-6	$-N(CH_3)_3OH$	>13
$-SO_3H$	0-1	$-N(CH_2OH)(CH_3)_2OH$	>13
$-CF_3COOH$	2	$-S(CH_3)_2OH$	>13
-COOH	4-6	$-P(CH_3)_3OH$	>13
$-PO_2H_2$ (pK_1)	2-3	$-NH_2$	7-9
$-PO_2H_2$ (pK_2)	7-8	-NH	7-9
Phenolic OH	9-10	-Aniline (NH_2)	5-6
$-C(CF_3)_3OH$	5-6		
$-CF_3SO_2NHR$	0-1		

In the early Membrane CDI (MCDI) research until 2010, only commercial IEMs were used. The most used commercial IEMs were ASTOM's Neosepta CMX (cation exchange membrane) and AMX (anion exchange membrane) (Biesheuvel and Van der Wal 2010). The detailed specifications provided by ASTOM are shown in Table II. 2 below. The MCDI performance (ion adsorption capacity, charge efficiency) with the commercial ion exchange membrane is about double the value of the conventional CDI (Kim and Choi 2010b, Li and Zou 2011, Omosebi et al. 2014). However, due to the high price of commercial IEMs (about $ 80 per m^2) (Weinstein and Dash 2013), a variety of ion exchange materials have been developed to replace them. Ion exchange materials for MCDI technology are classified into membrane type and coating type.

Table II. 2 Characteristics of Neosepta CMX and AMX (Xu 2005).

	Type	Transport number	Electric resistance ($\Omega \cdot cm^2$) [a]	Thickness (mm)	Temp. (^oC)	pH	Application
CMX	Strong acid (Na type)	0.97	3	0.17	< 40	0 - 10	Desalination, Hardness & Nitrogen control
AMX	Strong base (Cl type)	0.97	2.4	0.14	< 40	0 - 8	

[a] Electric resistance: Equilibrated with a 0.5N-NaCl solution at 25ºC

2.2.2. The role of Ion exchange membrane (IEM) in MCDI

Due to the IEM, MCDI has 3 major advantages in comparison with conventional CDI system. First, MCDI showed much better deionization performances than CDI (Kim and Choi 2010b, Li and Zou 2011, Omosebi et al. 2014). This is because the IEM in MCDI allows the penetration of the counter-ions, not the co-ion (Biesheuvel and Van der Wal 2010). Thus, MCDI effectively alleviate the co-ion expulsion, leading to the great enhancement of the deionization performance. Additionally, Second, MCDI is superior in performance retention compared to conventional CDI (Omosebi et al. 2014). This seems to be because the IEM protects the CDI electrode from oxidation-induced aging. It was reported that the oxidation of the electrode proceeds due to the dissolved oxygen in the feed water, resulting in a decrease in performance. The IEM in MCDI inhibited the oxidation of the electrode by alleviating the permeation of dissolved oxygen from the bulk solution to the electrode. According to Omosebi et al., The MCDI mitigated the performance degradation of the MCDI (Fig II. 2, (Omosebi et al. 2014)). Third, MCDI can reduce the amount of the concentrated stream (Biesheuvel and Van der Wal 2010). At the discharging step, the voltage can be reversed by a ‘concentrate’-step while the flow rate is reduced to zero due to the IEM.

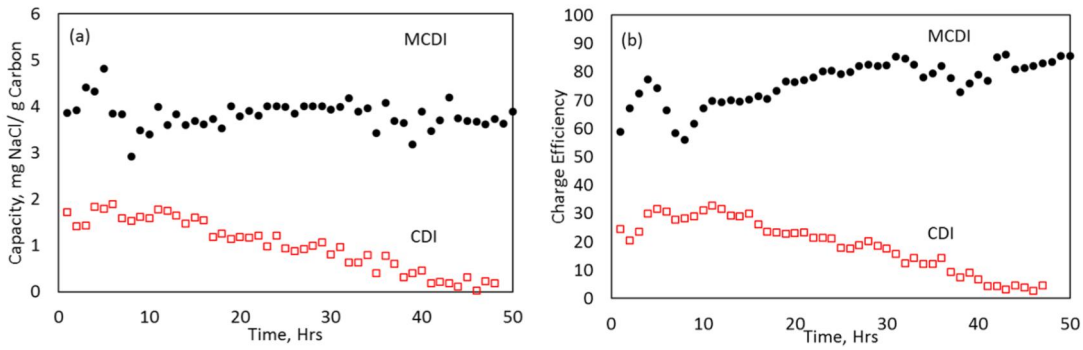

Figure II. 2 Deionization capacity (a) and charge efficiency (b) of MCDI and CDI with respect to time (Omosebi et al. 2014).

2.2.3. New membrane materials for MCDI

Table 3 summarized the materials and preparation method of the IEMs that have been studied for application to the MCDI.

First, several examples of IEM for MCDI have recently been reported which are synthesized by copolymerization. The copolymerization is a method of synthesizing a polymer using two or more monomers. In Hwang's group, vinylbenzyl chloride-styrene-ethyl methacrylate copolymer was used as an IEM material. And anion exchanging functional group was added through copolymerization and amination (Koo et al. 2012). The synthesized anion exchange membrane showed relatively good electrical resistance (1.5 $\Omega \cdot cm^2$) compared to Neosepta AMX (3.5 $\Omega \cdot cm^2$), which is a commercial anion exchange membrane. In this group, NaSS-MAA-MMA copolymer (Kwak et al., 2012) and Na Vinylbenzene Sulfonate-Grafted PVDF were investigated as cation exchange membrane materials (Kang et al. 2015). The cation exchange function utilized the $-SO_3^-$ group contained in the existing monomers. In the study using NaSS-MAA-MMA copolymer, Nafion 117 was selected as a comparative group. In aspect of electrical resistance, NaSS-MAA-MMA copolymer (0.7 $\Omega \cdot cm^2$) showed better values than Nafion 117 (1.5 $\Omega \cdot cm^2$). The IEMs in this group were superior in electrical and physicochemical properties to commercial cation exchange membranes. However, they did not report the directly evaluated performance in

MCDI system.

Table II. 3 Materials and preparation of ion exchange membrane for MCDI.

Group	Type	Material	Preparation
Taek Sung Hwang (Korea)	AEM	Vinylbenzyl chloride-styrene-ethyl methacrylate copolymer	Copolymerization with post-treatment
	CEM	NaSS–MAA–MMA copolymer	Copolymerization
	CEM	Na Vinylbenzene Sulfonate-Grafted PVDF	Copolymerization
Bradley P. Ladewig (Australia)	CEM	Random and multiblock side-chain sulfonated PES	Copolymerization with post-treatment
Ling Liu (China)	AEM	Cross-linked quaternised PVA	Post-treatment & Cross-linking
Linda Zou (UAE)	AEM	RGO/Polyaniline/PVDF	Simple mixing

NaSS: 4-styrenesulfonic acid sodium salt hydrate, MAA: methacrylic acid MMA: methyl methacrylate, PVDF: Polyvinylidene fluoride, PES: Poly(ethersulfone), PVA: Polyvinyl alcohol, RGO: Reduced grphene oxide

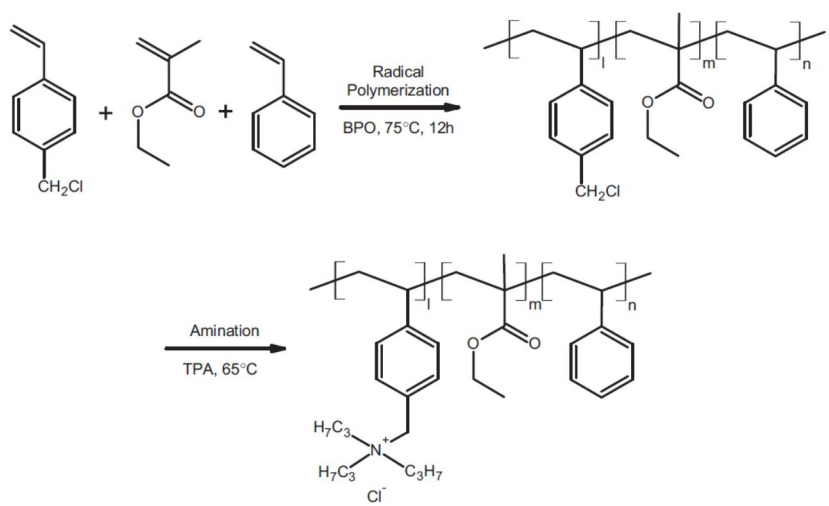

Figure II. 3 Scheme for the synthesis of the 4-vinylbenzyl chloride-styrene-ethylmethacrylate anion-exchange membranes (Koo et al. 2012).

Second, some research group utilized post-treatment method to prepare ion exchange membrane.

Ladewig group (Asquith et al. 2013) reported PES copolymers for copolymerization method. After the copolymerization, the polymer was functionalized through sulfuric acid treatment. In this study, the migration, electrical resistance, and ion exchange capacity showed better than the commercial Neosepta CMX, but they did not report the MCDI performance with their IEM.

Liu group synthesized anion exchange membrane by using Post-treatment & Cross-linking. They prepared polyvinyl alcohol with Glutaldehyde which a representative cross-linker. Then, the quaternary ammonium group was added with the post-treatment (Tian et al. 2014). In this study, the prepared IEMs were adhered to the electrodes by compressing. The performance of the ion exchange membranes was improved about double the value of that of CDI. Interestingly, this study compared the deionization performances in which one is a traditional MCDI and the other is a system with a coated electrode by casting method. It is noted that both systems used same ion exchange polymers. As a result, the deionization performance with coated electrode was lower than that of MCDI. The reasons for the above results are described by the authors of the group as

follows. The use of ion-adsorption area seems to be reduced by ion-exchange polymers invading and covering the effective surface area of the electrode during the coating process. In addition, in this study, the pseudo-first-order model of Lagergren is presented as the ion adsorption model. And they showed good correlation trend between the model values and the results obtained from the experiments. This model has shown a similar tendency from previous research results (Li et al. 2011, Li et al. 2010). (Li et al. 2011, Li et al. 2010).

$$\log(q_e - q) = \log q_e - (\frac{kt}{2.303})$$

q (mg / g) is the final desalting capacity of the electrode, q (mg / g) is the desalting capacity with time, k (1 / min) is the first rate constant and t (min) is the time.

Third, Zou group used a composite polymer to prepare IEM. The Zou group prepared anion-exchange membranes by mixing reduced graphene oxide (RGO) and polyaniline polymers with Poly (vinylidene) fluoride (PVDF) (Zhang et al. 2015). Each material was used for each function. First, the PVDF was used as backbone substrate. And, the polyaniline was added to provide the anion exchange group (i.e. amine group). RGO contributed to the improvement of the conductivity of the IEM. The deionization performance was also improved with increasing

RGO / polyaniline content (~ 3.5 times).

2.2.4. New coating materials for MCDI

Figure. II 4 showed various method of ion exchange polymer coating on to the MCDI electrode such as casting, dipping method, spray coating, electrodeposition and simple mixing. The materials of the ion exchange coating reported so far are summarized in the following Table. II 4. Ion exchange polymer coating has been introduced as a technique to replace the simple assembly of IEM in the traditional MCDI. And the ion exchange polymer coated electrodes are expected to be beneficial when constructing a device stack.

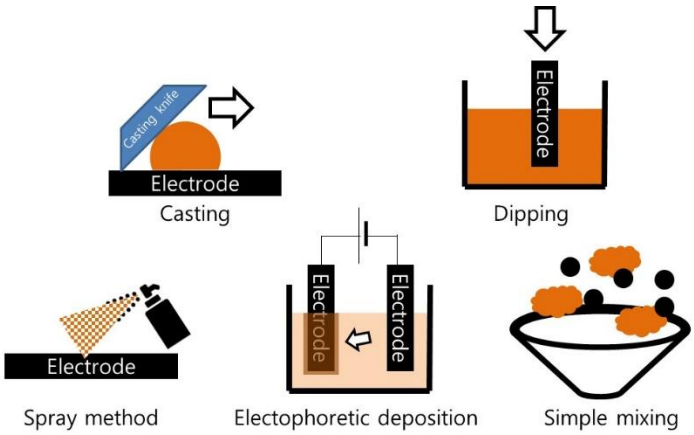

Figure II. 4 Various methods of ion exchange polymer coating on to the CDI electrode.

Table II. 4 Ion exchange material and their coating method for CDI electrode

Group	Type	Material	Coating method
Jae-Hwan Choi, Korea (2010)	CE	Polyvinyl alcohol/Sulfosuccinic acid	Direct casting
Bradley P. Ladewig, Australia (2014)	CE	Sulfonated poly(arylene ether sulfone) random copolymer	Direct casting
Ji Won Rhim, Korea (2015)	CE/AE	Sulfonated poly(phenylene oxide) / Aminated polysulfone	Direct casting
	CE/AE	Polyvinyl alcohol/Sulfosuccinic acid / Aminated polysulfone	Direct casting
Jieshan Qiu (China)	CE	Sulfonated reduced-graphene oxide	Dip-coating
Seung-Hyeon Moon Korea, (2011)	CE	Bromomethylated poly (2,6-dimethyl-1,4-phenylene oxide)	Spray coating
Haibo Li, China (2014)	CE	Sulfonated reduced-graphene oxide	Electophoretic deposition
Linkun Pan (China)	CE	CNT-polyacrylic acid	Electophoretic deposition
	CE/AE	Polyethyleneimine / Dimethyl diallyl ammonium chloride	Simple mixing (Binder)

Figure II. 5 shows one example of the ion exchanging materials coated carbon electrode using direct casting method, which was first introduced by Prof. Choi, Jae-Hwan group (Kim and Choi 2010b). In this study, polyvinyl alcohol (PVA) polymer was used as a backbone polymer. And sulfosuccinic acid (SSA) played a role of cross-linker and provided ion exchanging functional group. As the concentration of SSA and the degree of cross-linking increased, the electrical resistance decreased, resulting in the good improvement in deionization performance. They discussed that the coating of the ion exchange material appears to have a positive effect by reducing the interfacial resistance between the electrode and the ion exchange coating layer as compared with the application of the IEM. However, the result in this study showed some contradictions with the Liu group's study (Tian et al., 2014) (Figure II. 6). In Liu's result, they insisted that the deionization performance is degraded due to ion exchange coating since they cover the electrode active area.

Nevertheless, after Choi's research, the casting method has been widely used for the coating method for ion exchange polymer. For instance, the Ladewig's group also reported the ion exchange coating material with direct casting method. They used sulfonated poly (arylene ether sulfone) random copolymer (Asquith et al. 2014). Although they did not provide deionization performance, the improvement of the capacitance was provided. In addition, Prof. Lim's group has

reported sulfonated poly (phenylene oxide) (Kim et al. 2015b) and PVA / SSA (Kim et al. 2016) as a cation exchange coating materials and aminated polysulfone as an anion exchange coating material (Kim et al. 2016), respectively. In their research, the performance improvement was remarkable, compared with the conventional CDI process.

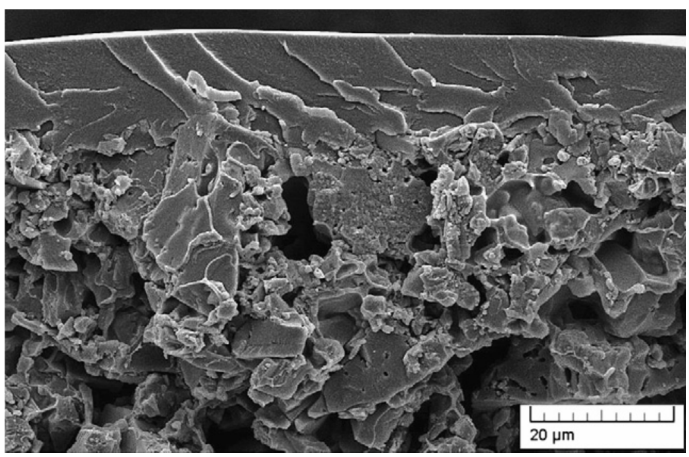

Figure II. 5 Cross-sectional image of Ion exchange polymer coated carbon electrode through casting method (Kim and Choi 2010b).

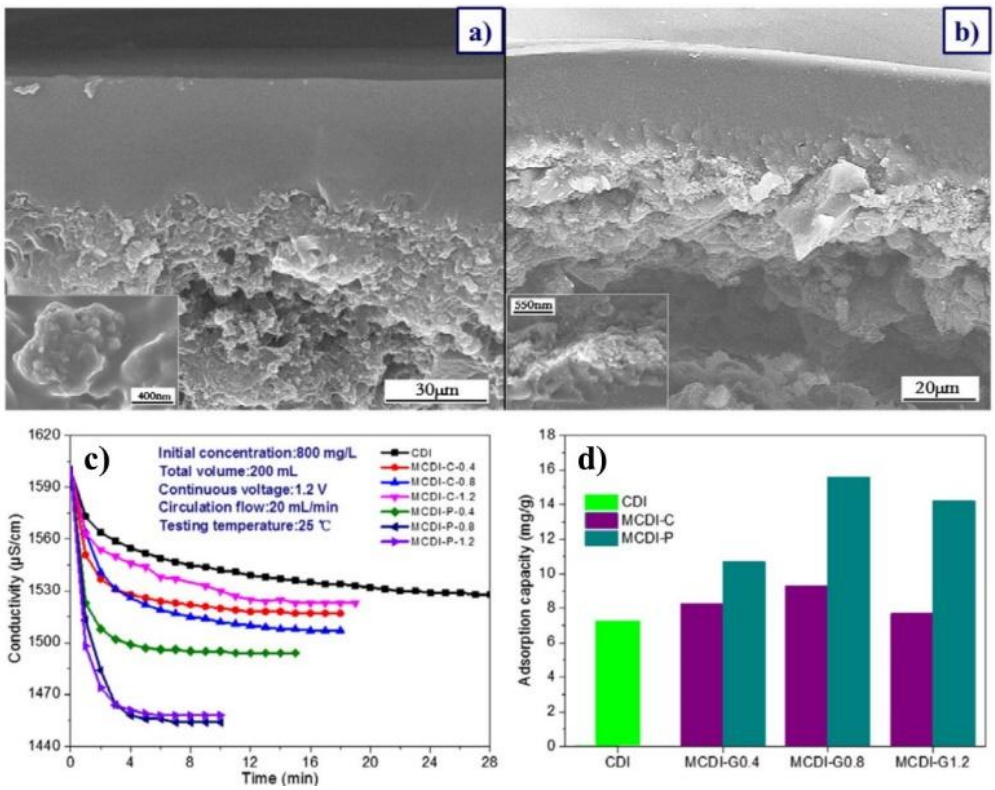

Figure II. 6 The SEM images of cross sections of the composite electrodes: (a) ACM-C (Activated carbon with N-Methyl-2-pyrrolidone coating); (b) ACM-P (Activated carbon with N-Methyl-2-pyrrolidone Pressed membrane). The adsorption effects of CDI and MCDI composite electrodes at various operation models: (c) adsorption behavior curves; (d) adsorption capacity. (Tian et al. 2014).

A study on the spray coating of ion - exchange polymer on the CDI electrode was developed by Moon's group (Lee et al. 2011). In this study, they described that the interfacial resistance between the electrode-ion exchange polymer could be saved due to the spray coating process. The polymer used in this study was bromomethylated poly (2,6-dimethyl-1,4-phenylene oxide. The results showed that the deionization performance of the proposed system was similar to that of conventional CDI, but the energy consumption was very low and showed excellent charge efficiency.

Electrodeposition method have been also getting attention as a good example of coating method for CDI electrode, reported by Li's group and Pan's group (Li et al. 2014, Nie et al. 2012). In Li's group the sulfonated graphene was electrodeposited on the carbon fiber cloth electrode under high voltage conditions (about 20 V) (Li et al. 2014) as shown in Figure II. 7. The adsorption potential varied from 0.6 V to 1.4 V. In all cases, deionization performance and charge efficiency were superior to those with pristine CDI electrodes. In addition, they analyzed the ion adsorption trends assigned to the Langmuir and Friedrich isotherm adsorption curves. As a result, the deionization capacity showed a high correlation with the Langmuir isotherm. This result explained that the system is efficiently operated in physisorption and adsorption / desorption would be efficient. In the Pan's group, 5 V was applied to a mixed solution of CNT and

polyacrylic acid to produce an electrode (Nie et al. 2012). With this electrode, they provided better the deionization performance than that with the commercial cation exchange membrane.

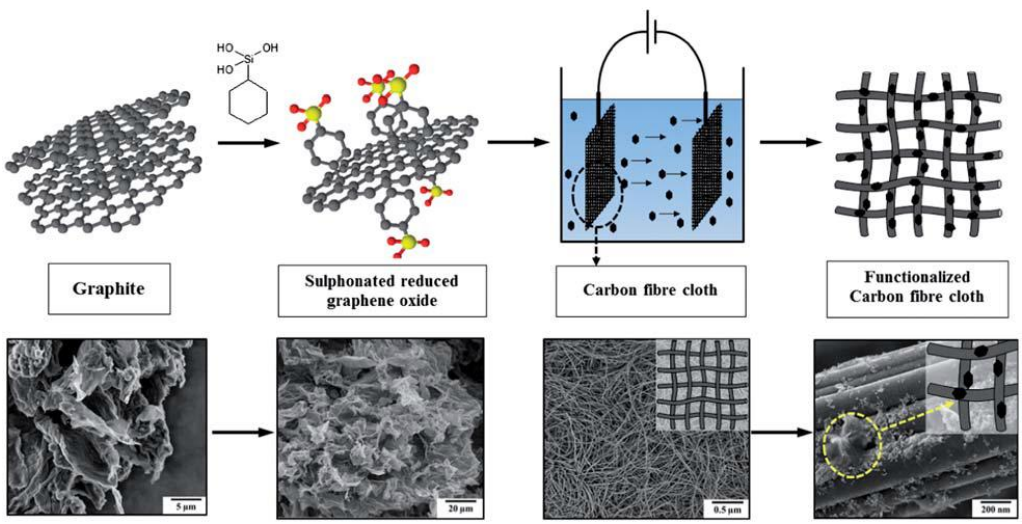

Figure II. 7 Sulfonated reduced graphene oxide coated using electrophoretic method (Li et al. 2014)

In the Pan's group, an electrode was prepared by simple mixing an electrode active material (CNT) and an ion exchange material (Liu et al. 2014). Polyethyleneimine and dimethyl diallyl ammonium chloride was mixed in the cathode preparation. Although the electrical resistance of the electrode tended to increase, but the desalination performance was improved. On the other hand, Linda Zou group introduced positive / anion exchange properties into the electrode material itself by introducing sulfuric acid / ammonium groups (Jia and Zou 2012). As a result, the capacitance of the control electrode was increased and the desalination rate was improved. However, there was a tendency for the electrode area to decrease during the functionalization process, which was described as having a negative effect on the deionization performance.

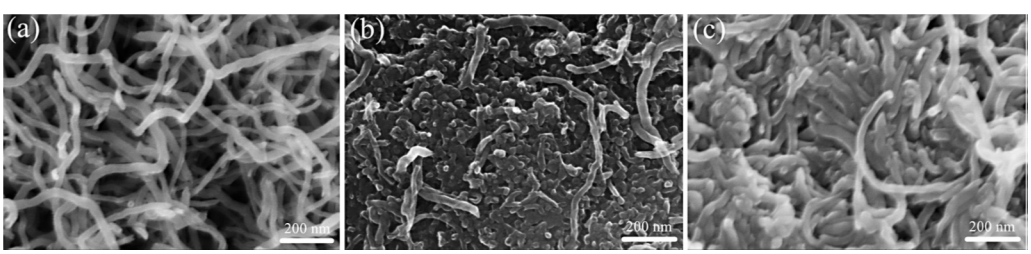

Figure II. 8 SEM images of (a) CNTs, (b) CNTs-PEI and (c) CNTs-DMDAAC electrodes (Liu et al. 2014).

Most studies have shown improved performance when ion exchange materials are applied. However many of them did not provide direct comparison with commercial IEM, which can be considered as a control. Although only a few studies have provided comparative results, there is a lack of information on the commercial ion exchange membranes used and the factors of performance improvement have not been clarified.

2.2.5. Stability of Cation/Anion exchange membrane

Compared to its importance, the stability issue of IEM in MCDI has not been actively discussed. However, when we look at the results of the subsequent studies, it can be seen that the stability issue of the IEM in MCDI should also be urgently reviewed.

IEM can be largely classified into cation exchange membrane and anion exchange membrane. First, the cation exchange membrane is relatively superior to the anion exchange membrane in aspect of chemical stability. This is because the sulfone group, which is the main functional group used for the cation exchange membrane, is highly resistant to chemical changes even when the pH changes (Bauer et al. 1990). In addition, the stability of the backbone polymer in the cation exchange membrane was improved remarkably through the perfluorination reaction. Based on this, Nafion® and Aciplex® Flemion® were developed well (Figure II. 9). Accordingly, the cation exchange membrane is used stably even under extreme pH harsh conditions.

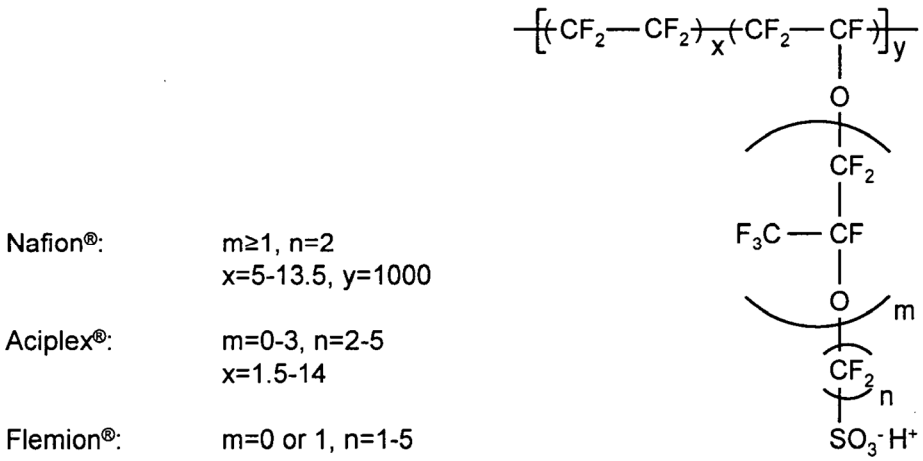

Figure II. 9 The structure of Nafion®, Aciplex® and Flemion® (Bürger 2017)

On the other hand, the chemical stability of the anion exchange membrane remains to be solved (Kneifel and Hattenbach 1980). In particular, anion exchange membranes have been shown to have significantly lower durability at high pH conditions (Matsui et al. 1986). It is known that functional groups of anion exchange membrane are easily damaged by hydroxide ion. This phenomenon occurs in Hofmann degradation. Specifically, hydroxide ions appear by supplying electrons to the B-H-atom of the carbon atom adjacent to the tertiary ammonium group. Through this, the tertiary amine group is removed and an olefin group is formed (Figure II. 10). This occurs actively under high pH and high temperature conditions (Bauer et al. 1990). In addition, anion exchange membranes using poly vinyl chloride as a backbone polymer have dehydrochlorination reaction at high pH, resulting in damage to the polymer structure. In the MCDI process, the pH of the solution changes according to the driving potential condition, so the possibility of anion exchange membrane damage is very high. However, the stability of ion exchange membranes in MCDI has not been systematically addressed.

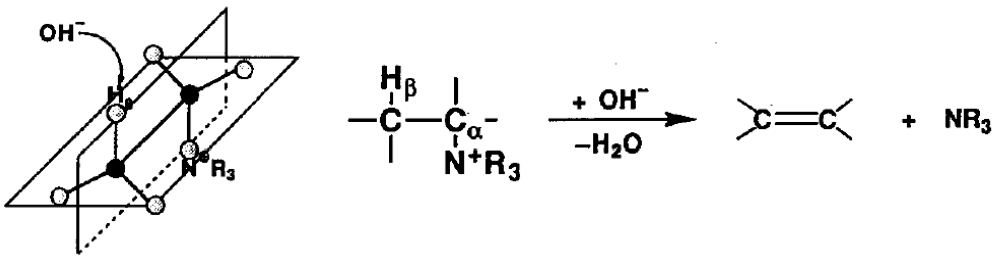

Figure II. 10 Reaction scheme illustrating the degradation of quatemary ammonium ions by the nucleophilic substitution reaction (Bauer et al. 1990).

2.3. Selective ion removal in capacitive deionization (CDI)

2.3.1. Selectivity in CDI carbon based electrode

Carbon based materials have been mainly used as CDI electrode. Therefore, the carbon electrode itself has no specific selectivity. Nonetheless, there is a selective removal tendency in the CDI carbon electrode due to the following two characteristics. One is the Columbic interaction and the other is the substitution phenomenon.

Columbic interaction is the magnitude of the electrostatic force between two point charges. The Columbic interaction is directly proportional to the product of the magnitudes of charge and inversely proportional to the distance between the two, as following.

$$|\mathrm{F}| = \frac{\mathrm{k_e}|q_1 q_2|}{r^2}$$

where k_e is Coulomb's constant ($k_e = 8.987\times10^9$ N m^2 C^{-2}), q_1 and q_2 are the signed magnitudes of the charges (C), the scalar r is the distance between the charges (m).

There have been several researches elucidating that Columbic interaction contributes to the ion selective removal in the CDI. For instance, in 2010, Moon's group found that divalent ions such as Ca^{2+} and Mg^{2+} can be selectively removed

by CDI electrodes (Seo et al. 2010). For example, it was observed that divalent cations, Mg ions and Ca ions were adsorbed more than monovalent Na ions. The above results are described as being influenced by both the valance charge of the ion and the hydrated radius. Specifically, the higher the valance charge and the lower the hydrated radius, the higher the removal rate. In addition, similar studies were conducted in the Hou Group in 2013 (Hou and Huang 2013)and in the Zhang Group in 2015 (Chen et al. 2015). Hou's group also showed a tendency to remove cations in the order of Ca> K> Na. Zhang group investigated the removal trends of the CDI carbon electrode for negative ions.

Recently, Wang's group reported interesting research works about the effect of the existing hydrated radius (Li et al. 2016) on to the removal tendency in CDI (in Figure II. 11). They insisted that the difference in hydrated radius is not clear in comparing the removal performance trends of ions with the same charge. This group presented a new influential factor called the 'hydration ratio'. The hydration ratio is the dimensionless factor of the hydrated radius divided by the atomic radius. Experimental results showed that when the ions having the same charge are compared, the lower the hydration ratio, the higher the removal amount. These trends were the same for both positive and negative ions.

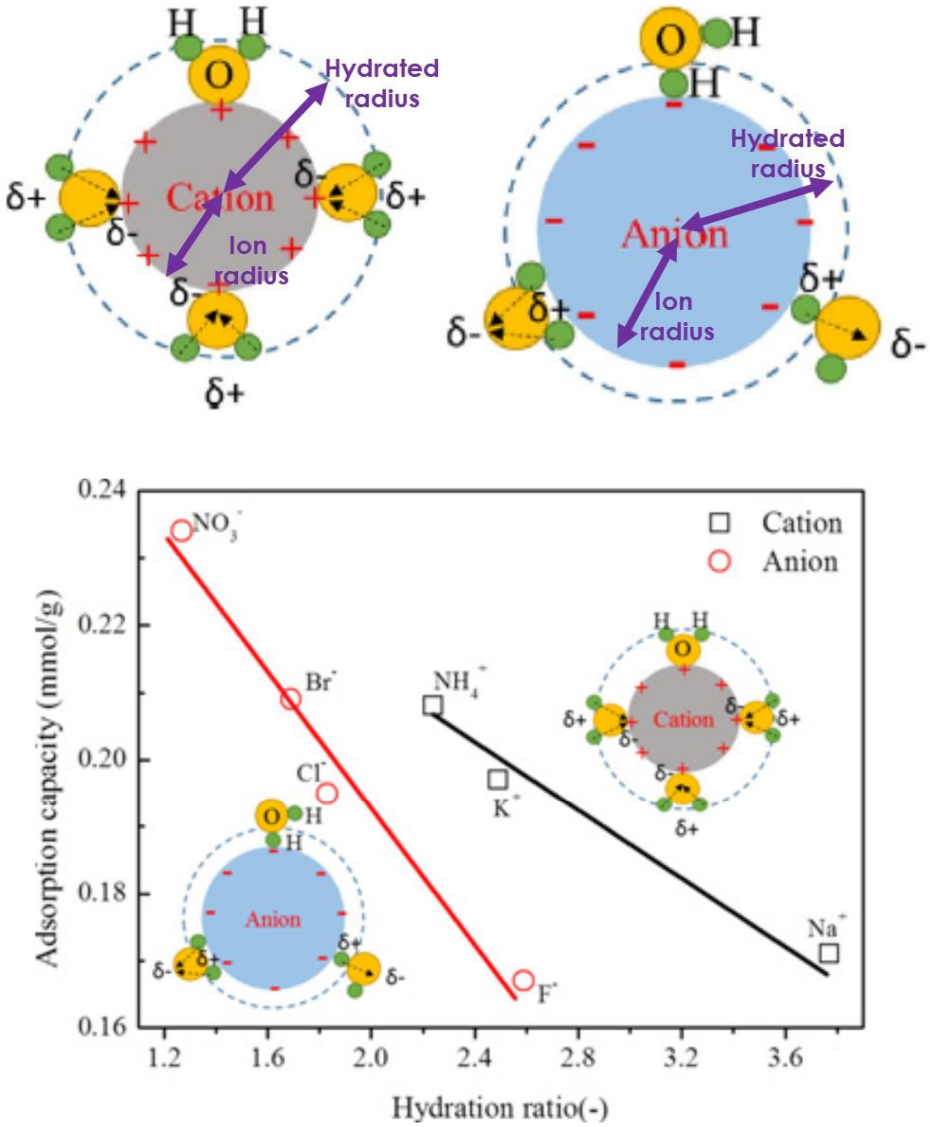

(a)

(b)

On the other hand, ion substitution have been regarded as an important factor affecting the selective removal in CDI. Ion substitutions have been observed in

Figure II. 11 Schematic of ion radius and hydrated radius (a) and adsorption capacity with hydration ratio (= hydrated radius divided by ion radius) (Li et al. 2016).

previous researches (Figure II.10). Substitution refers to a phenomenon in which ions in a bulk are adsorbed on a carbon electrode while pushing the adsorbed ions into a bulk solution. These results were observed in the researches of Moon's Group, Wang's Group, and Zhang's Group (Chen et al. 2015, Li et al. 2016, Seo et al. 2010) as shown in Figure II. 12. For example, in a study by Moon et al., About 10 minutes after the adsorption step, the Na concentration of the produced water was higher than that of the raw water. In Wang's group, the NO_3^- and Cl^- mixed solutions were tested. And it was found that the NO_3^- ion concentration in the bulk solution was steadily decreasing around 20 minutes after the adsorption step, whereas the Cl^- ion concentration increased. Zhang's group also showed a similar tendency.

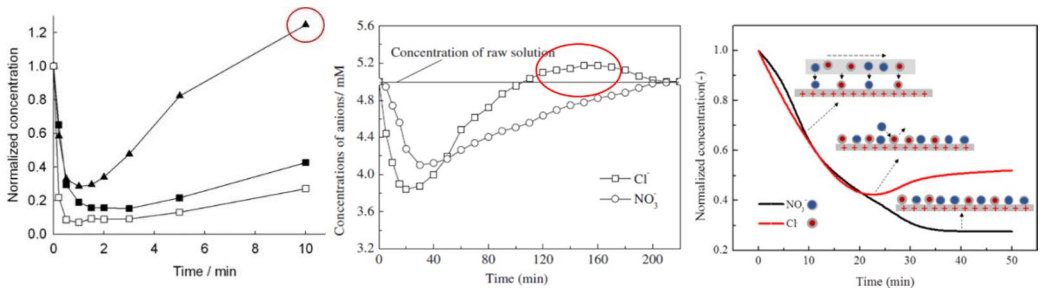

(a) (b) (c)

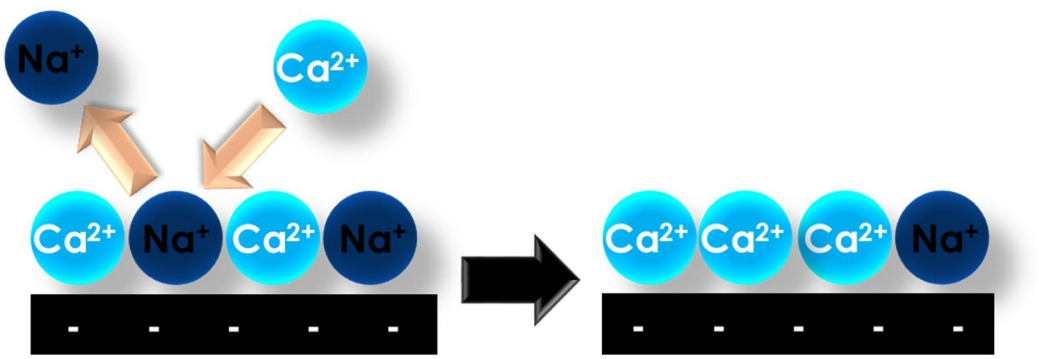

(d)

Figure II. 12 The examples of substitution in the capacitive deionization (CDI) system (a-c) and the schematic of substitution on the CDI carbon electrode (Chen et al. 2015, Li et al. 2016, Seo et al. 2010).

2.3.2. Selectivity in membrane capacitive deionization (MCDI)

MCDI is a system assembled with IEMs and a pair of carbon based electrode. Therefore, the selective ion removal trends in MCDI could be influenced by the IEM and ion exchange coating material. It is reported that the permselectivity of IEMs is affected by the type of functional groups and degree of cross-linking of polymers. For example, carboxyl groups are known to have a positive effect on the permeation selectivity for divalent cations compared to sulfonated groups (Sata 2007). And, it has been reported that when the degree of crosslinking of the polymer is increased, the permeation selectivity of the monovalent cation is positively influenced in comparison with that of the multivalent cation (Xu 2005). This is because the conductivity of the multivalent cation decreases as the size of the channel through which the ions permeate is smaller.

A representative study on ion selectivity in MCDI was published in 2012 by Prof. Choi (Kim and Choi 2012). In this study, ion exchange coating materials with excellent selectivity to nitrate ions were developed. The ion exchange coating material was made by mixing nitrate ion selective commercial anion exchange resins (BHP55, Bonlite Co., Republic of Korea) with other polymers. As a result of the study, they have reported that the selectivity to nitrate ion is improved with respect to chloride ion as a competitive substance. In the following year, this group developed another coating material that enhanced selectivity to

nitrate ions over chloride and sulfate ions (Kim et al. 2013b). The major material for this coating material was a commercial anion exchange resin used as in the previous study (BHP55, Bonlite Co., Republic of Korea). In the same year, Prof. Choi reported on the effect of ion adsorption selectivity of the ion exchange membrane itself on MCDI deionization selectivity (Yeo and Choi 2013). However, the results in this study showed a contradiction with previous studies. Previous research has shown that the higher the ion adsorption selectivity of the ion exchange membranes, the lower the actual permeation selectivity (Sata 2007). It seems that a systematic study is needed in the future.

Recently, Hong's group has constructed a MCDI system that utilizes a commercial cation exchange membrane to exhibit selective removal of monovalent cations (Figure II. 13, (Choi et al. 2016)). As a result, the selectivity to Na^+ over $Ca^{2+}$was about 2 times was observed. This group described that the MCDI system with monovalent cation selective membrane is superior in aspect of energy consumption to nanofiltration processes. Based on these results, it is suggested that MCDI can be utilized as a process for producing divalent cationic concentrated water.

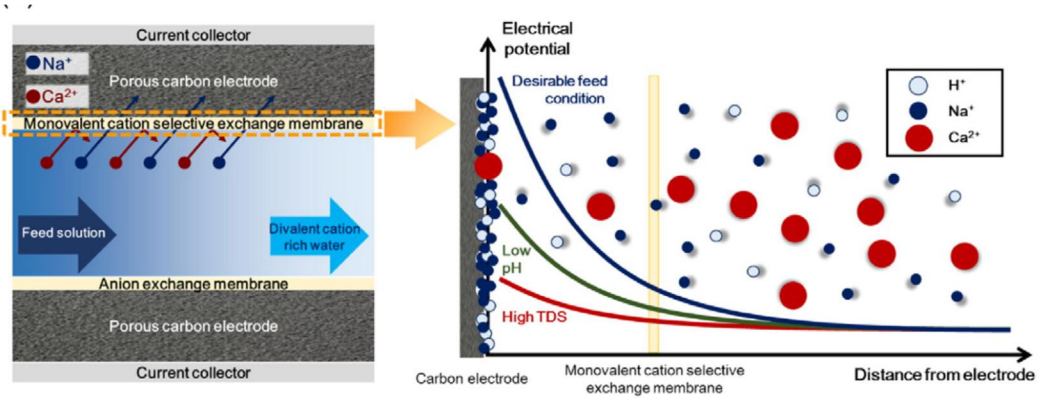

(a)

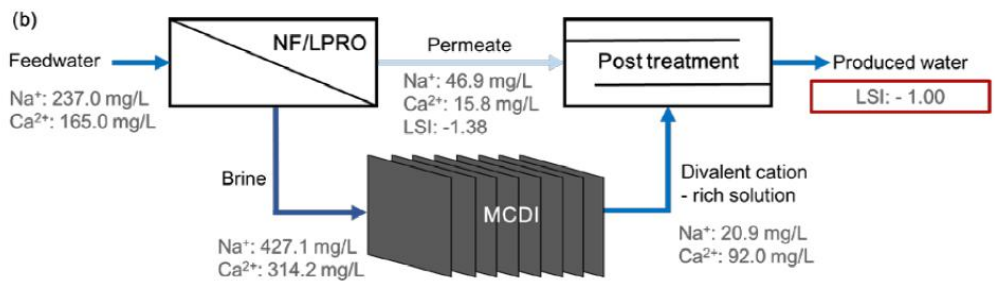

(b)

Figure II. 13 conceptual illustration for selective removal of monovalent and divalent cations by a MCDI cell with a monovalent cation permselective exchange membrane and conceptual illustration of MCDI process producing Ca^{2+}-rich water as a post-treatment in NF/LPRO treatment system (Choi et al. 2016).

2.3.3. Selectivity in capacitive deionization with faradaic reaction and aqueous battery desalination system

Recently, CDI technology using the faradaic reaction and an aqueous battery desalination system for ion selective removal process have been actively reported. The electrode materials in these studies utilized specific affinity such as intercalation or charge transfer reaction. Unlike conventional CDI or MCDI, which utilize carbon electrodes, this study utilizes a variety of organic / inorganic electrode materials.

For example, in Liu's group, a flow-through CDI system was constructed using nitrogen-doped graphene as an electrode material (Figure II. 14, (Ji et al. 2015)). Nitrogen-doped graphene electrodes have been described as having chelating properties for toxic heavy metal ions and show excellent selective removal performance. In particular, this electrode showed excellent selectivity for lead, cadmium, and mercury ions (Pb, Cd, Hg) compared to competitive ions such as Na, K, Ca, and Mg ions.

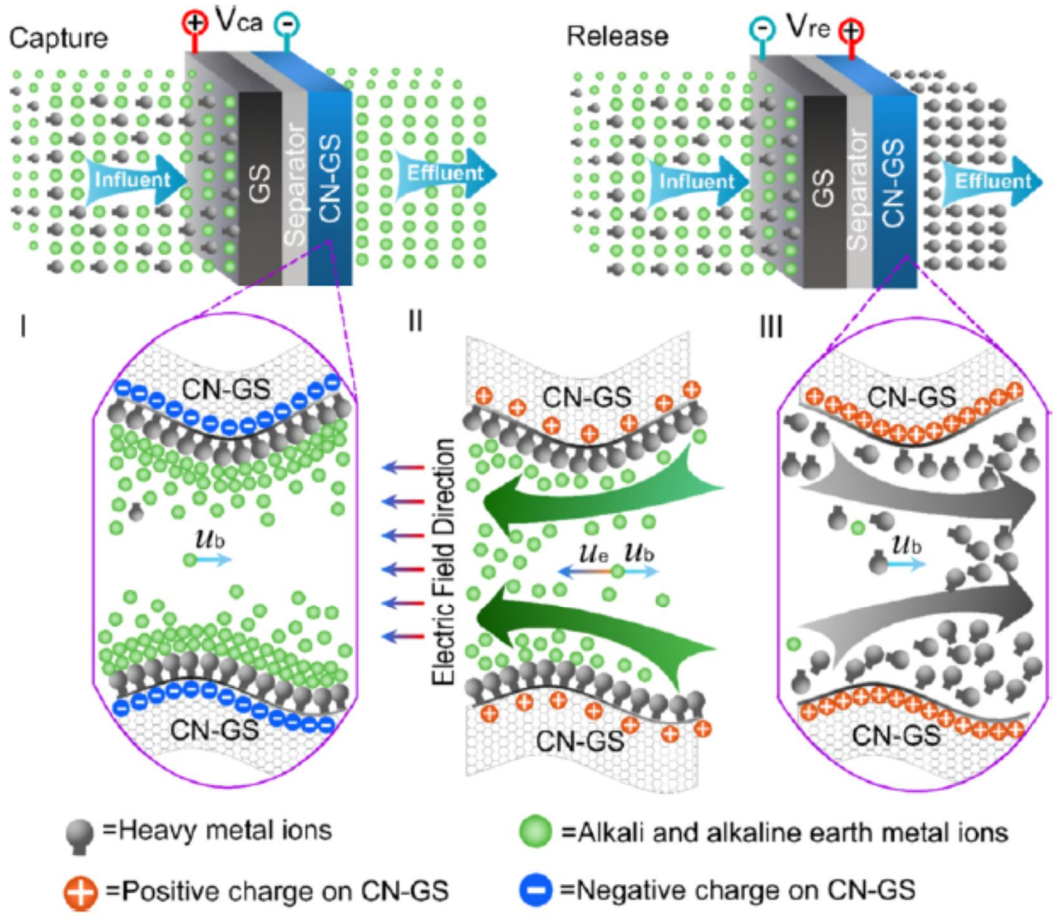

Figure II. 14 Schematics explaining the mechanism of the separation of aqueous metal ions using flow-through CDI system with N-doped graphene based electrode (Upper). Illustration of ion species during charging and discharging (Lower).

Prof. Yoon's group has constructed an aqueous battery desalination system and a hybrid CDI system using lithium manganese oxide electrode (Figure II. 15, (Kim et al. 2015b, Kim et al. 2017, Lee et al. 2013)). The electrode introduced in this study showed significant selectivity for Li ion compared to competitive ions such as Na, K, Mg and Ca through intercalation reaction. So far, lithium recovery have been conducted by the traditional systems based on the adsorption and sedimentation. According to their research results, the proposed system has overwhelmingly shortened the consumption time in recovering lithium compared to the traditional system. They also reported a battery desalination system showing sodium selectivity using a sodium manganese oxide electrode (Kim et al. 2017).

Wang et al. developed a selective electrode for nickel and copper extracting using an A-layered alpha-zirconium phosphate nanosheet and poly (2,6-pyridinedicarboxylic acid) as electrode materials, respectively (Wang et al. 2014a, Wang et al. 2014b). And, in the Ma group, a good CDI system was constructed showing good performance for Ca removal using zeolite as an electrode material (Liu et al. 2013). However, this study does not have the specific results of evaluating the selectivity of the solution mixed with two or more ions.

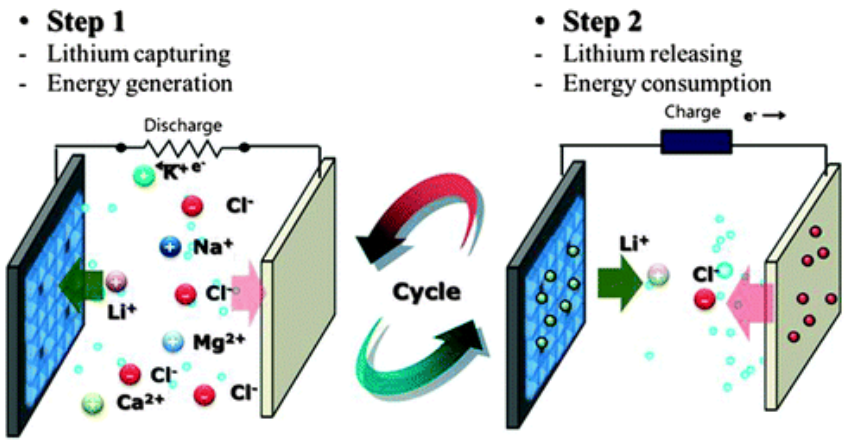

(a)

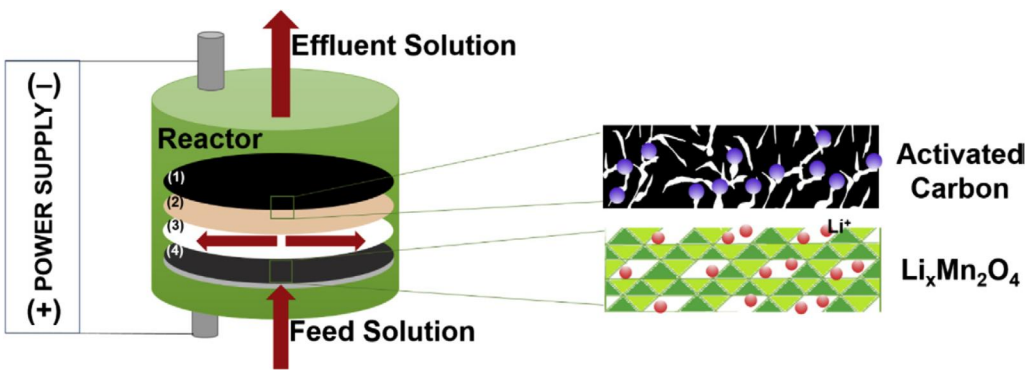

(b)

Figure II. 15 Illustrations of battery desalination system (a) and hybrid capacitive deionization system for lithium selective separation process (Kim et al. 2015b, Lee et al. 2013).

2.3.4. Application of CDI selectivity

Due to the ion removal selectivity, CDI have been expected to be used in a variety of applications for particular removal processes. First, the most active field using CDI selectivity would be the wastewater treatment process. The typical target material is nitrate ion (NO_3^-) (Farmer et al. 1996, Kim and Choi 2012, Kim et al. 2013b). CDI carbon electrode exhibited excellent selective removal characteristics for nitrate ion as compared with competitive ion such as chloride ion. Because it has been reported that the selectivity of nitrate ions in the carbon electrode is induced from the ion substitution (Kim and Choi 2012, Yeo and Choi 2013). However, as reported in some studies, the selectivity between chloride and nitrate ions was not evident in terms of removal rate capability (Chen et al. 2015, Li et al. 2016). Therefore, as reported by Choi, it seems advantageous to utilize nitrate selective ion exchange membranes and ion exchange materials to improve the rate capability.

Second, the application field of CDI selectivity is the hardness control process. Hardness-inducing species are typically Ca, Mg, Fe ions. Since they are all of the multivalent cations, the the CDI carbon electrode exhibit excellent selective removal characteristics due to Columbic interaction (Seo et al. 2010). However, it is speculated that the selectivity might be reduced by the introduction of the common IEM or ion exchanging polymer in the MCDI system. This is because, in

the case of the multivalent ions, the conductivity in the common IEM or ion exchange polymer is significantly lowered as compared with the monovalent ion (Svetličić and Konrad 1979). Therefore, IEMs and ion-exchange polymer materials that can maintain the ion-selective selectivity as much as possible should be utilized for effective hardness control.

Third, the application field of CDI selectivity is the resource recovery process. Typical target materials are lithium and copper ions (Li, Cu). Lithium ions can be removed with high selectivity in the hybrid CDI process using lithium manganese oxide as an electrode material (Kim et al. 2015b). Although copper ions have not been introduced in the CDI research, it is expected that poly (2,6-pyridinedicarboxylic acid) as an electrode material would exhibit high selective removal characteristics compared to the competitive ions (Na, K, Mg, Ca) (Wang et al. 2014b). The resource recovery process seems to have many aspects to be improved not only in materials but also in terms of systems. This is because not only removing the target ions from the raw water but also effectively concentrating the recovered ions in the other reservoir.

Fourth, toxic heavy metal ion removal process. The target material is Cd and Pb, etc (Ji et al. 2015). The targeted ions are removed by chelating properties of

the electrode as described in Section 2.3.3. In this study, the flow though CDI system was constructed by utilizing these electrodes.

3. Capacitive deionization with Ca-alginate coated-carbon electrode for hardness control

3.1. Introduction

Treating hard water is crucial in reducing industrial and domestic problems such as pipe clogging, membrane fouling, lime scaling in heaters, and decrease in cleaning efficiency (Gabrielli et al. 2006, Park et al. 2007). Chemical precipitation (Dean et al. 1972, Nagarajan and Paine 1984), ion-exchange process (resins) (Wiers et al. 1982), nanofiltration/reverse osmosis membrane techniques (Ghizellaoui et al. 2005, Hauck and Sourirajan 1969), and electrodialysis (Yeon et al. 2004) have been used as conventional technologies to control the hardness of water. These techniques inevitably require additional chemicals, intensive energy, and are, thereby, expensive (Song et al. 2005). Therefore, an environmentally benign, low cost and low energy consuming process is required to remove hard water minerals.

Recently, capacitive deionization (CDI) has been investigated in the demand for an efficient alternative to control hard water (Seo et al. 2010). CDI is a technology that removes ion species through electrochemical sorption/desorption on electrodes (Oren 2008, Porada et al. 2013, Suss et al. 2015b). As a potential is applied, an electric double layer forms on the surface of the electrodes to store oppositely charged ions. Recently, membrane assisted CDI (MCDI) system has

been emerged to enhance the performance of CDI (Biesheuvel and Van der Wal 2010). After Lee at al. reported on the superior desalination performance of MCDI (Lee et al. 2006), many studies have been actively conducted to improve operating conditions (García-Quismondo et al. 2013, Lee and Choi 2012, Zhao et al. 2012) and recovering the energy of the MCDI system (Długołęcki and van der Wal 2013).

However, commercially available ion exchange membranes (IEMs) are expensive and limit module assembly, which lowers the competitiveness of MCDI over conventional technologies (Kim and Choi 2010b). To overcome these limitations, various ion-exchange coating materials have been developed to achieve a similar phenomenon as that of IEMs resulting in an improved CDI performance. For example, polyvinyl alcohol/sulfosuccinic acid was cast as a cation exchange resin on a negative electrode which greatly advanced the CDI performance (Kim and Choi 2010b). Sulfonated or aminated polymer resins were coated on an electrode with the spray method by Lee et al. (Lee et al. 2011). In addition, Nie et al. utilized the electrodeposition method to coat polyacrylic acid as a cation exchanger achieving a good regeneration ability (up to 30 cycles) (Nie et al. 2012). Ion-exchange resin was also applied as polymeric binders (Liu et al. 2014). Nevertheless, the preparation and deposition of ion-exchange resins require hazardous chemicals (organic solvents, crosslinkers, etc.) and changes in process

parameters (pH, temperature, applied voltage, etc.). Therefore, for practical applications, the ion-exchange resin is recommended to be non-toxic, easy processability and high performance.

Alginate, an eco-friendly and low-cost ion exchange polymeric material (Sata 2004), can be simply changed into a gel form via calcium substitution reaction (Aslani and Kennedy 1996). Calcium alginate (Ca-alginate) is widely used as a clean material in food (Siragusa and Dickson 1992), medicine (Blandino et al. 1999, Yoshioka et al. 2003), wastewater treatment (Kim et al. 2013a), batteries (Kovalenko et al. 2011), and membranes (Sata 2004, Yang et al. 2000, Zhang et al. 1997). In addition, Ca-alginate is well known as an ion exchange material for multivalent cations that harden water (Chen et al. 2002, Chen and Wang 2001, Zhang et al. 1999). In this study, we propose Ca-alginate as a cation exchange coating material and used it in CDI and MCDI systems to control the hardness in water. The effect of the Ca-alginate coating was quantitatively analyzed by measuring the deionization capacity.

3.2. Materials & methods

3.2.1. Electrode preparation

The carbon electrode was fabricated with the following procedure (Kim et al.

2014, Kim and Yoon 2013). Activated carbon (MSP-20X, Kansai Coke and Chemicals, Japan), carbon black (Super P, TIMCAL Graphite & Carbon, Swiss), and polytetrafluoroethylene (PTFE, Sigma-Aldrich, USA) were mixed with a weight ratio of 86:7:7 to prepare the electrode. The mixture was blended in a few milliliters of ethanol for homogeneity and roll-pressed to make a sheet-type carbon electrode with a 300 μm thickness. The fabricated electrode was then dried in a vacuum oven at 120^{o}C for 12 h. After drying, the carbon sheet was cut into circular pieces with diameters of 18 and 20 mm. In the larger piece, a 4 mm diameter hole was made in the center for water passage. The two circular pieces were subsequently used for the electrochemical characterization and desalination performance test, respectively.

3.2.2. Calcium alginate coating on the carbon electrode

The fabricated carbon electrode was coated with Ca-alginate as following procedures. Sodium alginate powder (Sigma-Aldrich, USA) was dissolved in deionized (DI) water using a mechanical stirrer for 12 h (MS3040, MTOPS, Seoul, Republic of Korea). Various sodium alginate concentrations (3.5, 6.5, and 10wt%) were used, and unless mentioned otherwise, the experiments were performed with the 10wt%. The prepared sodium alginate solution was degassed for 6 h using

ultrasonicator (Ultrasonic cleaners, 1510E-DTH, Brason Ultrasonics, USA). The sodium alginate solution was cast on one-side of the carbon electrode with a casting knife (Elcometer, UK). The height of the casting knife was set at 350 μm. The cast electrode was then rapidly dipped in 2 M calcium chloride solution at room temperature (Sigma-Aldrich, USA) for 30 min. As the sodium ions in the sodium alginate solution were exchanged with calcium ions, the alginate solution changed to a gel phase (we will refer to calcium exchanged alginate as Ca-alginate). The Ca-alginate coated-electrode was fully rinsed with DI water and stored in DI water at room temperature for more than 12 h before use. It is noted that only about $6 per m^2 was consumed in the preparation of Ca-alginate coating. The final thickness of the Ca-alginate layer ranged from 90 μm (3.5wt%) to 140 μm (10wt%).

3.2.3. Characterization of the Ca-alginate layer

The physical and chemical properties of the Ca-alginate coating layer were investigated. The surface morphologies of the Ca-alginate coated electrode and carbon electrode were obtained with a scanning electron microscope (SEM, JSM-6700F, JEOL, Republic of Korea). The physical strength of the electrode was determined by measuring elongation at a break with a universal testing machine

(LS1SC, LLOYD Instruments, UK). The samples were fully dried and prepared to match the ASTM standard D638 (Type V dog-bone shaped samples; W = 3.18 ± 0.03 mm, L = 9.53 ± ± 0.08 mm, G = 7.62 ± 0.02 mm, and R = 12.7 ± 0.08 mm) (Testing and Materials 1998). Also, the surface hydrophilicity of the electrode was analyzed by the sessile drop method with a contact angle analyzer (DSA 100, KRUSS, Hamburg, Germany). The functional groups on the electrode surfaces were identified by ATR-FTIR (Attenuated total reflection Fourier transform infrared spectroscopy) (Nicolet spectrophotometer 5700, Thermo Electron, USA) with a wave number range of 4,000-650 cm^{-1}. The atomic composition was characterized by X-ray photoelectron spectroscopy (XPS) (SigmaProbe, Thermo VG, UK). The spectra were scanned from 0 to 999 eV in 1 eV steps. The Ca-alginate layer was fully rinsed with DI water to remove residual ions on the surface.

3.2.4. Electrochemical characterization of the Ca-alginate coated-electrode

Figure III. 1 describes the schematic of experimental cell to examine the electrochemical characteristics of Ca-alginate coated electrode. Cyclic voltammetry (CV), electrical impedance spectroscopy (EIS), and galvanostatic

charging/discharging were measured to determine the electrochemical properties of the electrodes by using a potentiostat (PARSTAT 2273, Princeton Applied Research, USA). The characterization cell consisted of an 18 mm diameter electrode, a graphite current collector and a cellulose nitrate separator (~110 µm thickness and ~0.45 µm pore size). CV and EIS were conducted in a three-electrode system with 1 M aqueous $CaCl_2$ electrolyte. Ca-alginate coated-electrode and pristine carbon electrode were used as the working electrodes. The pristine carbon electrode was used as the counter electrode, and an Ag/AgCl (sat. KCl) electrode was used as the reference electrode.

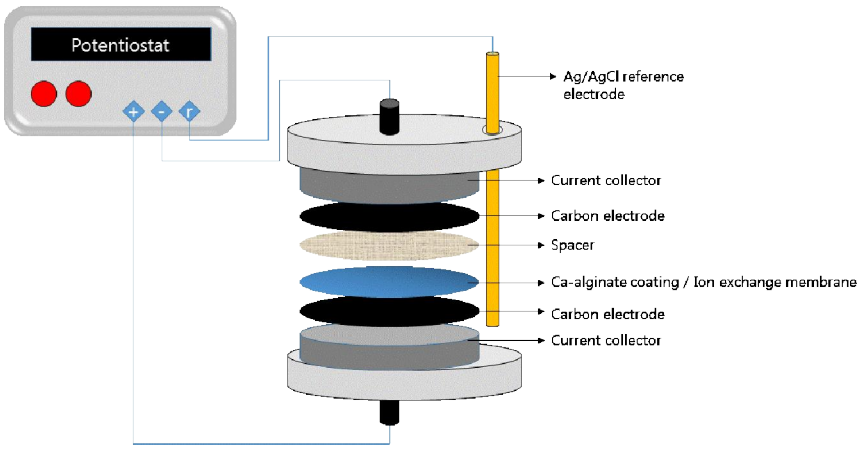

Figure Ⅲ. 1 Schematic of the experimental cell for the electrochemical characteristics of the Ca-alginate coating

CV measurements were made to calculate the change in specific capacitances of the electrodes. The scan rate was set as 2 mV/s with a potential range from 0 V (zero voltage) to 0.6 V (vs. Ag/AgCl sat. KCl). The specific capacitances of the electrodes were calculated from the specific current in the CV as in Eq. (2) (Bockris et al. 2001):

$$C = \frac{i}{vm} \tag{2}$$

where C is the specific capacitance (F/g), i is the current (A), v is the potential scan rate (V/s), and m is the total mass of the carbon electrodes (g).

The resistance of the Ca-alginate coating layer was determined with the EIS method. In this study, the impedance value at a higher frequency (100 Hz) was provided to measure the equivalent series resistance (ESR) comprised of the electrolyte solution, the Ca-alginate coating layer, and the electrodes (Kim and Choi 2010b). The impedance spectra were obtained at a frequency range from 100 Hz to 20 mHz at 0.0 V (Yoon et al. 2000). Since the ESRs were measured in the same electrolyte solution (1 M $CaCl_2$) and the electrode (carbon electrode), its difference was employed as the resistance of the Ca-alginate coating layer (R_m).

To determine the electrochemical stability of the Ca-alginate coated electrode, galvanostatic charge/discharge tests were conducted in a two-electrode

configuration. 1 M $CaCl_2$ solution was used as the electrolyte, and voltage profiles were obtained at a current density of 10.0 mA/cm^2 in a potential range from 0.0 to 0.6 V. Galvanostatic charge/discharge tests were performed for 400 cycles, and for each cycle, the normalized capacity and columbic efficiency were calculated. The normalized capacity was obtained according to Eqs. (4) and (5) (Lee et al. 2014) as follows:

$$C_n = \frac{2i\Delta t}{m\Delta V} \tag{4}$$

$$\text{Normalized capacity} = \frac{C_n}{C_o} \tag{5}$$

where C_n is the specific capacitance at the n^{th} cycle (F/g), C_0 is the specific capacitance at the first cycle (F/g), i is the current (A), Δt is the charging time (s), ΔV is the potential difference in the charging step (V), and m is the mass of the electrode (g).

3.2.5. Deionization performance test

Figure III. 2 describes the schematic assembly of the CDI with the Ca-alginate coated carbon electrode. The deionization performance was conducted in a

custom-made CDI system with graphite current collectors. The CDI consisted of the Ca-alginate coated electrode as a negative electrode, a pristine carbon electrode as a positive electrode and a nylon spacer. This system was referred to as Ca-alginate coated-CDI (CA-CDI). Experiments were carried out in single pass mode with a volumetric flow rate of 2 mL/min. 10 mM $CaCl_2$ was supplied as a representative hardness species. Ion adsorption (charging) and desorption (discharging) steps were performed with a cycler (WBCS3000, WonATech, Republic of Korea), which alternatingly applied a constant voltage of 1.2 V and 0 V (zero voltage) for 10 min each, respectively. These processes were repeated for 3 cycles to reach a steady-state. During the operation, the conductivity of the treated outlet stream was monitored with a flow-type conductivity meter (3583-10C, HORIBA, Japan). From the conductivity of the solution, we could deduce the concentration of $CaCl_2$. As a comparison, an identical test was performed with a pristine CDI system. Additionally, an MCDI system with a Ca-alginate coated-electrode and AEM (CA-MCDI) was prepared and compared to a conventional MCDI system. The conventional MCDI was assembled with carbon electrodes with CEM and AEM (CMX and AMX Neosepta, ASTOM, Japan). Note that the CEM and AEM used in this study are representative commercial membranes, which have excellent ion-exchange performance and have already been actively applied in various MCDI researches (Kim and Choi 2010a, Omosebi et al. 2014,

Zhao et al. 2012). In addition, we used MCDI without CEM as another comparison (denoted as half MCDI).

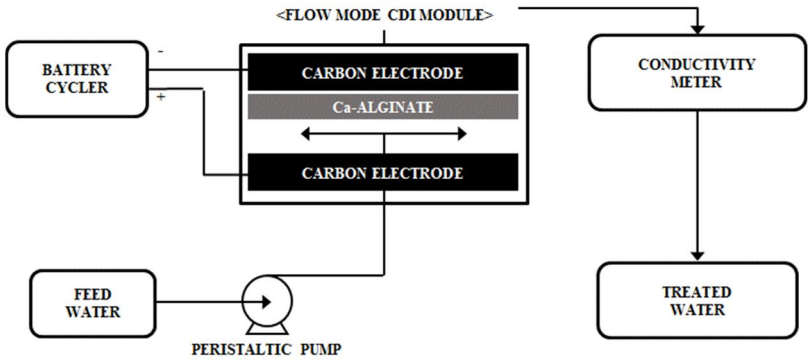

Figure III. 2 Schematic of capacitive deionization with the Ca-alginate coated cathode.

In this study, the deionization capacity (mg/g) was calculated from the integration of the conductivity change during the charging step in the 3rd cycle (Kang et al. 2014, Kim et al. 2014, Kim and Yoon 2013) shown in Eq. (6):

$$\text{Deionization capacity} = \frac{M_w \times \int (C_i - C_0)\Phi dt}{M_e} \quad (6)$$

where M_w is the molecular weight of $CaCl_2$ (g/mole), C_i and C_0 are the influent and effluent concentration (mM), respectively, during the charging step. Φ is the flow rate (mL/min), and M_e is the total mass of the electrodes (g).

The charge efficiency was then obtained from the deionization capacity and current profile (Kang et al. 2014, Zhao et al. 2012). The representative results from duplicate or triplicate experiments are presented with the standard deviation in this work.

3.2.6. Ion selective removal test

A selective ion removal test was conducted in similar conditions as described in 3.2.4 with mixed feed solutions of 5 mM $CaCl_2$ and 5 mM NaCl. During the third charging step, the effluent was sampled to analyze its ion composition by ion chromatography to quantify the ion selectivity (DIONEXICS-1100, Thermo-

Fisher Inc., Republic of Korea). The deionization capacity was calculated by integrating the ion concentration profile of the effluent at charging step of the 3rd cycle. For practical application, same test was performed with the synthetic hard water which has similar cationic composition of ground water in Yemen (Ca: 6.47 mM, Na: 1.19 mM, Mg: 0.98 mM, K: 0.11 mM) (Wadie and Abuljalil 2010).

3.3. Results and Discussion

3.3.1. Characteristics of the Ca-alginate coated-electrode

Figure III. 3 (a) - (c) show the top and cross-sectional morphology of the pristine and Ca-alginate coated-carbon electrode pictured with scanning electron microscope (SEM). As shown in Figure III. 3 (a) and (b), it was observed that the rough surface of the pristine carbon electrode was covered by the Ca-alginate layer. In Figure III. 3 (c), the Ca-alginate was well adhered to the carbon surface with an 80 μm thick dried-Ca-alginate layer. A fully swelled-Ca alginate layer had a thickness of 140 – 160 μm which is similar to the thickness of the commercial cation exchange membrane used in this study. It is noted that the percentage increase of total elongation at fracture increased from 26% (pristine electrode) to 44% (Ca-alginate coated-electrode) after coating Ca-alginate on the activated carbon surface, indicating the improvement in physical strength.

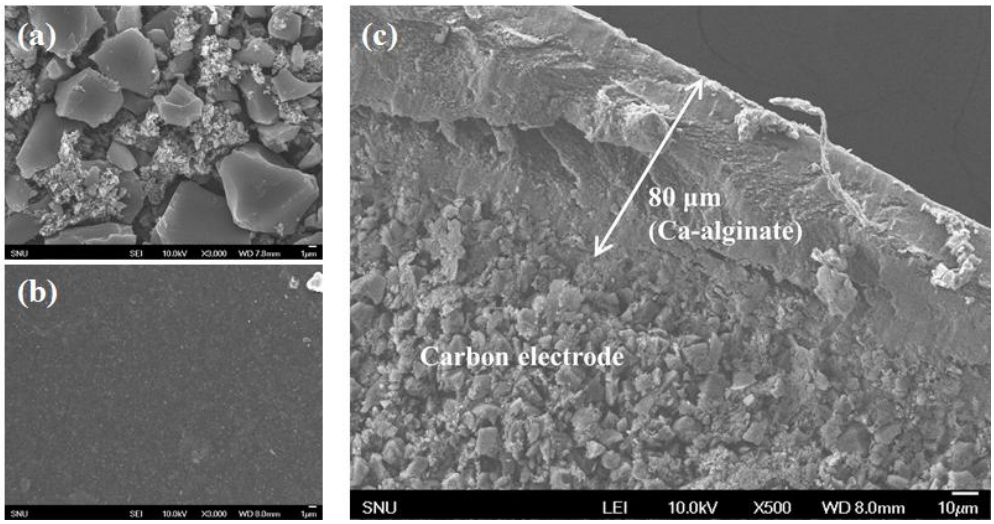

Figure III. 3 Morphology of the Ca-alginate coated carbon electrode analyzed by scanning electron microscope (SEM), top view images of (a) pristine carbon electrode, and (b) Ca-alginate coating layer and (c) cross-section image (thickness of Ca-alginate: ~80 µm).

Figure III. 4 (a) - (e) present the surface characterization of the pristine and Ca-alginate coated-electrode, in which the chemical/electrochemical properties were studied with ATR-FTIR, XPS, contact angle, and CV. Figure III. 4 (a) shows the ATR-FTIR spectra with a range of 4,000 - 650 cm^{-1} confirming the presence of an acetate group. In Figure III. 4 (a), an intensive peak at 1026 cm^{-1} and a broad peak range of 3,500 - 3,000 cm^{-1} were observed, which indicate the typical stretching bands of a C-O single bond and -OH bond, respectively. In addition, the C=O stretching bands of the acetate group in the alginate were observed with a strong peak at 1,620-1,575 cm^{-1}. Thus, the presence of a carboxyl group was confirmed in Ca-alginate and is expected to provide cation-exchanging properties at a neutral pH (Schafer 1970). On the other hand, in the pristine carbon electrode, no specific functional group was observed.

Figure III. 4 (b) presents the XPS spectrum of the Ca-alginate layer. As shown in Figure III. 4 (b), the alginate layer captured divalent cation such as Ca^{2+}, while it did not allow anions such as Cl^- to remain in the polymer chain. For instance, intensive peaks indicating carbon (284.80, 286.30, and 287.95 eV), oxygen (531.59 and 532.91 eV), and calcium (288.94 eV) were distinctively detected. Quantitatively, 2.3% of the calcium and a negligible chloride content (0.1%) were found in the Ca-alginate layer. Note that the chloride ion was the only anion in the procedure for the Ca-alginate coating. Overall, as shown in Figure III. 4 (a) and

(b), the Ca-alginate layer well contained the properties of a cation exchange material.

Figure III. 4 (c) and (d) show the contact angle images of the pristine carbon electrode and Ca-alginate coated-electrode, respectively. The hydrophobicity of the electrode dramatically decreased through the Ca-alginate coating. The contact angle value was significantly reduced from 125° to 27°. Ca-alginate, a well-known hydrophilic material, contributed to wetting on the carbon electrode surface which could be one of the positive effects on the CDI performance (Kim et al. 2014).

In addition, Figure III. 4 (e) shows the cyclic voltammogram (CV) of the Ca-alginate coated carbon electrode and the pristine carbon electrode within a potential window of 0 - 0.6 V. Both displayed a rectangular shaped CV which is a typical representative charge/discharge voltammogram of a capacitor indicating no charge transfer reaction within the 0 - 0.6 V potential range.

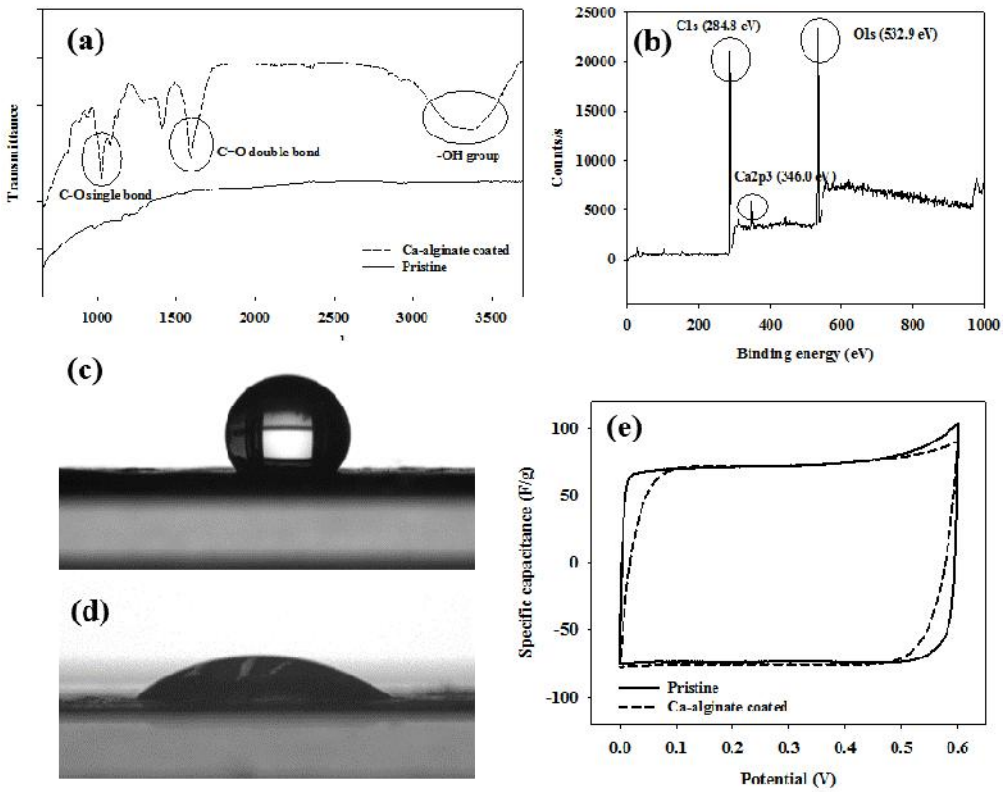

Figure III. 4 Surface characterization of the Ca-alginate coated-carbon electrode analyzed by (a) Attenuated total reflectance (ATR)-Fourier transform infrared spectroscopy (FTIR), (b) X-ray photoelectron spectroscopy (XPS) and (c, d) contact angle ((c) pristine and (d) Ca-alginate coated electrode), and (e) Cyclic voltammogram (2 mV/s, Electrolyte: 1 M $CaCl_2$, Potential range: 0 – 0.6 V, Ref.: Ag/AgCl (Sat' KCl), 25 ± 1^{o}C)

3.3.2. Deionization performance

Figure III. 5 (a) - (c) show the representative conductivity profile, deionization capacity, and current profile of the CA-CDI compared with those of the CDI. The deionization capacities (Figure III. 5 (b)) were obtained from the effluent conductivity profiles in Figure III. 5 (a) by Eq. (6). As shown in Figure III.5 (b), the CA-CDI demonstrated notable deionization performance for hardness species (Ca^{2+}) compared to the control CDI, while consuming a similar amount of current in both systems (Figure III. 5 (c)). For example, as shown in Figure III. 5 (b), the deionization capacity of the CA-CDI was 14.2 mg/g while only 9.8 mg/g for CDI, indicating that CA-CDI allocated the charges more efficiently than CDI by calculating the charge efficiency. More specifically, the charge efficiency of CDI (55 ± 3%) improved upto 85 ± 6% for the CA-CDI (Figure III. 5 (b) and (c)). Additionally, the deionization capacity and the charge efficiency were increased with the increase in the concentration of the alginate solution as shown in in Figure III. 6.

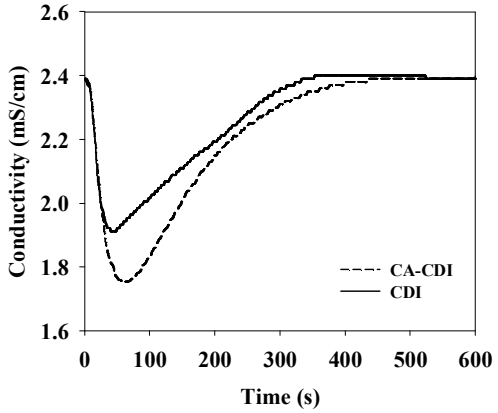

(a)

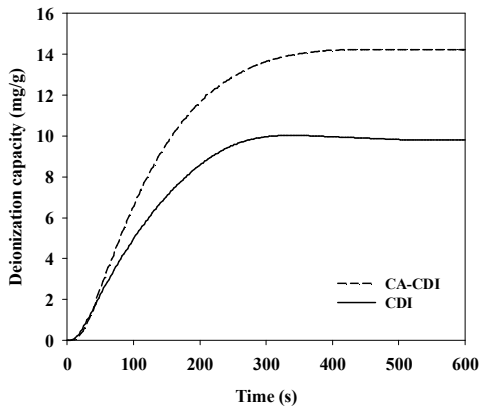

(b)

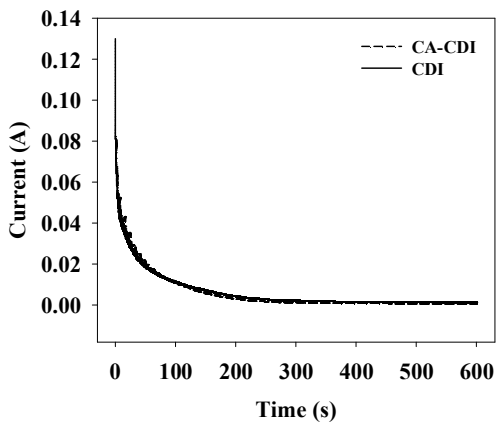

(c)

Figure III. 5 Conductivity profile (a), deionization capacity (b) and consumed current (c) of Ca-alginate coated CDI (CA-CDI) compared with the control CDI with time (10 mM $CaCl_2$, Charging/Discharging: 1.2 V/0 V (zero voltage) 10 min, 2 mL/min, 25 ± 1^{o}C, sodium alginate solution: 10wt%).

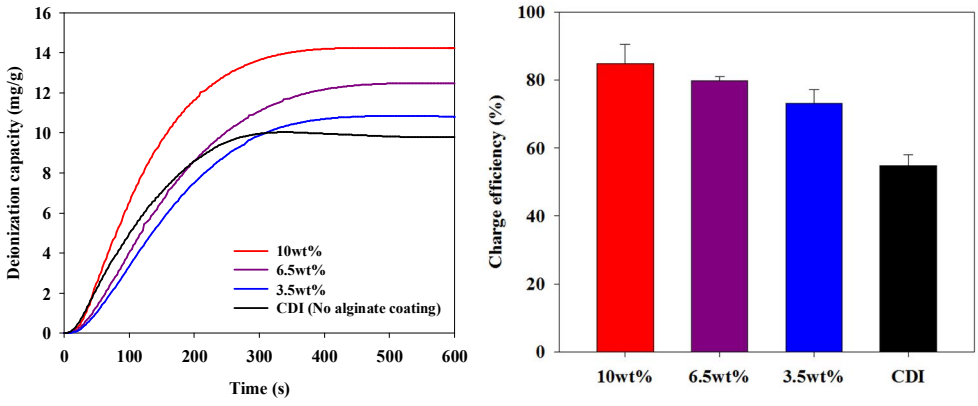

(a) **(b)**

Figure III. 6 (a) Deionization capacity and (b) charge efficiency of Ca-alginate coated asymmetric CDI (CA-CDI) with varying alginate solutions (from 3.5wt% to 10wt%) in comparison with those of conventional CDI (10 mM $CaCl_2$, Charging/Discharging, 1.2 V/0 V 10 min, 2 mL/min, 25 ± 1°C).

Figure III. 7 shows the deionization capacity of the CA-MCDI (Ca-alginate/AEM) compared to that of the MCDI (CEM/AEM) and half MCDI (CEM only). For comparison purposes, the deionization capacity of the CA-CDI (Ca-alginate) from Figure III.5 is shown in Figure III. 7. Based on the results in Figure III. 7, two important observations can be made. First, CA-MCDI showed that Ca-alginate coating showed the comparable deionization performance with commercial CEM in MCDI system. For instance, CA-MCDI and MCDI showed a similar deionization capacity of 15.6 mg/g and 15.1 mg/g, respectively, for 10 min charging. Also the charge efficiency of the CA-MCDI (95 ± 2%) was higher than that of the MCDI (88 ± 2%) (refer to Figure III. 8). Second, the CA-CDI showed a slightly higher deionization performance than the half MCDI. For example, CA-CDI had a deionization performance of 14.2 mg/g and a charge efficiency of 85 ± 6% while half MCDI cell had respective performances of 12.0 mg/g and 73 ± 3%. In addition, the CA-MCDI not only effectively controlled the Ca^{2+} ions but also removed other divalent ions such as Zn^{2+} and Mn^{2+} (refer to Figure III. 9). Moreover, the MCDI system with Ca-alginate coated-electrode showed excellent stability which was evaluated by galvanostatic charge/discharge test. For example, 97% of the specific capacity and 99% of the columbic efficiency were retained for 400 cycles (refer to Figure III. 10).

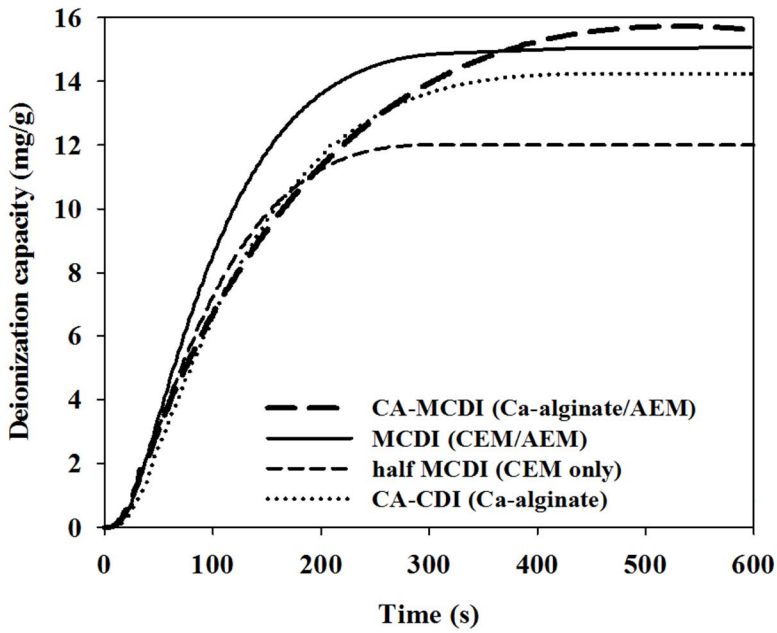

Figure III. 7 Deionization capacity of the Ca-alginate coated membrane CDI (CA-MCDI), MCDI, Ca-alginate coated CDI (CA-CDI), and half MCDI (10 mM $CaCl_2$, Charging/Discharging: 1.2 V/ 0 V (zero voltage) 10 min, 2 mL/min, 25 ± 1^{o}C, sodium alginate solution: 10wt%).

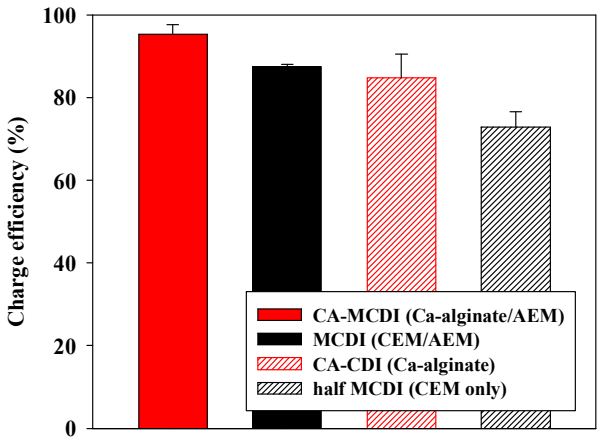

Figure III. 8 Charge efficiency of Ca-alginate coated asymmetric membrane CDI (CA-MCDI), MCDI, Ca-alginate coated asymmetric CDI (CA-CDI), and half MCDI (10 mM $CaCl_2$, Charging/Discharging, 1.2 V/0 V 10 min, 2 mL/min, 25 ± 1^{o}C, sodium alginate solution: 10wt%).

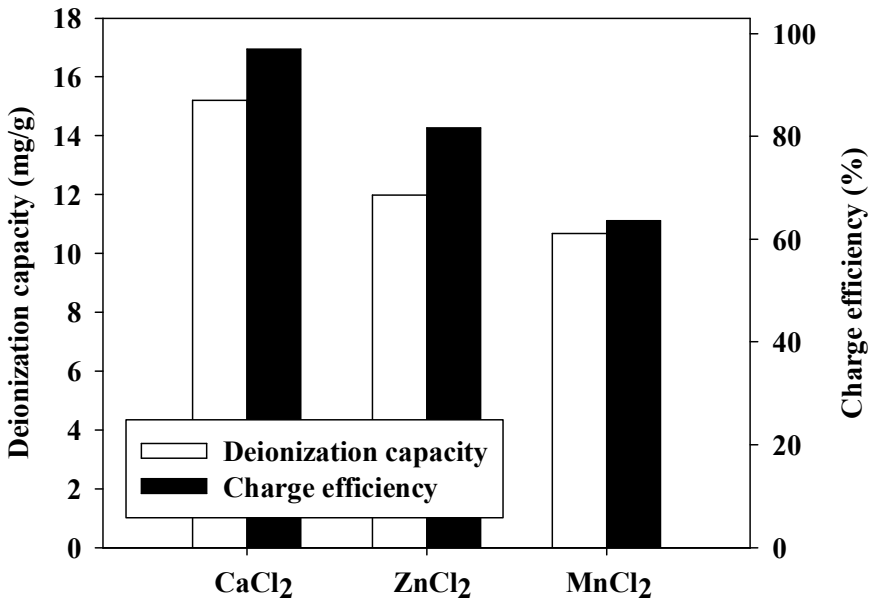

Figure III. 9 Deionization capacity and charge efficiency of Ca-alginate coated asymmetric membrane CDI (CA-MCDI) as the feed solution varied with Ca^{2+}, Mn^{2+}, and Zn^{2+} containing solution, respectively (10 mM feed solution of $CaCl_2$, $MnCl_2$, and $ZnCl_2$), Charging/Discharging: 1.2 V/0 V 10 min each 3 cycle, 2 mL/min, 25 ± 1°C).

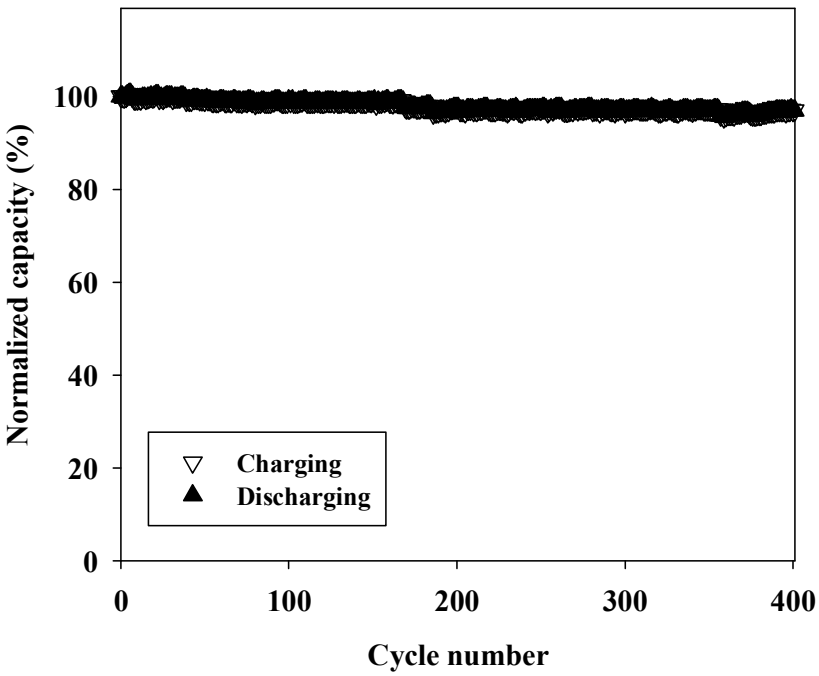

Figure III. 10 Normalized charge and discharge capacity of CA-MCDI for 400 cycles (Electrolyte: 1 M $CaCl_2$, Potential range: 0 – 0.6 V, Ref.: Ag/AgCl (Sat' KCl) Current density: 10 mA/cm^2, 25 ± 1^oC).

3.3.3. Deionization performance with a mixed solution

Figure III. 11 (a) and (b) indicate the cation concentration of Na^+ and Ca^{2+} in the effluent and their corresponding deionization capacity with time, respectively. In Figure III. 11 (b), the cumulative individual cation deionization capacity with respect to time was calculated from Figure III. 11 (a) to analyze selective performances, quantitatively. From Figure III. 11 (a) and (b), two important observations can be obtained. First, Ca^{2+}, a representative hardness species, was efficiently removed compared to Na^+ in the CA-MCDI, showing that the CA-MCDI operates well in hard water that contains Na^+ ions. According to Figure III. 11 (b), for the same charging period, 0.12 mmole/g of Ca^{2+} and 0.04 mmole/g of Na^+ were removed. This result can be explained by the difference in Coulombic interaction (charge valence and hydrated radius). More Ca^{2+} ions migrated towards the negative electrode as a result of a stronger attractive force exerted on the divalent cation (Ca^{2+}) than on the monovalent cation (Na^+). This tendency was also found in CDI system without ion exchange materials (refer to Figure III. 12) where more multivalent cations were adsorbed onto the carbon electrode. On the other hand, magnesium ion which is one of hardness components is reported to have similar deionization trend with calcium ion since magnesium has same charge valence and similar hydrated radius with calcium ion. In the synthetic hard water with more cation species (Wadie and Abuljalil 2010), CA-MCDI showed

stronger affinity towards hardness species such as divalent cation as well, indicating that this system is practically applicable (refer to Figure III. 13). Second, as shown in Figure III. 11 (b), it is interesting to observe that in a multi cationic solution, each deionization capacity did not stabilize even after 8 min. This result is explained as follows. Ca^{2+} gradually substituted the adsorbed Na^{+} as a result of the higher selectivity of Ca^{2+} over Na^{+} (Seo et al. 2010).

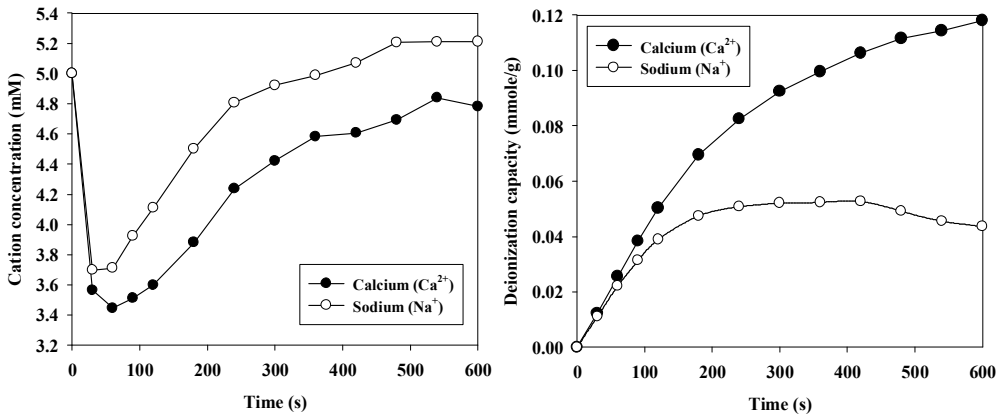

(a) (b)

Figure III. 11 Deionization performance of Ca-alginate coated MCDI (CA-MCDI) expressed as (a) cation concentration of effluent and (b) selective deionization capacity in a mixed feed solution of 5 mM $CaCl_2$ and 5 mM NaCl (Charging/Discharging: 1.2 V/ 0 V (zero voltage) 10 min 3 cycle, 2 mL/min, 25 ± 1^{o}C, sodium alginate solution: 10wt%).

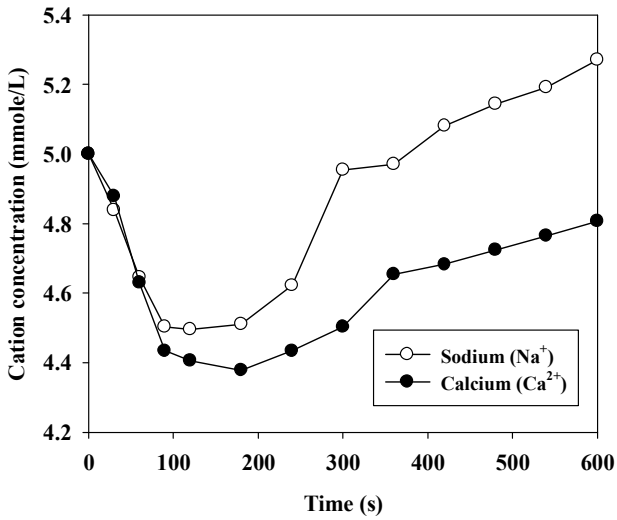

Figure III. 12 Deionization performance of Ca-alginate coated asymmetric MCDI (CA-MCDI) expressed as cation concentration of effluent in a mixed feed solution of 5 mM $CaCl_2$ and 5 mM NaCl (Charging/Discharging: 1.2 V/0 V 10 min 3 cycle, 2 mL/min, 25 ± 1^oC, sodium alginate solution: 10wt%).

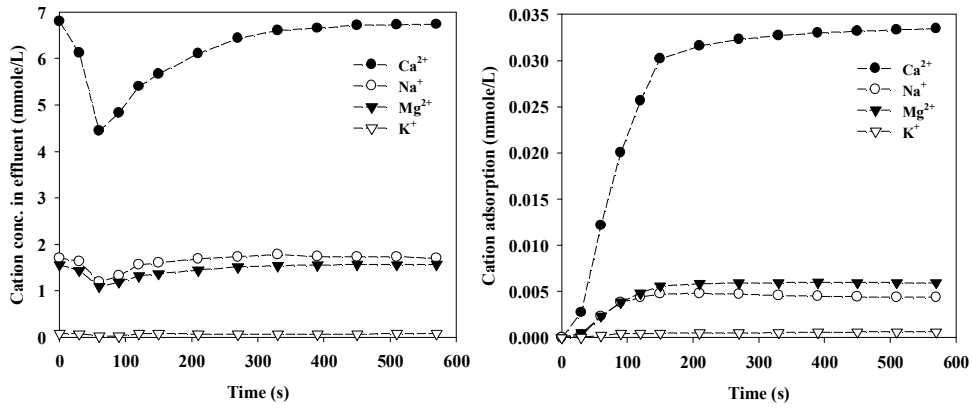

(a) (b)

Figure III. 13 Deionization performance of Ca-alginate coated asymmetric MCDI (CA-MCDI) expressed as (a) cation concentration of effluent and (b) selective deionization capacity in a synthetic hard water (Discharging: 1.2 V/0 V 10 min 3 cycle, 2 mL/min, 25 ± 1°C, sodium alginate solution: 10wt%, pH: 7.8, Cationic composition in feed: Ca: 6.47 mM, Na: 1.19 mM, Mg: 0.98 mM, K: 0.11 mM).

3.4. Summary

In this study, Ca-alginate, a cation exchange material, was successfully applied in CDI and MCDI systems to treat hard water. Ca-alginate coated electrode assembled CDI demonstrated superior enhancement in deionization capacity and excellent charge efficiency compared to the conventional CDI. Moreover, CA-MCDI displayed comparable performance to conventional MCDI system with good stability and selectivity for hardness species, indicating that Ca-alginate can be an appropriate alternative to commercial cation exchange membrane. In conclusion, Ca-alginate is speculated as an appropriate material for CDI system to control hardness in water.

4. Hybrid capacitive deionization with Ag coated carbon composite electrode

4.1. Introduction

Capacitive deionization (CDI) is an alternative desalination technology based on electrochemical adsorption/desorption (Porada et al. 2013, Suss et al. 2015a). CDI stores ionic species in the electrical double layer (EDL) formed on the surface of electrodes. CDI has been gaining attention for its high energy-efficiency especially in deionizing low-grade saline water (Anderson et al. 2010, Zhao et al. 2013). Thus, various applications have been reported such as brackish water desalination (Xu et al. 2008), distilled water production (Lee and Choi 2012), wastewater treatment (Lee et al. 2006), and hardness control (Seo et al. 2010, Yoon et al. 2016).

However, CDI still has an intrinsic limitation regarding the low capacity of the electrode because traditional CDI electrodes store ions only in the EDL at the surface of the electrodes. There have been several approaches to improve the CDI performance. For example, CDI electrode materials were developed to have a large surface and hierarchically porous structure (El-Deen et al. 2014, Kim and Yoon 2013, Leonard et al. 2009, Li et al. 2010, Mayes et al. 2010, Wimalasiri and Zou 2013, Yang et al. 2014, Zhang et al. 2012a, Zhang et al. 2012b). In addition, novel innovative CDI systems such as membrane assisted CDI (MCDI), inverted-

CDI and Flow-CDI have been introduced (Gao et al. 2015, Jeon et al. 2013, Lee et al. 2006, Lee et al. 2011, Liu et al. 2014, Park and Choi 2010).

Recently, hybrid capacitive deionization (HCDI) was reported opening new stage of CDI technology (Lee et al. 2014). HCDI is an asymmetric system consisting of two different types of electrodes: a capacitive electrode from CDI and a battery electrode from a battery desalination system (Pasta et al. 2012). In the battery electrode where sodium manganese oxide, manganese dioxide-carbon composite, sodium iron pyrophosphate, silver nanoparticles, and MoS_2 have been employed (Kim et al. 2016b, Lee et al. 2014, Liu et al. 2016, Tsai and Doong 2016, Xing et al. 2017, Yang et al. 2011), the ions are stored through the charge transfer reaction, which contributes to the large amount of electrical capacity. Indeed, HCDI demonstrated superior deionization capacity compared to the conventional CDI (Lee et al. 2014). Although not in HCDI, MXene and nickel hexacyanoferrate were used as battery materials for CDI and cation intercalation desalination, respectively (Porada et al. 2016, Srimuk et al. 2016). However, no researches in HCDI field have been reported using a Ag-carbon composite electrode which has both the characteristics of a battery and a capacitor as one of the electrodes in the system.

Here, new HCDI with an Ag-coated carbon composite electrode (Ag coated HCDI) is proposed where this composite electrode has the characteristics of a battery and a capacitor together (Figure IV. 1). The Ag coated carbon composite electrode is fabricated by coating Ag onto the capacitive carbon electrode so that it has both characteristics of a battery and a capacitor. In this study, as a battery composite material, Ag was chosen due to its anion capturing ability through the charge transfer reaction ($Ag + Cl^- \leftrightarrows AgCl + e^-$) and electrochemical stability of Ag in an aqueous system with a large amount of electrical capacity (Bates et al. 1956). Since Ag is an expensive rare metal, small amount of Ag was deposited onto the capacitive carbon electrode with a photo induced reduction (Liao et al. 2010, Shi et al. 2004).

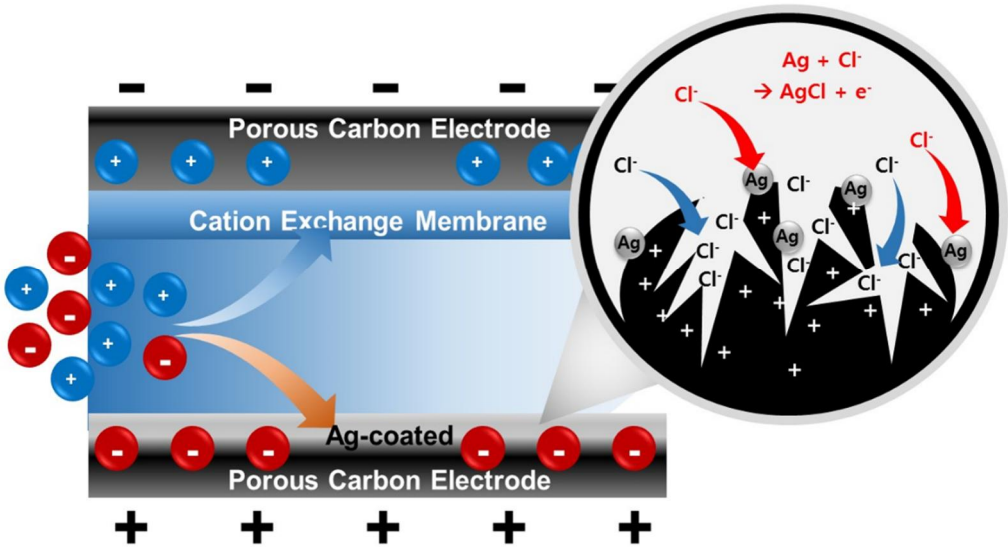

Figure IV. 1 Schematic of HCDI with Ag-coated carbon composite electrode (Ag coated HCDI)

4.2. Materials & methods

4.2.1. Preparation of the capacitive carbon electrode

The carbon electrode was fabricated as previously described (Kim and Yoon 2013, Lee et al. 2014, Yoon et al. 2016). Activated carbon (YP50, Kuraray Chemical Co, Japan), carbon black (super P, TIMCAL Graphite & Carbon, Swiss), and polymeric binder (polytetrafluoroethylene, Sigma-Aldrich, USA) were mixed to prepare the electrode. The mixture was blended and roll-pressed to make a sheet-type carbon electrode.

4.2.2. Silver coated carbon composite electrode

The Ag coated carbon composite electrode was prepared by ultraviolet radiation and Ag reduction (refer to Figure IV. 2 for the details). The carbon electrode was radiated for 30 min with UV-C (TUV 8W G8 T5, Philips, USA) in a solution of $AgNO_3$ varied from 3 to 100 mM. Unless mentioned otherwise, the concentration of $AgNO_3$ was 50 mM. Subsequently, the electrode was immersed into 0.1 M NaOH for few seconds and was immediately rinsed with deionized water. The electrode was then dried in a vacuum oven at 120^{o}C.

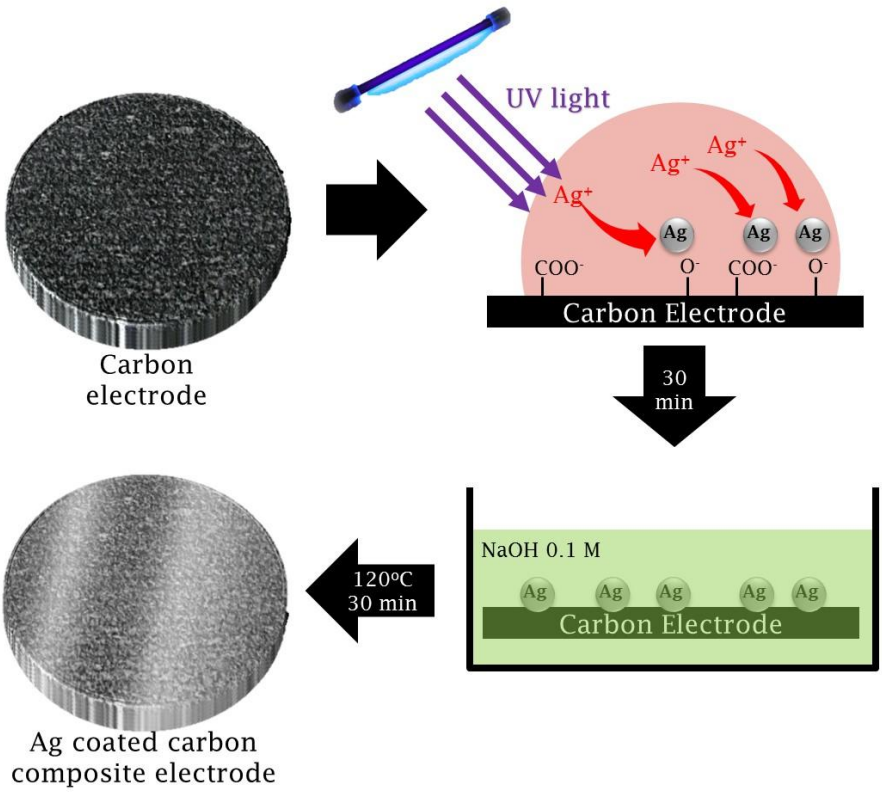

Figure IV. 2 Procedure for fabricating the Ag coated carbon composite electrode with UV radiation using the carbon electrode in this study.

4.2.3. Characterization of the Ag coated CDI carbon electrode

The surface morphologies and atomic composition of the Ag coated carbon composite electrode were obtained with a scanning electron microscope (SEM-EDX, JSM-6700F, JEOL, Japan). Pore volume and specific surface area were measured according to the Brunauer–Emmett–Teller (BET) equation (ASAP 2010, Micromeritics Instrument Corp., USA). The surface hydrophilicity of the electrode was analyzed by the sessile drop method with a contact angle analyzer (DSA 100, KRUSS, Hamburg, Germany).

Cyclic voltammetry (CV) and galvanostatic charging/discharging were measured with a potentiostat (PARSTAT 2273, Princeton Applied Research, USA) to determine the electrochemical properties of the electrodes. A characterization cell was used as previously described (Yoon et al. 2016). A pristine carbon electrode and an Ag/AgCl (sat. KCl) electrode were used as the counter electrode and the reference electrode, respectively. The scan rate (v) was set at 2 mV s^{-1}. The specific capacity (mAh g^{-1}) was measured from the galvanostatic charging/discharging profile in a 3-electrode system. The galvanostatic profile was obtained with a current density of 0.5 mA cm^{-2}. The potential range was -0.10 ~ 0.25 V.

In addition, the electrochemical stability of the specific capacity was evaluated

in a two-electrode system. 2 M NaCl was used as an electrolyte. The current density was set at 10 mA cm^{-2} in a potential range from zero to 0.7 V.

Galvanostatic charge/discharge tests were performed, and for each cycle, the capacity retention ratio and the coulombic efficiency were calculated as follows (Eqs. (1) and (2)) (Lee et al. 2014, Yoon et al. 2016):

$$\text{Capacity retention ratio} = \frac{C_i}{C_0} \left(C_i = \frac{2I \cdot \Delta t_i}{m \cdot \Delta V_i}\right) \quad (1)$$

$$\text{Coulombic efficiency} = \frac{C_{i,d}}{C_{i,c}} \quad (2)$$

, where C_i is the specific capacity at the i^{th} cycle (mAh g^{-1}); C_0 is the specific capacity at the first cycle (mAh g^{-1}); $C_{i,c}$ and $C_{i,d}$ are the specific capacity at the charing and discharging in the i^{th} cycle (mAh g^{-1}); I is the current (A); Δt_i is the charging time at the i^{th} cycle (s); ΔV_i is the potential difference at the i^{th} cycle (V); and m is the mass of the electrode (g).

4.2.4. Deionization performance test

The deionization performance was evaluated with a lab-scale CDI system as previously described (Kim and Yoon 2013, Lee et al. 2014, Yoon et al. 2016). The deionization capacity, deionization rate, and charge efficiency were measured to

examine the CDI performance.

The Ag coated HCDI was assembled with the Ag coated carbon composite electrode (anode), pristine carbon electrode (cathode) and cation exchange membrane (CEM) (CMX, ASTOM corp., Japan). A CDI with a CEM system was used as the control assembled with a pair of pristine carbon electrodes and one CEM. A conventional MCDI, assembled with a pair of pristine carbon electrodes, a CEM, and an anion exchange membrane, was also compared with the Ag coated HCDI. The diameter of the electrode in test cell was 2 cm. As a feed solution, 10 mM NaCl solution was used with a flow rate of 2 mL min^{-1}. The Ag coated HCDI was evaluated under a constant voltage operation (WBCS3000, WonATech, Korea). 0.7 V charging /-0.7 V discharging condition was chosen taking into consideration its charge efficiency with respect to the applied voltage (refer to the details in Figure IV. 3). Note that the 1.2 V operation as a typical condition for CDI and MCDI was chosen for comparison in this study (Zhao et al. 2012).

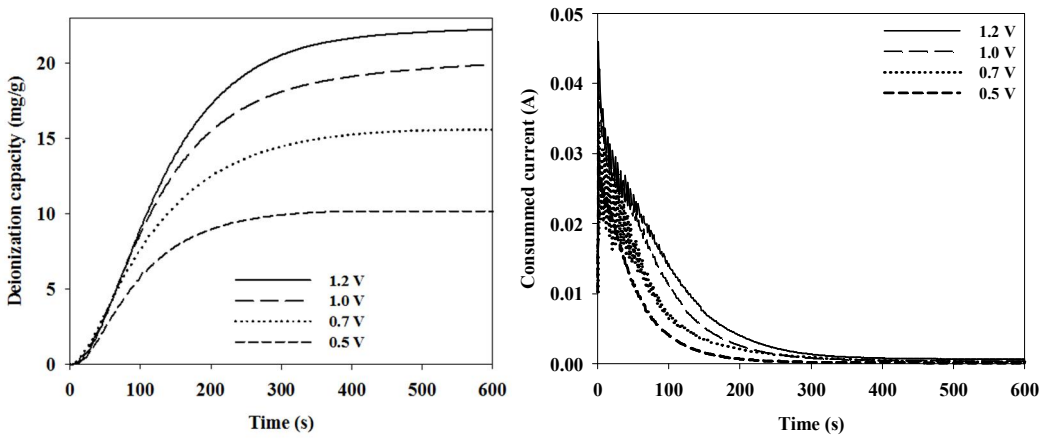

(a) (b)

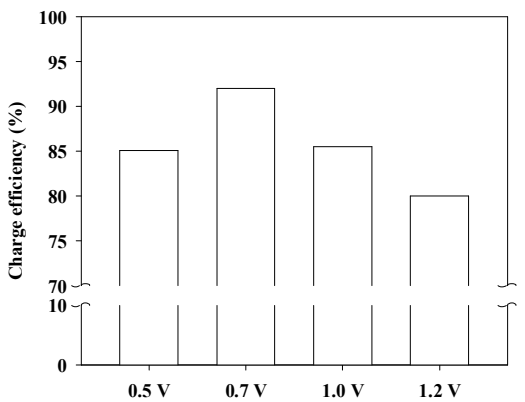

(c)

Figure IV. 3 (a) Deionization capacity, (b) consumed current, and (c) charge efficiency of the Ag coated HCDI with respect to the applied voltage (Charging/Discharging: 0.5 V~1.2 V / -0.5 V~ - 1.2 V, 10 mM NaCl, 2 mL min^{-1}, 25 ± 1°C).

The conductivity of the treated outlet stream was monitored with a flow-type conductivity meter (3583-10C, HORIBA, Japan) to deduce the deionization capacity and rate (Kim et al. 2016b, Lee et al. 2014). The charge efficiency is the deionization capacity divided by the consumed current shown in Eq (3):

$$\text{Charge efficiency (\%)} = \frac{\int (C_i - C_0) \cdot \Phi \cdot dt \cdot F}{\int I \cdot dt} \quad (3)$$

, where C_i and C_0 are the influent and effluent concentration (mM), respectively, during the charging step. Φ is the flow rate (mL min^{-1}); I is the consumed current (A); and F is the faradaic constant (96485 C $mole^{-1}$).

In addition, the energy consumption per removed ions was calculated with Eq (4):

$$\text{Energy consumption (kJ mole}^{-1}) = \frac{V \cdot \int I \, dt}{\int (C - C_0) \cdot \Phi \cdot dt} \quad (4)$$

, where V is the applied voltage (V); I is the consumed current (A); t is the time (s); C is the NaCl concentration in the outlet (M); C_0 is the NaCl concentration in the inlet (M); and Φ is the flow rate (mL min^{-1}).

The concentration in the effluent of total Ag was measured with an inductively coupled plasma atomic emission spectrometer (ICPS-8100, SHIMADZU, Japan).

4.2.5. Performance test of Ag coated HCDI with real river water

For practical application, Ag coated HCDI was tested with the water from the Ilkwang River (Busan, Republic of Korea) (Lee et al. 2017). The river water had a concentration of 73.9 meq L^{-1} (Na^{+}: 60 mM; K^{+}: 4.5 mM; Mg^{2+}: 3.5 mM; Ca^{2+}: 1.2 mM). The feed was pre-filtered prior to use. The diameter of the electrode for this test cell was 5 cm. Flow rate was set as 5 mL mi^{-1}n. During the charging step, the deionization capacity for each ions was analyzed by ion chromatography (DIONEXICS-1100, Thermo-Fisher Inc., Republic of Korea).

4.3. Results and Discussion

Figure IV. 4 shows the SEM images of the pristine carbon electrode (a), Ag coated carbon composite electrode with UV irradiation (b), and Ag coated carbon composite electrode with base treatment following UV irradiation (c)), respectively. As shown in Figure IV. 4 (a), the top-view images of the pristine carbon electrode appear to be clear. On the other hand, the Ag coated carbon composite electrode with UV irradiation with UV irradiation (Figure IV. 4 (b)) has small Ag seeds (200 ~ 400 nm) with a good distribution on the activated carbon. Figure IV. 4 (c) shows the top view SEM image of the Ag coated carbon composite electrode with the base treatment following UV irradiation. From the image in Figure IV. 4 (c), thickly grown Ag coating layers were observed, which are clearly distinguishable from the Ag seeds in Figure IV. 4 (b). The growth of the Ag coating layers can be explained by the additional reduction of Ag ions due to the base treatment (Pasricha et al. 2009). It is interesting to observe that the Ag coated carbon composite electrode with the base treatment with no UV irradiation had a poor distribution of Ag on the activated carbon (refer to Figure IV. 5). On the Ag coated carbon composite electrode, about 26 atomic% of Ag was detected by EDX (data not shown) and 1.3 mg cm^{-1} of Ag was measured. Even though the carbon electrode was coated with an Ag layer, there was no significant change in

the specific surface area and total pore volume of the electrode (refer to Figure IV. 6). The hydrophilic nature of the Ag coated carbon composite electrode was observed from the relatively low contact angle (31^{o}) compared to the pristine electrode (118^{o}) (refer to Figure IV. 7).

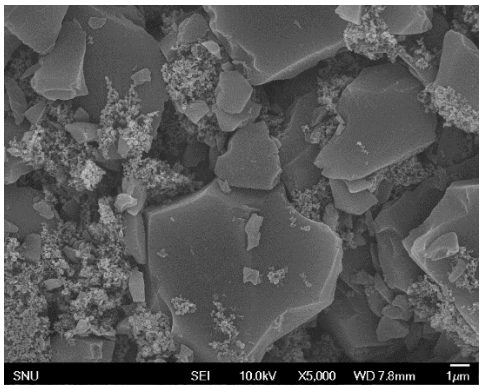

(a)

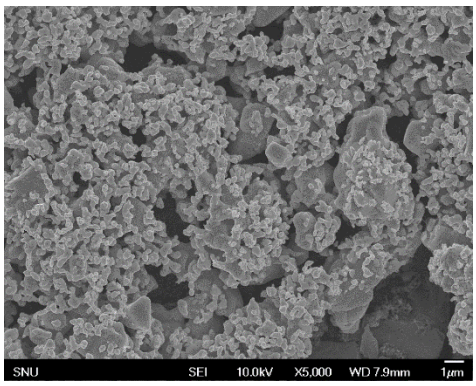

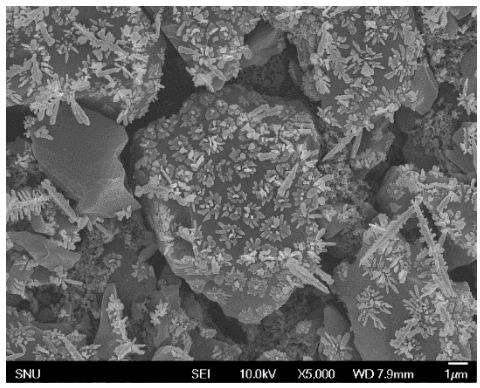

(b) (c)

Figure IV. 4 Scanning electron microscopic (SEM) images showing the morphologies of (a) the pristine carbon electrode and (b) Ag coated carbon composite electrode with UV irradiation, and (c) Ag coated carbon composite electrode with base treatment (NaOH 0.1 M) following UV irradiation

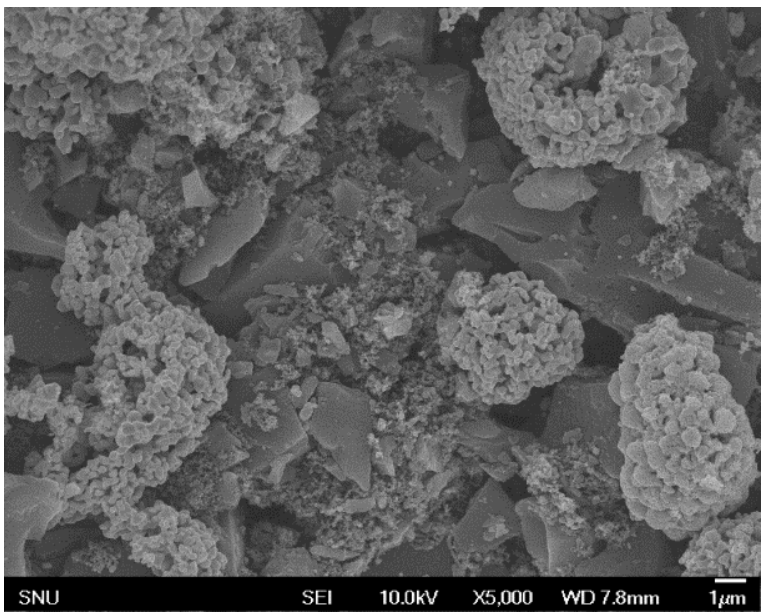

Figure IV. 5 Scanning electron microscopy (SEM) image showing the morphologies of the Ag coated carbon electrode with the immersion step in the base solution (NaOH 0.1 M) without UV radiation.

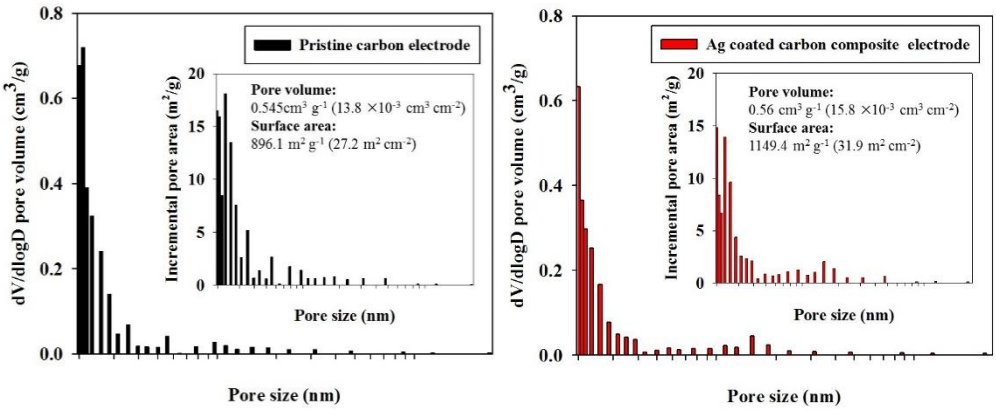

(a) **(b)**

Figure IV. 6 Pore volume (cm^3/g) and incremental pore area (m^2/g) of (a) the pristine carbon electrode and (b) Ag coated carbon composite electrode analyzed by the BET method.

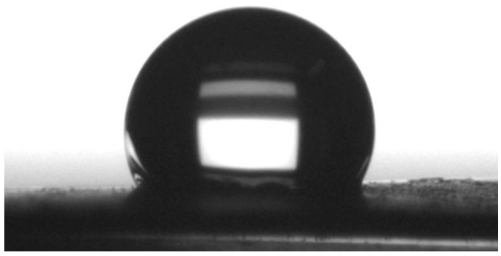

(a)

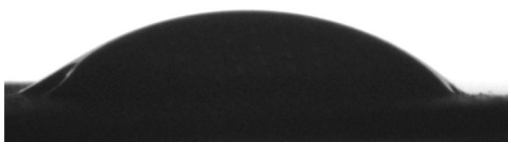

(b)

Figure IV. 7 Contact angle of the pristine carbon electrode (118^{o}, (a)) and the Ag coated carbon composite electrode (31^{o}, (b)).

Figure IV. 8 shows the cyclic voltammogram (CV) of the pristine carbon electrode (a) and the Ag coated carbon composite electrode (b), and the specific electrochemical capacity (c) and the capacity retention ratio (d) of the Ag coated carbon composite electrode analyzed by galvanostatic charging/discharging test, respectively. Several interesting observations can be made from Figure IV. 8.

First, as seen in Figure IV. 8 (a) and (b), the Ag coated carbon composite electrode exhibits both the characteristic of a battery and a capacitive electrode. For instance, Figure IV. 8 (a) shows the rectangular shape of a CV profile indicating that the electrode is a typical capacitor electrode (Kim and Yoon 2013). The CV profile in Figure IV. 8 (b) has a quasi-rectangular shape with reversible redox peaks around at 0-0.1 V ($Ag + Cl^- \leftrightarrows AgCl + e^-$) which are typically observed in a pseudocapacitor electrode (Chen et al. 2014) indicating that the electrode has the characteristic of both a capacitor and a battery. Second, Figure IV. 8 (c) shows that the specific capacity of the Ag coated carbon composite electrode was significantly increased compared with that of the pristine electrode, although tiny amount of Ag was coated (1.3 mg cm^{-2}). For example, the electrical capacity of the Ag coated carbon composite electrode was 0.23 mAh cm^{-2} which was more than double the value of the pristine carbon electrode (0.12 mAh cm^{-2}) in the potential range of -0.1 to 0.25 V. Third, the Ag coated carbon composite electrode exhibited good electrochemical stability (Figure IV. 8 (d)). The capacity

retention ratio was evaluated by galvanostatic charge/discharge test. As shown in Figure IV. 8 (d), 98% of the capacity and 99% of the coulombic efficiency (Eq (2)) were retained until 1,100 cycles.

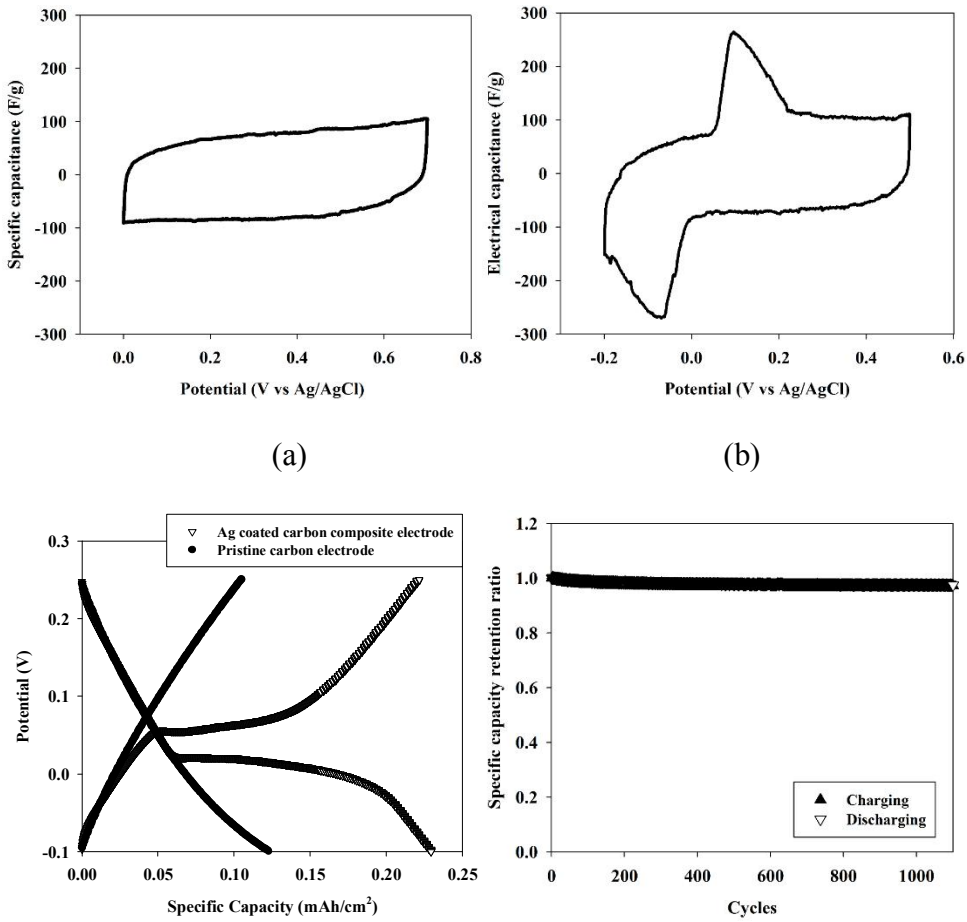

Figure IV. 8 Cyclic voltammetry profile (2 mV s^{-1}) of (a) the Ag coated carbon composite electrode and (b) pristine carbon electrode. (c) Galvanostatic charging/discharging profile of the Ag coated carbon composite electrode compared with the pristine carbon electrode. (d) Capacity retention of the Ag coated HCDI system with respect to the cycle number (2 M NaCl, Ag/AgCl, 25 ± 1^{o}C)

Figure IV. 9 shows the deionization performances of the Ag coated HCDI expressed as the effluent conductivity (a), deionization capacity (b), and deionization rate (c), respectively. To investigate the effect of the Ag coating, CDI with CEM was employed as a control system. As shown in Figure IV. 9 (a), the Ag coated HCDI demonstrated an enhanced deionization capacity compared with the CDI with CEM, in which the effluent conductivity of the Ag coated HCDI was much lower than that of the CDI with CEM. With the result of one cycle selected in Figure IV. 9 (a), the deionization capacity and rate are shown in Figure IV. 9 (b) and (c), respectively. For example, the Ag coated HCDI had a deionization capacity of 15.6 mg g^{-1} whose value is much higher (88% more) than that of the CDI with CEM (8.2 mg g^{-1}). The maximum deionization rate of the Ag coated HCDI was 0.078 mg g^{-1} s^{-1}, which was faster than that of the CDI with CEM (0.056 mg g^{-1} s^{-1}) (Figure IV. 9 (c)). The significant improvement in the deionization performance is explained by the enhanced specific capacity in Ag coated carbon composite electrode (Figure IV. 8 (c)). As a capacitor property, the increase in capacity of one electrode contributes to the enhancement in the total system capacity ($1/C_{total} = 1/C_{cathode} + 1/C_{anode}$) (Kim and Yoon 2013) as previously observed in the previous HCDI studies (Kim et al. 2016b, Lee et al. 2014). Note that the release of Ag in the effluent was negligible (< 2 ug L^{-1}) for each cycle (data not shown). In addition, in the real river water, Ag coated HCDI

showed much better deionization capacity (23.2 mg g^{-1} (= 0.77 meq g^{-1})), compared to that of synthetic water (15.6 mg L^{-1} (= 0.53 meq g^{-1})) in Figure IV. 9, showing its applicability as desalination technology (data not shown). This better deionization capacity in the real river water (3,900 mg L^{-1} (= 147.8 meq L^{-1})) is explained by its higher salt concentration than synthetic water (584 mg L^{-1} (= 20 meq L^{-1}).

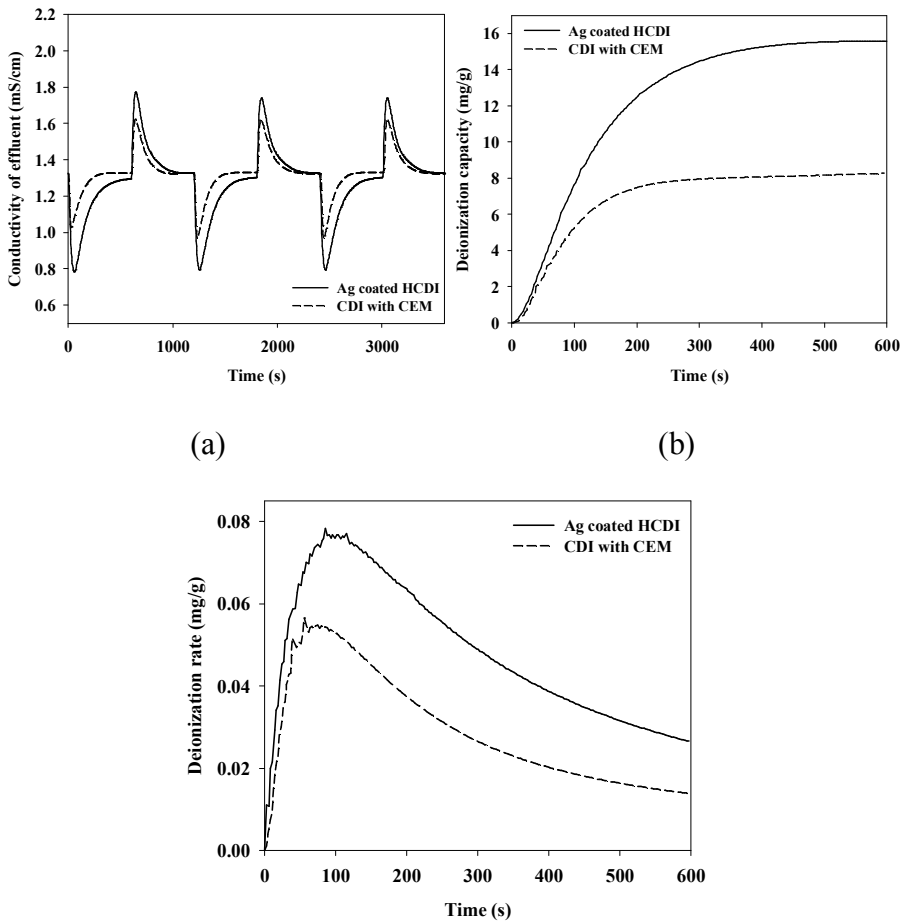

Figure IV. 9 Effluent conductivity (a), deionization capacity (b), and deionization rate (c) of the Ag coated HCDI over time compared to CDI with CEM (cation exchange membrane) (0.7 V / -0.7 V, 10 mM NaCl, 2 mL min^{-1}, 25 ± 1^{o}C).

Table IV. 1 shows the deionization capacity and the charge efficiency of the Ag coated HCDI with respect to the amount of coated-Ag which was obtained by varying the Ag ion concentration in the coating solution (3 – 100 mM). Two important observations can be made from Table IV. 1.

First, the deionization capacity of the Ag coated HCDI was clearly increased with respect to the amount of coated-Ag on the CDI carbon electrode. For example, the deionization capacity was enhanced from 11.6 mg g^{-1} to 16.8 mg g^{-1} as the amount of coated-Ag increased from 0.3 mg cm^{-2} to 1.7 mg cm^{-2} in the composite electrode. This observation supports the previous explanation that the specific capacity was enhanced as a result of combining the capacitance of carbon electrode with Ag mediated charge transfer reaction, which leads to the improvement in the deionization capacity.

Second, the Ag coating positively influenced the charge efficiency in the Ag coated HCDI system although it was not exactly linear. For example, the charge efficiency of the Ag coated HCDI was 92.2% (with 1.3 mg cm^{-2} of coated-Ag), while that of the CDI with CEM (no Ag coated carbon composite electrode) was 76.1%. Although the charge efficiency dropped when the Ag coating was 1.7 mg cm^{-2}, its value (88.5%) was still much higher than that of the control (76.1%). One

explanation for the enhanced charge efficiency of the Ag coated HCDI is that it was induced by the selective reaction of Ag with the chloride ion. In the traditional CDI carbon electrode, a fraction of the current is inevitably consumed due to 'co-ion repulsion' at the charging step (Biesheuvel and Van der Wal 2010). However, in the case of the Ag coated carbon composite electrode in the Ag coated HCDI, the counter ions (Cl^-) were directly stored in the Ag layer through the Ag/AgCl charge transferring reaction, not only in the EDL. Accordingly, the Ag coated carbon composite electrode appeared to save the waste of the current from the co-ion repulsion leading to a higher charge efficiency.

Table IV. 1 Deionization capacity and charge efficiency of the Ag coated HCDI with respect to the amount of coated-Ag (10 mM NaCl, 0.7 / -0.7 V, 10 min, 2 mL min^{-1}, 25 ± 1°C)

Amount of coated-Ag ($mg\ cm^{-2}$)	Deionization capacity ($mg\ g^{-1}$)	Charge efficiency (%)
0.0	7.6	76.1
0.3	11.6	87.7
0.5	13.8	90.2
1.3	15.6	92.2
1.7	16.8	88.5

Figure IV. 10 compared the deionization capacity (a) and the energy consumption (b) of the Ag coated HCDI (operated at 0.7 V) with those of the MCDI and the CDI with CEM operated at 1.2 V (2 mL min^{-1}, 25 ± 1°C, 10 mM NaCl). As shown in Figure IV. 10, the deionization capacity (a) and the energy consumption (b) of the Ag coated HCDI were much better than those of the CDI with CEM and the MCDI, respectively. For example, the deionization capacity of the Ag coated HCDI was 15.6 mg g^{-1} while that of the MCDI, the CDI with CEM, and the CDI were 14.5, 12.1 and 7.5 mg g^{-1} respectively. For energy consumption, the Ag coated HCDI consumed 73.3 kJ $mole^{-1}$, which was much lower than that of the MCDI (136.7 kJ $mole^{-1}$), the CDI with CEM (194.8 kJ $mole^{-1}$) and the CDI (257.5 kJ $mole^{-1}$) (obtained from Eq (4)). The low energy consumption in the Ag coated HCDI for deionization is because the Ag coated HCDI can be operated well at a lower voltage (0.7 V) than that of other systems (1.2 V). The 0.7 V operation can theoretically save 42% energy compared to the 1.2 V operation considering that the energy consumption is obtained by multiplying the charge with the applied voltage. Considering that Ag coated HCDI showed competitive deionization capacity with MCDI with the absence of anion exchange membrane, its good energy efficiency is expected to be one of the promising advantages of Ag coated HCDI.

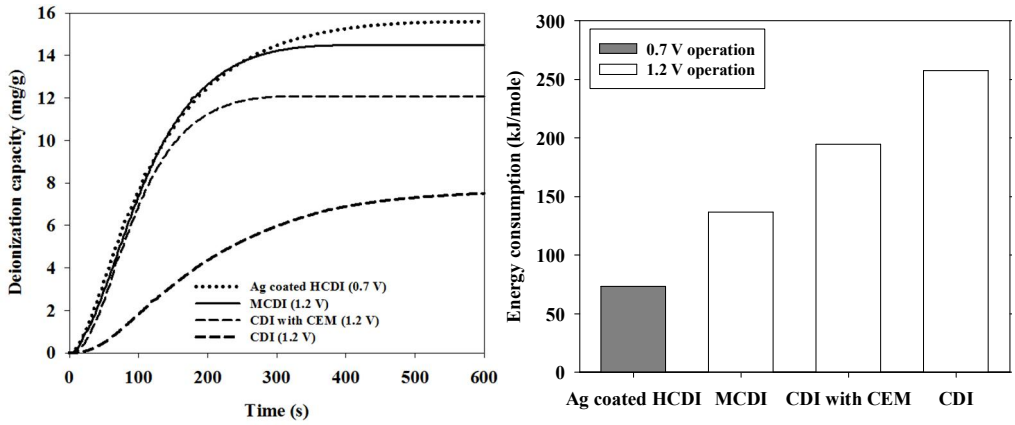

(a) **(b)**

Figure IV. 10 Comparison of (a) the deionization capacity and (b) energy consumption of the Ag coated HCDI, operated at 0.7 V with those of the MCDI and CDI with CEM operated at 1.2 V (2 mL/min, 25 ± 1°C, 10 mM NaCl).

4.4. Summary

In this study, a new HCDI system with an Ag coated carbon composite electrode (Ag coated HCDI) was investigated where this HCDI consists of an Ag coated composite carbon electrode and one carbon electrode. The composite electrode was prepared by the tiny amount of coating Ag (1.3 mg cm^{-2}) as a battery material onto a carbon electrode by photo induced Ag reduction. As the major results, the CDI deionization capacity was dramatically enhanced (88% more) due to Ag coating. In addition, its maximum deionization rate (0.056 mg g^{-1} s^{-1} → 0.078 mg g^{-1} s^{-1}) and charge efficiency (76% → 92%) were also notably improved. The enhancement in the deionization performances is caused by the improved electrochemical capacity combining the capacitance in the carbon electrode with Ag mediated charge transfer reaction. Moreover, the Ag coated HCDI (73.3 kJ $mole^{-1}$) is superior to the MCDI (136.7 kJ $mole^{-1}$) in terms of energy consumption for deionization because the Ag coated HCDI can operate well even at a lower voltage (0.7 V) compared to that of the traditional CDI operating condition (~1.2 V). This study reports that Ag coated HCDI has a potential for improving the deionization performance and energy efficiency in CDI technology.

5. Relationship between the characteristics of cation exchange membrane and their desalination performances in membrane capacitive deionization

5.1. Introduction

Desalination such as distillation and reverse osmosis considered as one of technologies that can effectively overcome water scarcity problem (Khawaji et al. 2008, Shannon et al. 2008, Subramani and Jacangelo 2015). Recently, capacitive deionization (CDI) which is driven by an electrical double layer (EDL) formation of an electrode surface has been attracting attention as a novel desalination technology (Suss et al. 2015a). Energy-efficient CDI for treating the low-grade saline water in comparison with the conventional desalination technology showed its great potential to be applied for the hardness control, wastewater treatment, producing distilled water (Lee et al. 2006, Lee and Choi 2012, Seo et al. 2010, Yoon et al. 2016, Zhao et al. 2013).

However, CDI has an intrinsic limitation that some of charges are wasted due to 'co-ion expulsion effect', leading to the deionization performance reduction (Avraham et al. 2009, Kim et al. 2015c). Because, when the EDL is formed, the co-ions (i.e. ions having same charge with the electrode) are expelled from the

electrode, inevitably consuming charges for attracting the counter-ions into the electrode. To overcome the limitation of CDI, membrane CDI (MCDI) system was introduced (Biesheuvel and Van der Wal 2010, Lee et al. 2006).

MCDI is a system which is assembled with a pair of CDI electrode and cation/anion exchange membranes (Kim and Choi 2010b, Zhao et al. 2012). Due to the ion exchange membranes (IEM), MCDI showed much better deionization performances than CDI (Biesheuvel and Van der Wal 2010). It is because that the IEMs in MCDI mitigate the above-mentioned co-ion repulsion. In addition, IEM contribute to maintaining deionization performance compared to conventional CDI (Omosebi et al. 2014). Despite its advantages, MCDI was limited due to the expensive price of commercial IEM. Therefore, various attempts have been made to develop ion exchanging materials that are expected to be competitive with commercial IEMs (Asquith et al. 2014, Dykstra et al. 2016, Gu et al. 2016, Kang et al. 2015, Kim et al. 2016a, Kim et al. 2015a, Kim and Choi 2010b, Koo et al. 2012, Kwak et al. 2012, Lee et al. 2011, Li et al. 2014, Li et al. 2017, Liu et al. 2014, Nie et al. 2012, Qian et al. 2015, Tian et al. 2014, Yoon et al. 2016, Zhang et al. 2015). For example, novel materials have been used as IEM to reduce the electrical resistance (Kang et al. 2015, Koo et al. 2012, Kwak et al. 2012, Tian et al. 2014, Zhang et al. 2015). In addition, facile coatings have been introduced to alleviate the interfacial resistance between electrode and the ion exchange

materials (Asquith et al. 2014, Dykstra et al. 2016, Gu et al. 2016, Kim et al. 2016a, Kim et al. 2015a, Kim and Choi 2010b, Lee et al. 2011, Li et al. 2014, Li et al. 2017, Liu et al. 2014, Nie et al. 2012, Qian et al. 2015, Yoon et al. 2016). Most of the previous researcher seem to intuitively recognize that the lowering the electrical resistance would be beneficial for the MCDI performance. However, until now, a systematic research has been limitedly conducted on how the overall characteristics of IEM, including electrical resistance, affect the performance of MCDI. In particular, the effect of the other IEM characteristics such as transport number, water content and ion exchange capacity onto the MCDI performance have not been examined yet.

The aim of this research is to investigate how the characteristics of cation exchange membrane (CEM) affects the MCDI performance which is evaluated by deionization capacity, maximum average deionization rate (MADR), and charge efficiency. As characteristics of IEM, electrical resistance, ion exchange capacity, water content, and transport number was examined. Sulfonated polyphenylene oxide (SPPO) based cation exchange membranes (CEM), Ca-alginate based cation exchange membrane and three commercials were used for an experimental group.

5.2. Materials & Methods

5.2.1. Electrode fabrication

The carbon electrode was prepared as our previous research (Kim and Yoon 2013, Yoon et al. 2016). Activated carbon (MSP-20X, Kansai Coke and Chemicals, Japan), carbon black (Super P, TIMCAL Graphite & Carbon, Swiss), and polytetrafluoroethylene (PTFE, Sigma-Aldrich, USA) were mixed with a weight ratio of 86:7:7 to prepare the electrode of MCDI employed in this study. The mixture was blended in a few milliliters of ethanol for homogeneity and roll-pressed to make a sheet-type carbon electrode with a 250 μm thickness. The fabricated electrode was then dried in a vacuum oven at 120℃ for 12 h. After drying, the carbon sheet was cut into circular pieces.

5.2.2. Cation exchange membrane

As the experimental group of CEM, SPPO based membrane and 3 commercials (Neosepta CMX, Neosepta CMB (ASTOM, Japan), and CMD (Asahi glass, Japan)) were used.

The SPPO was prepared in Kilo-Lab in KRICT (Korean Research Institute of Chemical Technology) as following procedure. First, PPO was dissolved in $CHCl_3$. Subsequently, this solution was sulfonated with chlorosulfonic acid. The solid phase SPPO was obtained from the solution through precipitation and

filtration step. The SPPO solution (22wt%) was prepared with dissolved in dimethylacetamide (DMAc). The prepared SPPO solution was casted on the glass plate. The membrane thickness was sensitively controlled by the casting knife. The casted SPPO solution was dried in the 70^{o}C oven for 60 min. Subsequently, it was dipped in the deionized water for the phase separation.

The Ca-alginate membrane was prepared by the previous research (Yoon et al. 2016). Sodium alginate powder (Sigma-Aldrich, USA) was dissolved in deionized (DI) water using a mechanical stirrer for 12 h (MS3040, MTOPS, Seoul, Republic of Korea). 12wt% of sodium alginate solution was used, and unless mentioned otherwise, the experiments were performed with the 10wt%. The prepared sodium alginate solution was degassed for 6 h using ultrasonicator (Ultrasonic cleaners, 1510E-DTH, Brason Ultrasonics, USA). The sodium alginate solution was cast on the flat glass plate (Elcometer, UK). The height of the casting knife was set at 150 μm. The cast electrode was then rapidly dipped in 2 M calcium chloride solution at room temperature (Sigma-Aldrich, USA) for 30 min. The ca-alginate membrane was fully rinsed with DI water and stored in DI water at room temperature for more than 12 h before use.

5.2.3. Characterization of cation exchange membrane

Electrical resistance, transport number, ion exchange capacity, and water content were examined as the major characteristics of CEM.

The electrical resistance of CEM was measured by the electrical impedance spectroscopy (EIS) method as previous research (Yoon et al. 2016). The carbon electrode was used as for working electrode and counter electrode. Ag/AgCl (sat. KCl) electrode was used as the reference electrode. EIS was analyzed in a three-electrode system with 2 M $CaCl_2$ electrolyte. Impedance value at a high frequency (100 Hz) was measured to obtain the equivalent series resistance (ESR) comprised of the electrolyte, IEMs and the electrodes. Since the ESR was measured in the identical electrolyte (2.5 mM $CaCl_2$) and the electrodes, ESR changes with or without CEM were used as the resistance of the CEM (R_{CEM}).

Transport number was measured by the calculation from membrane potential (Sata 2007) as shown in Figure V.1. The CEM was placed to divide a reservoir into two, and each was filled with 2.5 mM and 5 mM $CaCl_2$ solution, respectively. A pair of Ag/AgCl electrodes were used to measure the membrane potential between both side of CEM. The transport number was obtained from the measured membrane potential as following Eq. (1) (Sata 2007).

$$V_m = -\left(\frac{3}{2}t_+ - 1\right)\frac{RT}{F}\ln\left(\frac{a_{\pm c}}{a_{\pm d}}\right) \quad (1)$$

Where V_m is voltage difference between CEM (V), R is gas constant (8.314 J $mole^{-1}K^{-1}$), T is absolute temperature (K), F is faradaic constant (96485 C $mole^{-1}$) $a_{\pm c}$ is $a_{\pm d}$ concentration of each reservoir respectively (mole L^{-1}).

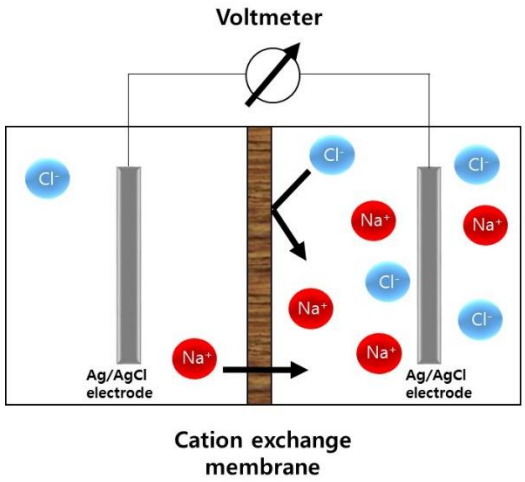

Figure V. 1 Schematic of the calculation from membrane potential to obtain transport number

Water content was obtained by the weight difference between before and after drying the CEM as following Eq. (2).

$$\text{Water content (\%)} = \frac{W_{wet} - W_{dry}}{W_{dry}} \times 100 \quad (2)$$

Where W_{wet} is the weight of fully wetted CEM, W_{dry} is the weight of dried CEM.

Ion exchange capacity was measured as following procedure (Helfferich 1962). First, the CEM sample was exposed to the HC1 1 M for 24 h, which was intended to substitute all cations in CEM matrix to H^+ ion. Second, the sample was dipped in 0.5 M NaCl solution for several hours. And then ion exchange capacity was calculated by measuring the concentration of H^+ ion.

5.2.4. Deionization performance test

Figure V. 2 shows the schematic of MCDI and its control (No CEM), which were used to evaluate the deionization performance. As shown in Figure V. 1, MCDI system was assembled with a pair of carbon electrodes, a CEM and an anion exchange membrane (AEM). As control, no CEM was assembled. 2 Nylon spacers were used as separator. All experiments were conducted as single pass

flow mode with a volumetric flow rate of 2 mL min^{-1}. For comparison under the same electrolyte resistance conditions (R_{sol}), the same concentration of CaCl2 (5 mM) was used unless otherwise noted. For example, Rsol of 5 mM CaCl2 solution is 12.7 Ω cm2 in the MCDI system used for this study.

Ion adsorption (purification) and desorption (concentration) steps were conducted with a cycler (WBCS3000, WonATech, Republic of Korea), which applied a constant voltage of 1.2 V and 0 V for 15 min each, respectively. The cycles were repeated for 3 times. The conductivity of the treated outlet stream was monitored with a flow-type conductivity meter (3583-10C, HORIBA, Japan). The deionization capacity was calculated from the integration of the concentration change expressed as the conductivity (Eq. (3)). The average deionization rate was obtained from the deionization capacity divided by the time (Eq. (4)). The charge efficiency was obtained from the deionization capacity divided by the consumed charges (Eq. (5)).

$$\text{Deionization capacity (mg g}^{-1}) = \frac{\int (C_i - C_0)\cdot\Phi\cdot dt\cdot M_w}{m} \quad (3)$$

$$\text{Average deionization rate (mg g}^{-1}\text{s}^{-1}) = \frac{\int (C_i - C_0)\cdot\Phi\cdot dt\cdot M_w}{m\int dt} \quad (4)$$

$$\text{Charge efficiency (\%)} = \frac{\int (C_i - C_0)\cdot\Phi\cdot dt\cdot F}{\int I\cdot dt} \quad (5)$$

, where C_i and C_0 are the influent and effluent concentration (mM), respectively, during the charging step. Φ is the flow rate (mL min^{-1}); I is the consumed current (A), and F is the faradaic constant (96485 C $mole^{-1}$). (Pasta et al. 2012)

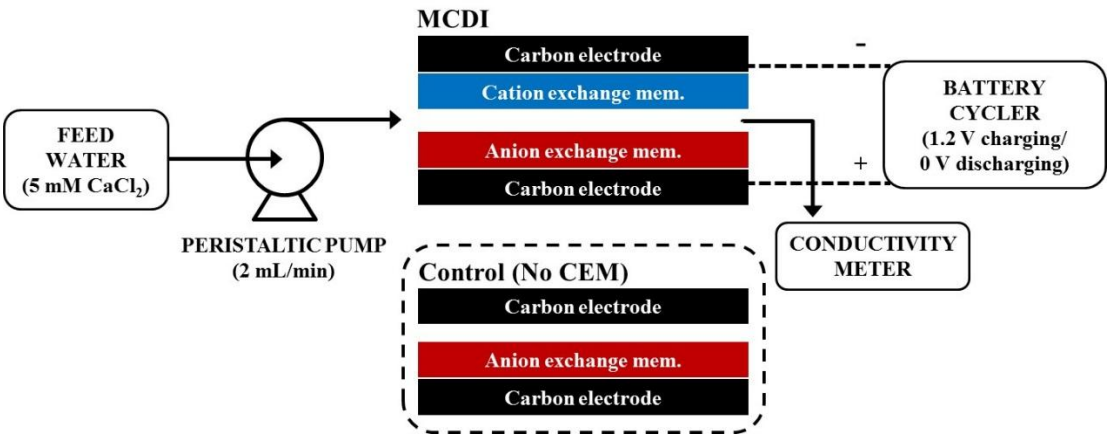

Figure V. 2 Schematic of membrane capacitive deionization (MCDI) and its control (No CEM).

5.3. Results and Discussion

Table V. 1 provides quantitative characteristics of CEMs used in this study expressed as membrane electrical resistance, transport number, water content and ion exchange capacity. As shown Table V. 1, quantitative characteristics of CEMs were distributed well in various ranges. For example, the membrane resistance of

the CEMs was varied in the range of 5.72 ~ 19.71 $\Omega \cdot cm^2$, and the ion exchange capacity was varied in the range of 0.004 to 0.064. In addition, the transport number and water content were varied in the range of 0.720 to 0.968, the water content was varied in the range of 17.7 to 45.4%. Note that the electrical resistance and transport number were evaluated in the low range of ion concentration solution (2.5 – 5 mM $CaCl_2$).

From the result in Table V. 1, 2 interesting observations can be made. First, as the thickness of SPPO membrane increased from 20 um to 250 um, the electrical resistance increased from 1.23 to 6.99 $\Omega \cdot cm^2$ and transport number increased from 0.901 to 0.968. the increase in the electrical resistance with the thickness appears simply to follow the Law of resistance (Resistance = resistivity × Length/Area) (Lawrence 1997). Second, transport number (0.901 → 0.968), water content (18.2 → 25%) and ion exchange capacity (0.005 → 0.05 meq cm^{-2}) also increased with the thickness. The change in the transport number, water content, and ion exchange capacity seems to be due to the increase in the number of sulfonated groups per area, as thickness increase. It is noted that that the sulfonated group is a negatively charged functional group, which repels the anions, improves hydrophilicity, and leads the adsorption of cations (Tedesco et al. 2016).

Table V. 1 Characteristics of ion exchange membrane expressed as membrane resistance, transport number, water content and ion exchange capacity. SPPO: Sulfonated polyphenylene oxide.

Model.	Mem. Res. (Ω cm^2)	Transport number	Water content (%)	Ion exchange capacity (meq/cm^2)
SPPO 20	5.85	0.901	20.0	0.005
SPPO 70	8.90	0.926	20.5	0.013
SPPO 150	12.18	0.968	21.9	0.028
SPPO 250	17.42	0.968	21.9	0.050
Neosepta CMX	7.37	0.966	20.7	0.041
Neosepta CMB	11.70	0.892	17.7	0.059
Selemion CMD	19.71	0.908	25.3	0.064
Ca-alginate	5.72	0.720	45.4	0.004

Figure V. 3 (a) – (c) shows deionization capacity, average deionization rate, and consumed current of MCDI with CEM (SPPO 20 um) in comparison with those in no CEM. The result in Figure V. 2 revealed that the MCDI performances were notably enhanced with the addition of CEM, which showed the similar trends reported in the previous research (Yoon et al. 2016). For instance, as shown in figure V. 2 (a) and (b), deionization capacity and MADR were improved from 13.8 to 19.7 mg g^{-1} and from 0.045 to 0.079 mg $g^{-1}s^{-1}$, respectively. In addition, the charge efficiency (48 → 84%) were also enhanced, which values were obtained from Eq. (6) with the consumed current in Figure V. 2 (c). Similar trends were observed in the results other CEMs in this study (refer to Figure V. 4).

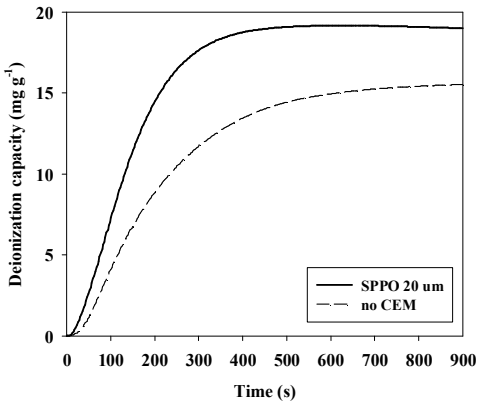

(a)

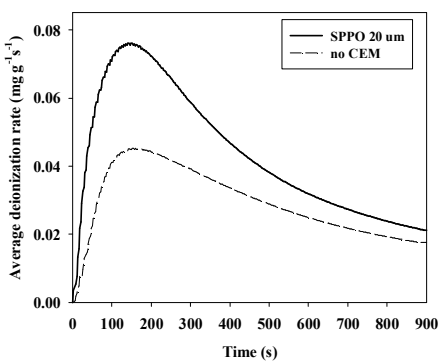

(b)

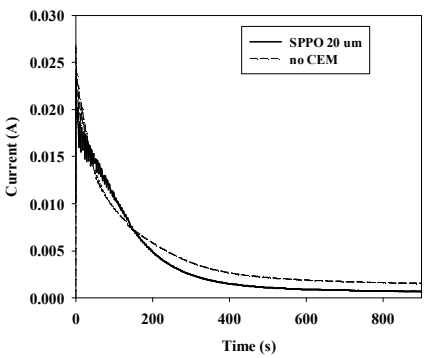

(c)

Figure V. 3 Representative deionization capacity (a), average deionization rate (b) and consumed current (c) in membrane capacitive deionization system in comparison with those in no CEM. 20 um sulfonated polyphenyleneoxide (20 um SPPO) membrane was used for the representative CEM ($CaCl_2$ 5 mM, 2 mL min^{-1}, 25^{o}C).

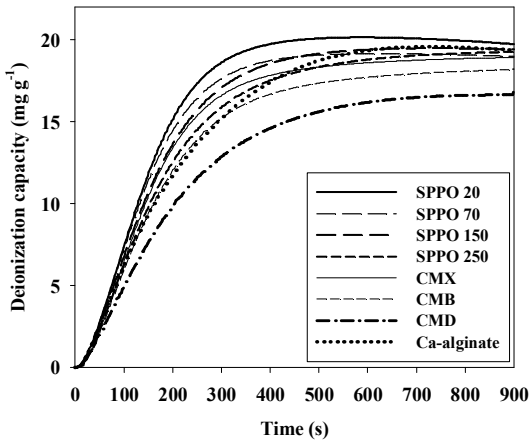

(a)

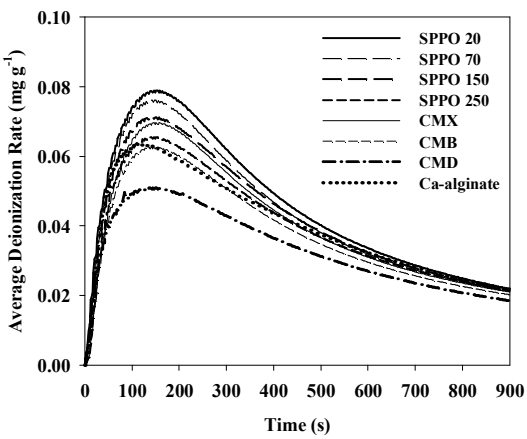

(b)

Figure V. 4 Representative deionization capacity (a), and average deionization rate (b) in membrane capacitive deionization system with various cation exchange membrane (CEM) ($CaCl_2$ 5 mM, 2 mL min^{-1}, 25°C, SPPO: sulfonated polyphenylene oxide). The representative results are obtained from triplicated experiments.

Table V. 2 summarized the deionization capacity, MADR and charge efficiency of MCDI with CEMs. In Table V. 2, the MADR varied within a significant range depending on the CEMs. As shown in Table V. 2, the MADR with SPPO 20 um was 0.0773 ± 0.0016 mg $g^{-1}s^{-1}$ and that with Neosepta CMD was 0.0519 ± 0.0030 mg $g^{-1}s^{-1}$. On the other hand, the deionization capacities and charge efficiencies were varied in narrow range within about 10%. For example, the deionization capacities were varied from 17.0 ± 1.1 mg g^{-1} to 18.9 ± 1.7 mg g^{-1} and charge efficiencies were varied from 81.8 ± 2.1% to 90.4 ± 4.1% depending on the CEMs. In addition, most results of deionization capacities and charge efficiencies overlapped within the error ranges. From the result in Table V. 2, it is speculated that the rate capability of MCDI among the deionization performances is sensitively influenced by the quantitative characteristics of MCDI.

Table V. 2 Deionization performances of membrane capacitive deionization expressed as deionization capacity, maximum average deionization rate, and charge efficiency. SPPO: Sulfonated polyphenylene oxide.

Model.	Deionization capacity (mg/g)	Maximum average deionization rate (mg/g/s)	Charge efficiency (%)
SPPO 20 um	18.8 ± 0.2	0.0773 ± 0.0016	86.7 ± 6.0
SPPO 70 um	18.9 ± 1.6	0.0691 ± 0.0038	90.4 ± 4.1
SPPO 150 um	18.9 ± 1.7	0.0639 ± 0.0016	87.5 ± 1.4
SPPO 250 um	18.2 ± 2.4	0.0587 ± 0.0019	88.7 ± 4.4
Selemion CMX	17.2 ± 1.4	0.0674 ± 0.0021	87.9 ± 5.1
Neosepta CMB	17.0 ± 1.1	0.0595 ± 0.0038	81.8 ± 2.1
Neosepta CMD	18.1 ± 1.1	0.0519 ± 0.0030	87.3 ± 2.5
Ca-alginate	18.0 ± 3.9	0.0647 ± 0.0025	92.9 ± 4.8

Figure V. 5 (a) – (b) show the MADR of MCDI with the inverse of electrical resistance of CEM, and transport number, respectively. From the results of Figure V. 5, it was observed that no significant correlation between MADR and CEM characteristics was observed. For instance, the MADR with the inverse of electrical resistance showed $R^2 = 0.63$, and that with the transport number showed $R^2 = 0.001$. This lack of relationship seems to be attributed to the following reasons.

First, although electrical resistance represents ionic conductivity, it cannot represent a positive contribution to the alleviation of co-ion repulsion as following Eq (6) (Sata 2007). Second, although the transport number can represent the alleviation of co-ion repulsion, but it does not provide the information of the ionic conductivity in CEM itself, which is expressed well in the following Eq (7).

$$R_{CEM} = \frac{1}{F(|z_+|u_+C_+ + |z_-|u_-C_-)} \quad (6)$$

$$t_+(transport\ number) = \frac{|z_+|u_+C_+}{|z_+|u_-C_- + |z_-|u_-C_-} \quad (7)$$

Where R_{CEM} is the electrical resistance of the CEM ($\Omega\ cm^2$), t_+ is the transport number of CEM, F is faradaic constant (96485 C/mole), z_+ and z_- are each ion valance, u_+ and u_- are each ion mobility in the membrane ($m^2\ s^{-1}\ V^{-1}$), C_+ and C_- are each ion concentration in the membrane (mole L^{-1}) and *l* is the thickness of the

membrane.

On the other hand, it is noted that no specific analysis has been conducted on the effects of the water content and ion exchange capacity on MADR in this study. Since the water content and ion exchange capacity are variables that can be obtained by reaching a certain equilibrium, so there is a limit to be considered as a factor directly affecting deionization rate capability such as MADR.

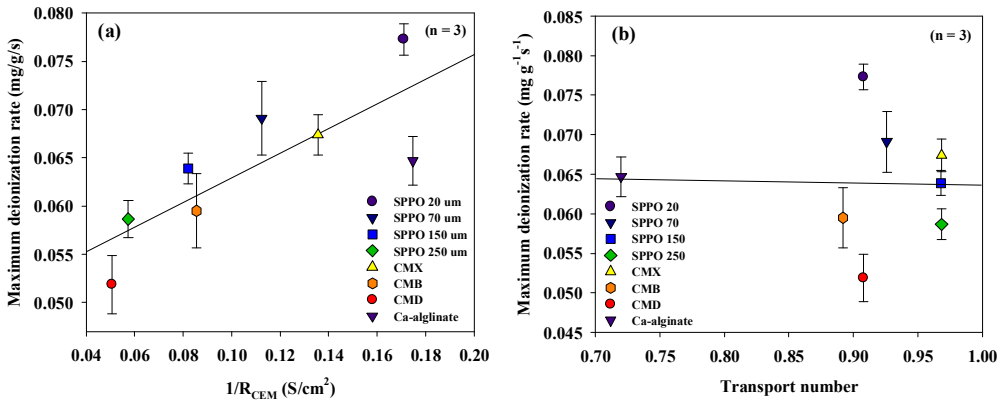

Figure V. 5 Maximum average deionization rate of membrane capacitive deionization with inverse of total electrical resistance ($1/R_{tot}$) (R^2 = 0.63) (a) and transport number (R^2 = 0.001) (b), SPPO: sulfonated polyphenylene oxide.

Figure V. 6 shows the MADR with the t_+/R_{CEM} (transport number divided by CEM electrical resistance), which is inspired from the results in Figure V. 5 and Eq. (6) and (7). As a results in Figure V. 6, the MADR was notably correlated with t_+/R_{CEM} (R^2 = 0.83). For instance, the MADR was enhanced from 0.052 ± 0.003 mg $g^{-1}s^{-1}$ to 0.077 ± 0.002 mg $g^{-1}s^{-1}$ while the t_+/R_{CEM} varied from 0.046 to 0.155 S cm^{-2}.

From the Eq. (6) and (7), the t_+/R_{CEM} can be expressed the following Eq. (8), which is related to the counter ion flux in the CEMs ($J_+ = |z_+|u_+C_+$). It is noted that the t_+ and R_{CEM} were evaluated in the same ionic concentration condition.

$$t_+/R_{CEM} = F(|z_+|u_+C_+) \quad (8)$$

Since the counter ion flux is a variable representing rate capability, the t_+/R_{CEM} is expected to show high relationship with the rate capability of the MCDI system. Accordingly, the result in Figure V. 6 showed better sensitive relationship, compared to the result in Figure V. 5 (a) and (b).

An insight from the result in Figure V. 6 is that the transport number and the electrical resistance in CEM should be considered together for fast rate capability in MCDI. Most of the researches to develop IEM for MCDI have tried to achieve only low electrical resistance. However, the introduction of t_+/R_{CEM} for IEM development can suggest a balanced development direction of MCDI performance.

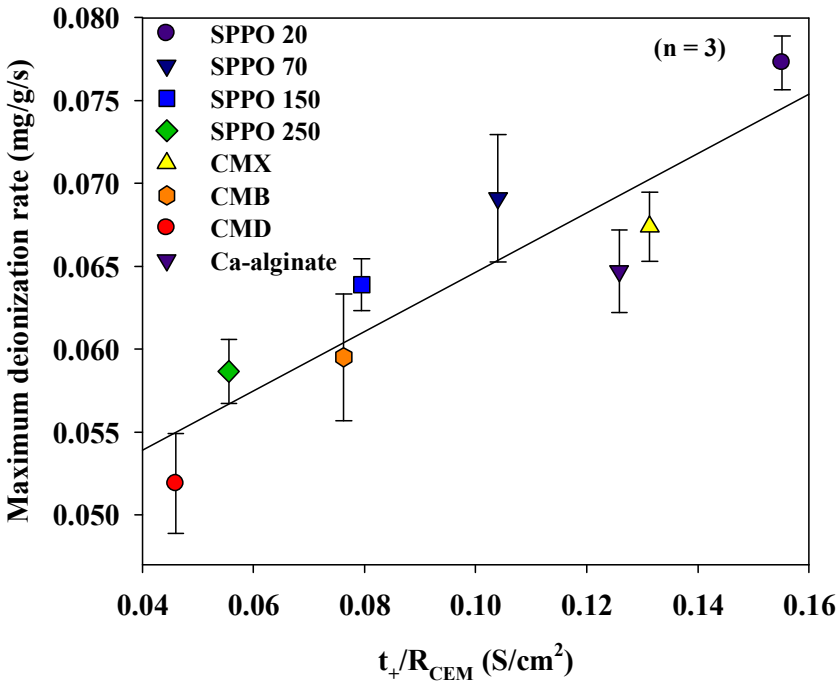

Figure V. 6 Maximum average deionization rate of membrane capacitive deionization with t_+/R_{CEM} (transport number divided by electrical resistance of cation exchange membrane), 5 mM $CaCl_2$, 2 mL min^{-1}, R^2 = 0.83).

5.4. Summary

In this study, how the characteristics of cation exchange membrane (CEM) affects the membrane CDI (MCDI) performance were examined in terms of

deionization capacity, maximum average deionization rate (MADR), and charge efficiency. As a major result, only MADR among MCDI performances was significantly varied by CEMs. In particular, MADR was found to have a significant correlation with the transport number divided by total electrical resistance (R^2 = 0.83). Accordingly, CEM with low electrical resistance and with high transport number would be beneficial for the fast deionization rate performance. The result in this study is expected to provide a good insight to develop of highly high rate-capable MCDI.

6. Conclusion

This study develops new and fascinated ion selective materials to enhanced CDI performance. In addition, it is investigated the influence of the ion selective materials on the CDI performances.

Firstly, Ca-alginate, a cation exchange material, was successfully applied in CDI and MCDI systems to treat hard water. Ca-alginate coated electrode assembled CDI demonstrated superior enhancement in deionization capacity and excellent charge efficiency compared to the conventional CDI. Moreover, CA-MCDI displayed comparable performance to conventional MCDI system with good stability and selectivity for hardness species, indicating that Ca-alginate can be an appropriate alternative to commercial cation exchange membrane. In conclusion, Ca-alginate is speculated as an appropriate material for CDI system to control hardness in water.

Secondly, Second, Ag coating on to the carbon composite electrode is proposed where this composite electrode has the characteristics of a battery and a capacitor together. The composite electrode was prepared by the tiny amount of coating Ag (1.3 mg cm^{-2}) as a battery material onto a carbon electrode by photo induced Ag reduction. As the major results, the CDI deionization capacity was dramatically enhanced (88% more) due to Ag coating. In addition, its maximum deionization

rate (0.056 mg g^{-1} s^{-1} → 0.078 mg g^{-1} s^{-1}) and charge efficiency (76% → 92%) were also notably improved. The enhancement in the deionization performances is caused by the improved electrochemical capacity combining the capacitance in the carbon electrode with Ag mediated charge transfer reaction. Moreover, the Ag coated CDI (73.3 kJ $mole^{-1}$) is superior to the MCDI (136.7 kJ $mole^{-1}$) in terms of energy consumption for deionization because the Ag coated HCDI can operate well even at a lower voltage (0.7 V) compared to that of the traditional CDI operating condition (~1.2 V). This study reports that Ag coated HCDI has a potential for improving the deionization performance and energy efficiency in CDI technology.

Third, how the characteristics of cation exchange membrane (CEM) affects the membrane CDI (MCDI) performance were examined in terms of deionization capacity, maximum average deionization rate (MADR), and charge efficiency. As a major result, only MADR among MCDI performances was significantly varied by CEMs. In particular, MADR was found to have a significant correlation with the transport number divided by total electrical resistance (R^2 = 0.83). Accordingly, CEM with low electrical resistance and with high transport number would be beneficial for the fast deionization rate performance. The result in this study is expected to provide a good insight to develop of high rate-capable MCDI.

Reference

Anderson, M.A., Cudero, A.L. and Palma, J. (2010) Capacitive deionization as an electrochemical means of saving energy and delivering clean water. Comparison to present desalination practices: Will it compete? Electrochimica Acta 55(12), 3845-3856.

Aslani, P. and Kennedy, R.A. (1996) Studies on diffusion in alginate gels. I. Effect of cross-linking with calcium or zinc ions on diffusion of acetaminophen. Journal of controlled release 42(1), 75-82.

Asquith, B.M., Meier-Haack, J. and Ladewig, B.P. (2014) Cation exchange copolymer enhanced electrosorption. Desalination 345, 94-100.

Avraham, E., Bouhadana, Y., Soffer, A. and Aurbach, D. (2009) Limitation of charge efficiency in capacitive deionization I. On the behavior of single activated carbon. Journal of the Electrochemical Society 156(6), P95-P99.

Bates, R., Guggenheim, E., Harned, H., Ives, D., Janz, G., Monk, C., Robinson, R., Stokes, R. and Wynne-Jones, W. (1956) Standard electrode potential of the silver, silver chloride electrode. The Journal of Chemical Physics 25(2), 361-361.

Bauer, B., Strathmann, H. and Effenberger, F. (1990) Anion-exchange membranes with improved alkaline stability. Desalination 79(2-3), 125-144.

Biesheuvel, P. and Van der Wal, A. (2010) Membrane capacitive deionization. Journal of membrane science 346(2), 256-262.

Blandino, A., Macías, M. and Cantero, D. (1999) Formation of calcium alginate gel

capsules: influence of sodium alginate and CaCl 2 concentration on gelation kinetics. Journal of bioscience and bioengineering 88(6), 686-689.

Bockris, J.O.M., Reddy, A.K. and Gamboa-Aldeco, M. (2001) Modern Electrochemistry 2B: Electrodics in Chemistry, Engineering, Biology and Environmental Science, Springer Science & Business Media.

Bürger, W. (2017) Use of an ionic fluoropolymer as antistatic coating, Google Patents.

Chen, J.P., Hong, L., Wu, S. and Wang, L. (2002) Elucidation of interactions between metal ions and Ca alginate-based ion-exchange resin by spectroscopic analysis and modeling simulation. Langmuir 18(24), 9413-9421.

Chen, J.P. and Wang, L. (2001) Characterization of a Ca-alginate based ion-exchange resin and its applications in lead, copper, and zinc removal. Separation science and technology 36(16), 3617-3637.

Chen, W., Xia, C., Rakhi, R. and Alshareef, H.N. (2014) A general approach toward enhancement of pseudocapacitive performance of conducting polymers by redox-active electrolytes. Journal of Power Sources 267, 521-526.

Chen, Z., Zhang, H., Wu, C., Wang, Y. and Li, W. (2015) A study of electrosorption selectivity of anions by activated carbon electrodes in capacitive deionization. Desalination 369, 46-50.

Choi, J., Lee, H. and Hong, S. (2016) Capacitive deionization (CDI) integrated with monovalent cation selective membrane for producing divalent cation-rich solution. Desalination 400, 38-46.

Dean, J.G., Bosqui, F.L. and Lanouette, K.H. (1972) Removing heavy metals from waste

water. Environmental science & technology 6(6), 518-522.

Długołęcki, P. and van der Wal, A. (2013) Energy recovery in membrane capacitive deionization. Environmental science & technology 47(9), 4904-4910.

Dykstra, J., Zhao, R., Biesheuvel, P. and Van der Wal, A. (2016) Resistance identification and rational process design in Capacitive Deionization. Water research 88, 358-370.

El-Deen, A.G., Barakat, N.A. and Kim, H.Y. (2014) Graphene wrapped MnO 2-nanostructures as effective and stable electrode materials for capacitive deionization desalination technology. Desalination 344, 289-298.

Elimelech, M. and Phillip, W.A. (2011) The future of seawater desalination: energy, technology, and the environment. science 333(6043), 712-717.

Farmer, J.C., Fix, D.V., Mack, G.V., Pekala, R.W. and Poco, J.F. (1996) Capacitive deionization of NaCl and NaNO3 solutions with carbon aerogel electrodes. Journal of the Electrochemical Society 143(1), 159-169.

Gabrielli, C., Maurin, G., Francy-Chausson, H., Thery, P., Tran, T. and Tlili, M. (2006) Electrochemical water softening: principle and application. Desalination 201(1), 150-163.

Gao, X., Omosebi, A., Landon, J. and Liu, K. (2015) Enhanced salt removal in an inverted capacitive deionization cell using amine modified microporous carbon cathodes. Environmental science & technology 49(18), 10920-10926.

García-Quismondo, E., Santos, C., Lado, J., Palma, J.s. and Anderson, M.A. (2013) Optimizing the energy efficiency of capacitive deionization reactors working under real-world conditions. Environmental science & technology 47(20), 11866-11872.

Ghizellaoui, S., Chibani, A. and Ghizellaoui, S. (2005) Use of nanofiltration for partial

softening of very hard water. Desalination 179(1), 315-322.

Gu, X., Deng, Y. and Wang, C. (2016) Fabrication of anion-exchange polymer layered graphene–melamine electrodes for membrane capacitive deionization. ACS Sustainable Chemistry & Engineering 5(1), 325-333.

Hauck, A.R. and Sourirajan, S. (1969) Performance of porous cellulose acetate membranes for the reverse osmosis treatment of hard and waste waters. Environmental science & technology 3(12), 1269-1275.

Hou, C.-H. and Huang, C.-Y. (2013) A comparative study of electrosorption selectivity of ions by activated carbon electrodes in capacitive deionization. Desalination 314, 124-129.

Jeon, S.-i., Park, H.-r., Yeo, J.-g., Yang, S., Cho, C.H., Han, M.H. and Kim, D.K. (2013) Desalination via a new membrane capacitive deionization process utilizing flow-electrodes. Energy & Environmental Science 6(5), 1471-1475.

Ji, Q., An, X., Liu, H., Guo, L. and Qu, J. (2015) Electric Double-Layer Effects Induce Separation of Aqueous Metal Ions. ACS nano 9(11), 10922-10930.

Kang, J., Kim, T., Jo, K. and Yoon, J. (2014) Comparison of salt adsorption capacity and energy consumption between constant current and constant voltage operation in capacitive deionization. Desalination 352, 52-57.

Kang, K.W., Hwang, C.W. and Hwang, T.S. (2015) Synthesis and properties of sodium vinylbenzene sulfonate-grafted poly (vinylidene fluoride) cation exchange membranes for membrane capacitive deionization process. Macromolecular Research 23(12), 1126-1133.

Khawaji, A.D., Kutubkhanah, I.K. and Wie, J.-M. (2008) Advances in seawater desalination technologies. Desalination 221(1-3), 47-69.

Kim, C., Lee, J., Kim, S. and Yoon, J. (2014) TiO 2 sol–gel spray method for carbon electrode fabrication to enhance desalination efficiency of capacitive deionization. Desalination 342, 70-74.

Kim, J.S., Jeon, Y.S. and Rhim, J.W. (2016a) Application of poly (vinyl alcohol) and polysulfone based ionic exchange polymers to membrane capacitive deionization for the removal of mono-and divalent salts. Separation and Purification Technology 157, 45-52.

Kim, J.S., Kim, C.S., Shin, H.S. and Rhim, J.W. (2015a) Application of synthesized anion and cation exchange polymers to membrane capacitive deionization (MCDI). Macromol. Res 23(4), 360-366.

Kim, S.-R., Oh, H.-S., Jo, S.-J., Yeon, K.-M., Lee, C.-H., Lim, D.-J., Lee, C.-H. and Lee, J.-K. (2013a) Biofouling control with bead-entrapped quorum quenching bacteria in membrane bioreactors: physical and biological effects. Environmental science & technology 47(2), 836-842.

Kim, S., Lee, J., Kang, J.S., Jo, K., Kim, S., Sung, Y.-E. and Yoon, J. (2015b) Lithium recovery from brine using a λ-MnO 2/activated carbon hybrid supercapacitor system. Chemosphere 125, 50-56.

Kim, S., Lee, J., Kim, C. and Yoon, J. (2016b) Na 2 FeP 2 O 7 as a Novel Material for Hybrid Capacitive Deionization. Electrochimica Acta 203, 265-271.

Kim, S., Yoon, H., Shin, D., Lee, J. and Yoon, J. (2017) Electrochemical selective ion separation in capacitive deionization with sodium manganese oxide. Journal of colloid and interface science 506, 644-648.

Kim, T., Dykstra, J., Porada, S., Van Der Wal, A., Yoon, J. and Biesheuvel, P. (2015c)

Enhanced charge efficiency and reduced energy use in capacitive deionization by increasing the discharge voltage. Journal of colloid and interface science 446, 317-326.

Kim, T. and Yoon, J. (2013) Relationship between capacitance of activated carbon composite electrodes measured at a low electrolyte concentration and their desalination performance in capacitive deionization. Journal of Electroanalytical Chemistry 704, 169-174.

Kim, Y.-J. and Choi, J.-H. (2010a) Enhanced desalination efficiency in capacitive deionization with an ion-selective membrane. Separation and Purification Technology 71(1), 70-75.

Kim, Y.-J. and Choi, J.-H. (2010b) Improvement of desalination efficiency in capacitive deionization using a carbon electrode coated with an ion-exchange polymer. Water research 44(3), 990-996.

Kim, Y.-J. and Choi, J.-H. (2012) Selective removal of nitrate ion using a novel composite carbon electrode in capacitive deionization. Water research 46(18), 6033-6039.

Kim, Y.-J., Kim, J.-H. and Choi, J.-H. (2013b) Selective removal of nitrate ions by controlling the applied current in membrane capacitive deionization (MCDI). Journal of membrane science 429, 52-57.

Kneifel, K. and Hattenbach, K. (1980) Properties and long-term behavior of ion exchange membranes. Desalination 34(1-2), 77-95.

Koo, J.S., Kwak, N.-S. and Hwang, T.S. (2012) Synthesis and properties of an anion-exchange membrane based on vinylbenzyl chloride–styrene–ethyl methacrylate copolymers. Journal of membrane science 423, 293-301.

Kovalenko, I., Zdyrko, B., Magasinski, A., Hertzberg, B., Milicev, Z., Burtovyy, R., Luzinov, I. and Yushin, G. (2011) A major constituent of brown algae for use in high-capacity Li-ion batteries. Science 334(6052), 75-79.

Kwak, N.-S., Koo, J.S., Hwang, T.S. and Choi, E.M. (2012) Synthesis and electrical properties of NaSS–MAA–MMA cation exchange membranes for membrane capacitive deionization (MCDI). Desalination 285, 138-146.

Lawrence, S. (1997) Physics for scientists and engineers. Jones &bartlett Learning 2, 732-733.

Lee, J.-B., Park, K.-K., Eum, H.-M. and Lee, C.-W. (2006) Desalination of a thermal power plant wastewater by membrane capacitive deionization. Desalination 196(1-3), 125-134.

Lee, J.-H. and Choi, J.-H. (2012) The production of ultrapure water by membrane capacitive deionization (MCDI) technology. Journal of membrane science 409, 251-256.

Lee, J.-Y., Seo, S.-J., Yun, S.-H. and Moon, S.-H. (2011) Preparation of ion exchanger layered electrodes for advanced membrane capacitive deionization (MCDI). Water research 45(17), 5375-5380.

Lee, J., Kim, S., Kim, C. and Yoon, J. (2014) Hybrid capacitive deionization to enhance the desalination performance of capacitive techniques. Energy & Environmental Science 7(11), 3683-3689.

Lee, J., Yoon, H., Lee, J., Kim, T. and Yoon, J. (2017) Extraction of Salinity-Gradient Energy by a Hybrid Capacitive-Mixing System. ChemSusChem 10(7), 1600-1606.

Lee, J., Yu, S.-H., Kim, C., Sung, Y.-E. and Yoon, J. (2013) Highly selective lithium

recovery from brine using a λ-MnO 2–Ag battery. Physical Chemistry Chemical Physics 15(20), 7690-7695.

Leonard, K.C., Genthe, J.R., Sanfilippo, J.L., Zeltner, W.A. and Anderson, M.A. (2009) Synthesis and characterization of asymmetric electrochemical capacitive deionization materials using nanoporous silicon dioxide and magnesium doped aluminum oxide. Electrochimica Acta 54(22), 5286-5291.

Li, H., Pan, L., Lu, T., Zhan, Y., Nie, C. and Sun, Z. (2011) A comparative study on electrosorptive behavior of carbon nanotubes and graphene for capacitive deionization. Journal of Electroanalytical Chemistry 653(1), 40-44.

Li, H., Zaviska, F., Liang, S., Li, J., He, L. and Yang, H.Y. (2014) A high charge efficiency electrode by self-assembling sulphonated reduced graphene oxide onto carbon fibre: towards enhanced capacitive deionization. Journal of Materials Chemistry A 2(10), 3484-3491.

Li, H. and Zou, L. (2011) Ion-exchange membrane capacitive deionization: a new strategy for brackish water desalination. Desalination 275(1), 62-66.

Li, H., Zou, L., Pan, L. and Sun, Z. (2010) Novel graphene-like electrodes for capacitive deionization. Environmental science & technology 44(22), 8692-8697.

Li, N., An, J., Wang, X., Wang, H., Lu, L. and Ren, Z.J. (2017) Resin-enhanced rolling activated carbon electrode for efficient capacitive deionization. Desalination 419, 20-28.

Li, Y., Zhang, C., Jiang, Y., Wang, T.-J. and Wang, H. (2016) Effects of the hydration ratio on the electrosorption selectivity of ions during capacitive deionization. Desalination 399, 171-177.

Liao, Y., Wang, Y., Feng, X., Wang, W., Xu, F. and Zhang, L. (2010) Antibacterial surfaces through dopamine functionalization and silver nanoparticle immobilization. Materials Chemistry and Physics 121(3), 534-540.

Liu, Y.-H., Hsi, H.-C., Li, K.-C. and Hou, C.-H. (2016) Electrodeposited manganese dioxide/activated carbon composite as a high-performance electrode material for capacitive deionization. ACS Sustainable Chemistry & Engineering 4(9), 4762-4770.

Liu, Y., Ma, W., Cheng, Z., Xu, J., Wang, R. and Gang, X. (2013) Preparing CNTs/Ca-Selective zeolite composite electrode to remove calcium ions by capacitive deionization. Desalination 326, 109-114.

Liu, Y., Pan, L., Xu, X., Lu, T., Sun, Z. and Chua, D.H. (2014) Enhanced desalination efficiency in modified membrane capacitive deionization by introducing ion-exchange polymers in carbon nanotubes electrodes. Electrochimica Acta 130, 619-624.

Matsui, K., Tobita, E., Sugimoto, K., Kondo, K., Seita, T. and Akimoto, A. (1986) Novel anion exchange membranes having fluorocarbon backbone: preparation and stability. Journal of applied polymer science 32(3), 4137-4143.

Mayes, R.T., Tsouris, C., Kiggans Jr, J.O., Mahurin, S.M., DePaoli, D.W. and Dai, S. (2010) Hierarchical ordered mesoporous carbon from phloroglucinol-glyoxal and its application in capacitive deionization of brackish water. Journal of Materials Chemistry 20(39), 8674-8678.

Nagarajan, M. and Paine, H. (1984) Water hardness control by detergent builders. Journal of the American Oil Chemists Society 61(9), 1475-1478.

Nie, C., Pan, L., Liu, Y., Li, H., Chen, T., Lu, T. and Sun, Z. (2012) Electrophoretic

deposition of carbon nanotubes–polyacrylic acid composite film electrode for capacitive deionization. Electrochimica Acta 66, 106-109.

Omosebi, A., Gao, X., Landon, J. and Liu, K. (2014) Asymmetric electrode configuration for enhanced membrane capacitive deionization. ACS applied materials & interfaces 6(15), 12640-12649.

Oren, Y. (2008) Capacitive deionization (CDI) for desalination and water treatment—past, present and future (a review). Desalination 228(1), 10-29.

Park, B.-H. and Choi, J.-H. (2010) Improvement in the capacitance of a carbon electrode prepared using water-soluble polymer binder for a capacitive deionization application. Electrochimica Acta 55(8), 2888-2893.

Park, J.-S., Song, J.-H., Yeon, K.-H. and Moon, S.-H. (2007) Removal of hardness ions from tap water using electromembrane processes. Desalination 202(1), 1-8.

Pasricha, R., Gupta, S. and Srivastava, A.K. (2009) A Facile and Novel Synthesis of Ag–Graphene-Based Nanocomposites. Small 5(20), 2253-2259.

Pasta, M., Wessells, C.D., Cui, Y. and La Mantia, F. (2012) A desalination battery. Nano letters 12(2), 839-843.

Porada, S., Bukowska, P., Shrivastava, A., Biesheuvel, P. and Smith, K.C. (2016) Nickel Hexacyanoferrate Electrodes for Cation Intercalation Desalination. arXiv preprint arXiv:1612.08293.

Porada, S., Zhao, R., Van Der Wal, A., Presser, V. and Biesheuvel, P. (2013) Review on the science and technology of water desalination by capacitive deionization. Progress in Materials Science 58(8), 1388-1442.

Qian, B., Wang, G., Ling, Z., Dong, Q., Wu, T., Zhang, X. and Qiu, J. (2015) Sulfonated Graphene as Cation-Selective Coating: A New Strategy for High-Performance Membrane Capacitive Deionization. Advanced Materials Interfaces 2(16).

Sata, T. (2004) Ion exchange membranes: preparation, characterization, modification and application, Royal Society of chemistry.

Sata, T. (2007) Ion exchange membranes: preparation, characterization, modification and application, Royal Society of chemistry.

Schafer, H. (1970) Carboxyl groups and ion exchange in low-rank coals. Fuel 49(2), 197-213.

Seo, S.-J., Jeon, H., Lee, J.K., Kim, G.-Y., Park, D., Nojima, H., Lee, J. and Moon, S.-H. (2010) Investigation on removal of hardness ions by capacitive deionization (CDI) for water softening applications. Water research 44(7), 2267-2275.

Shannon, M.A., Bohn, P.W., Elimelech, M., Georgiadis, J.G., Mariñas, B.J. and Mayes, A.M. (2008) Science and technology for water purification in the coming decades. Nature 452(7185), 301-310.

Shi, Z., Neoh, K. and Kang, E. (2004) Surface-grafted viologen for precipitation of silver nanoparticles and their combined bactericidal activities. Langmuir 20(16), 6847-6852.

Siragusa, G.R. and Dickson, J.S. (1992) Inhibition of Listeria monocytogenes on beef tissue by application of organic acids immobilized in a calcium alginate gel. Journal of Food Science 57(2), 293-296.

Song, J.-H., Yeon, K.-H., Cho, J. and Moon, S.-H. (2005) Effects of the operating parameters on the reverse osmosis-electrodeionization performance in the production of

high purity water. Korean Journal of Chemical Engineering 22(1), 108-114.

Srimuk, P., Kaasik, F., Krüner, B., Tolosa, A., Fleischmann, S., Jäckel, N., Tekeli, M.C., Aslan, M., Suss, M.E. and Presser, V. (2016) MXene as a novel intercalation-type pseudocapacitive cathode and anode for capacitive deionization. Journal of Materials Chemistry A 4(47), 18265-18271.

Subramani, A. and Jacangelo, J.G. (2015) Emerging desalination technologies for water treatment: a critical review. Water research 75, 164-187.

Suss, M., Porada, S., Sun, X., Biesheuvel, P., Yoon, J. and Presser, V. (2015a) Water desalination via capacitive deionization: what is it and what can we expect from it? Energy & Environmental Science 8(8), 2296-2319.

Suss, M., Porada, S., Sun, X., Biesheuvel, P., Yoon, J. and Presser, V. (2015b) Water desalination via capacitive deionization: what is it and what can we expect from it? Energy & Environmental Science.

Svetličić, V. and Konrad, Z. (1979) Study of the electrical resistivity of alkaline earth ions in cation-exchange membranes. Journal of membrane science 5, 129-134.

Tedesco, M., Hamelers, H. and Biesheuvel, P. (2016) Nernst-Planck transport theory for (reverse) electrodialysis: I. Effect of co-ion transport through the membranes. Journal of membrane science 510, 370-381.

Testing, A.S.f. and Materials (1998) Standard Test Method for Tensile Properties of Plastics, ASTM.

Tian, G., Liu, L., Meng, Q. and Cao, B. (2014) Preparation and characterization of cross-linked quaternised polyvinyl alcohol membrane/activated carbon composite electrode for

membrane capacitive deionization. Desalination 354, 107-115.

Tsai, Y.-C. and Doong, R.-a. (2016) Hierarchically ordered mesoporous carbons and silver nanoparticles as asymmetric electrodes for highly efficient capacitive deionization. Desalination 398, 171-179.

Wadie, A. and Abuljalil, G. (2010) Assessment of hydrochemical quality of groundwater under some urban areas with Sana'a Secretariat. Eclética Química 35(1), 77-84.

Wang, Z., Feng, Y., Hao, X., Huang, W. and Feng, X. (2014a) A novel potential-responsive ion exchange film system for heavy metal removal. Journal of Materials Chemistry A 2(26), 10263-10272.

Wang, Z., Ma, Y., Hao, X., Huang, W., Guan, G. and Abudula, A. (2014b) Enhancement of heavy metals removal efficiency from liquid wastes by using potential-triggered proton self-exchange effects. Electrochimica Acta 130, 40-45.

Weinstein, L. and Dash, R. (2013) Capacitive Deionization: Challenges and Opportunities. Desalin. Water Reuse 23, 34-37.

Welgemoed, T. and Schutte, C. (2005) Capacitive deionization technology™: an alternative desalination solution. Desalination 183(1-3), 327-340.

Wiers, B.H., Grosse, R.J. and Cilley, W.A. (1982) Divalent and trivalent ion exchange with zeolite A. Environmental science & technology 16(9), 617-624.

Wimalasiri, Y. and Zou, L. (2013) Carbon nanotube/graphene composite for enhanced capacitive deionization performance. Carbon 59, 464-471.

Xing, F., Li, T., Li, J., Zhu, H., Wang, N. and Cao, X. (2017) Chemically exfoliated MoS 2 for capacitive deionization of saline water. Nano Energy 31, 590-595.

Xu, P., Drewes, J.E., Heil, D. and Wang, G. (2008) Treatment of brackish produced water using carbon aerogel-based capacitive deionization technology. Water research 42(10), 2605-2617.

Xu, T. (2005) Ion exchange membranes: state of their development and perspective. Journal of membrane science 263(1), 1-29.

Yang, G., Zhang, L., Peng, T. and Zhong, W. (2000) Effects of Ca 2+ bridge cross-linking on structure and pervaporation of cellulose/alginate blend membranes. Journal of Membrane Science 175(1), 53-60.

Yang, J., Zou, L., Song, H. and Hao, Z. (2011) Development of novel MnO 2/nanoporous carbon composite electrodes in capacitive deionization technology. Desalination 276(1), 199-206.

Yang, S.J., Kim, T., Lee, K., Kim, Y.S., Yoon, J. and Park, C.R. (2014) Solvent evaporation mediated preparation of hierarchically porous metal organic framework-derived carbon with controllable and accessible large-scale porosity. Carbon 71, 294-302.

Yeo, J.-H. and Choi, J.-H. (2013) Enhancement of nitrate removal from a solution of mixed nitrate, chloride and sulfate ions using a nitrate-selective carbon electrode. Desalination 320, 10-16.

Yeon, K.-H., Song, J.-H. and Moon, S.-H. (2004) A study on stack configuration of continuous electrodeionization for removal of heavy metal ions from the primary coolant of a nuclear power plant. Water research 38(7), 1911-1921.

Yoon, H., Lee, J., Kim, S.-R., Kang, J., Kim, S., Kim, C. and Yoon, J. (2016) Capacitive deionization with Ca-alginate coated-carbon electrode for hardness control. Desalination

392, 46-53.

Yoon, S., Lee, J., Hyeon, T. and Oh, S.M. (2000) Electric double-layer capacitor performance of a new mesoporous carbon. Journal of the Electrochemical Society 147(7), 2507-2512.

Yoshioka, T., Tsuru, K., Hayakawa, S. and Osaka, A. (2003) Preparation of alginic acid layers on stainless-steel substrates for biomedical applications. Biomaterials 24(17), 2889-2894.

Zhang, D., Wen, X., Shi, L., Yan, T. and Zhang, J. (2012a) Enhanced capacitive deionization of graphene/mesoporous carbon composites. Nanoscale 4(17), 5440-5446.

Zhang, D., Yan, T., Shi, L., Peng, Z., Wen, X. and Zhang, J. (2012b) Enhanced capacitive deionization performance of graphene/carbon nanotube composites. Journal of Materials Chemistry 22(29), 14696-14704.

Zhang, L., Zhou, D., Wang, H. and Cheng, S. (1997) Ion exchange membranes blended by cellulose cuoxam with alginate. Journal of Membrane Science 124(2), 195-201.

Zhang, L., Zhou, J., Zhou, D. and Tang, Y. (1999) Adsorption of cadmium and strontium on cellulose/alginic acid ion-exchange membrane. Journal of Membrane Science 162(1), 103-109.

Zhang, Y., Zou, L., Wimalasiri, Y., Lee, J.-Y. and Chun, Y. (2015) Reduced graphene oxide/polyaniline conductive anion exchange membranes in capacitive deionisation process. Electrochimica Acta 182, 383-390.

Zhao, R., Biesheuvel, P. and Van der Wal, A. (2012) Energy consumption and constant current operation in membrane capacitive deionization. Energy & Environmental Science

5(11), 9520-9527.

Zhao, R., Porada, S., Biesheuvel, P. and Van der Wal, A. (2013) Energy consumption in membrane capacitive deionization for different water recoveries and flow rates, and comparison with reverse osmosis. Desalination 330, 35-41.

국문 초록

축전식 탈염 기술 (CDI)은 차세대 담수화 공정으로 주목을 받고 있습니다. 축전식 탈염 기술은 증발법이나, 역삼투법 과 같은 기존 담수화 공정에 비해 에너지 효율 측면에서 유리할 것으로 기대 되어왔습니다. 그러나, 본 기술은 “동전하 반발 현상 (Co-ion expulsion)이라는 필연적인 한계점을 갖고 있습니다. 이는 전극 표면의 전기 이중층이 형성이 될 때, 일부 전하가 낭비되는 현상이며, 탈염 효율 및 성능 감소를 야기합니다. 이러한 단점을 해결하고자, 최근 이온교환막과 배터리 전극 물질 같은 이온 선택성 물질이 적용이 되었습니다. 최근 다양한 물질들이 개발 되어왔으나, 여전히 축전식 탈염 기술에 적합한 이온 선택적 물질의 개발이 요구되고 있습니다. 본 박사학위 논문에서는 축전식 탈염 기술의 성능을 증대시키고자 새로운 이온 선택적 물질을 개발했습니다. 또한, 양이온 교환막의 특성이 축전식 탈염 기술의 탈염 성능에 미치는 영향에 대해서 체계적으로 분석했습니다.

우선, Ca-alginate 을 양이온교환막을 대체 했으며, 경도 제어 공정에 적용했습니다. Ca-alginate 를 음전극에 이온 치환 반응을 통해서 성공적으로 코팅하였습니다. 주요 결과로써, Ca-alginate 코팅을 통하여 약 44%의 탈염 용량 향상을 나타냈습니다. 또한, 상용 양이온교환막과 비교하도 비견할만한 탈염 용량 및 전하 효율을 나타냈습니다.

둘째, 은 (Ag) 코팅을 통하여 음이온교환막을 대체했으며 탈염 성능 향상을 보였습니다. 주요 결과로, 은 코팅이 도입된 축전식 탈염 기술 (Ag coated HCDI)은 은 코팅의 영향으로 탈염 용량 (88% 이상), 속도 (39% 이상), 전하효율 (76% → 92%) 측면에서 향상된 성능을 보였습니다. 이러한 탈염 성능 향상은 코팅된 은이 탄소 전극의 전기화학적 용량 향상에 기여함에 따라 나타난 것으로 보입니다. 한편, 은 코팅이 도입된 축전식 탈염 기술 (Ag coated HCDI)은 에너지 소모 측면에서도 탁월함을 나타냈습니다. 이는 은 코팅이

도입된 축전식 탈염 기술 (Ag coated HCDI)은 기존의 막결합 축전식 탈염 기술 (MCDI)에 비해 낮은 전위에서 운전함에도 탁월한 탈염 성능을 보였기 때문입니다.

마지막으로, 양이온교환막의 특성이 막 결합 축전식 탈염 (MCDI) 성능 향상에 미치는 영향에 대해서 분석하는 연구를 수행했습니다. 탈염 성능으로써 탈염 용량, 최대 탈염 속도, 전하 효율이 평가 되었습니다. 주요 결과로써, 우선 세 가지 탈염 성능 중에 최대 탈염 속도가 양이온교환막의 종류에 따라 민감하게 변하는 결과를 관찰했습니다. 뿐만 아니라, 양이온교환막의 이동수와 전기 저항을 함께 고려한 변수를 적용할 때 (i.e. t_+/R_{CEM}) 최대 탈염 속도와의 관계성이 향상되었습니다 (R^2=0.83).

결론적으로, 본 학위 논문에서 수행된 연구를 통해서 Ca-alginate 와 은코팅과 같은 탁월한 이온 선택성 재료 개발을 통해 담수화 성능 향상을 달성했으며, 적용 가능성을 보였습니다. 또한, 이동수와 전기 저항이 함께 고려된 변수 (i.e. t_+/R_{CEM})와 최대 탈염 속도간의 관계성을 확인함으로써 향후 막결합 축전식 탈염 기술용 이온 교환막 개발에 중요한 정보를 제공할 것으로 기대 됩니다.

주요어: 수처리 공정, 담수화, 축전식 탈염 공정, 은, 칼슘 알지네이트

학번: 2013-30283